

https://dspace.org/

# Wave propagation in a homogenous piezoelectric solid cylinder of transversely isotropic material

**Yenwong-Fai, Alfred Sevidzem**

**2009-02-04T08:53:36Z**
http://hdl.handle.net/10539/6000

Downloaded from a DSpace repository. https://dspace.org/

# Wave Propagation in a Homogeneous Piezoelectric Solid Cylinder of Transversely Isotropic Material

**Alfred Sevidzem Yenwong-Fai**

A dissertation submitted to the Faculty of Science, University of the Witwatersrand, Johannesburg, in fulfilment of the requirements for the degree of Master of Science.

**Johannesburg, 2008**

## Declaration

I declare that this dissertation is my own, unaided work. It is being submitted for the Degree of Master of Science in the University of the Witwatersrand, Johannesburg. It has not been submitted before for any degree or examination in any other University.

_____

A.S. Yenwong-Fai

____ day of _____ 2008

# Acknowledgements

I thank my supervisors Prof A.G. Every and Prof M. Shatalov, for giving me the opportunity to study towards an MSc under their supervision and for giving me rigorous training in the fundamentals of scientific research methodology.

I am grateful to Dr Craig Long, for his help while I used latex and X-fig packages and also for answering some of my questions in solid mechanics. I would like to thank Dr Philip Loveday for also willing to answer some questions related to this project. I am also indebted to Jeremy Wallis and Kiri Nicolaides for always ensuring that I had all I needed to carry out my project smoothly while working at the CSIR Pretoria. I want to express my heartfelt thanks to Dr Nomusa Dlodlo, Kudakwashe Jakata, the AIMS alumni at the University of the Witwatersrand, Ally Mahlangu, David Seshai, and all the employees at the sensor science and technology competence area at the CSIR for the support and encouragement in the course of the project.

I owe a special dept of gratitude to my sponsors AIMS (Cape town), Prof A.G. Every and the CSIR for giving me the opportunity to be trained in scientific research. I want to express my gratitude and love to my family, for their love, support, emotional sustenance and prayers during the course of this project. Above all I am grateful to God Almighty, for sustaining and seeing me through the project by His love, mercy and mighty hand (Isaiah 41:10).

# Abstract

The ultrasonic nondestructive evaluation (NDE) of composite cylinders is dependent on the thorough understanding of the propagation characteristics of the wave modes in these materials. In this dissertation the propagation of free harmonic non-axisymmetric (flexural) waves in a homogeneous piezoelectric solid cylinder of transversely isotropic material is studied, on the basis of the linear theory of elasticity and linear electromechanical coupling of the elastic and electric variables. The equations of motion of the cylinder are developed using the constitutive relations of a piezoelectric material possessing transversely isotropic symmetry properties, with the symmetry direction collinear with the axis of the cylinder. The physically allowed boundary conditions are derived from Hamilton's variational principle. Four displacement and three electric potentials satisfying Helmholtz's equation are used to solve the equations of motion of the cylinder. The characteristic equation (dispersion relation) is obtained by the application of the boundary conditions satisfied by the elastic and electric variables. The characteristic equation is solved numerically by a novel method which makes use of the three dimensional plot of the log of the modulus of the left hand side of the characteristic equation. The results are numerically illustrated via dispersion curves of a sample PZT-4 composite cylinder. Significant changes in the propagating wave modes are revealed by the dispersion curves, when compared with a corresponding non-piezoelectric model of a PZT-4 cylinder. It is also observed that the dispersion curves are sensitive to the form of the electric boundary conditions.

# Contents

**1 Introduction** **1**

1.1 Elastic Wave Phenomena and Piezoelectricity . . . . . 1

1.2 Preview . . . . . 10

**2 Elastodynamics and Piezoelectricity** **12**

2.1 Introduction . . . . . 12

2.2 Strain . . . . . 13

2.3 Stress . . . . . 18

2.4 Hooke's Law . . . . . 21

2.5 Voigt Contracted Notation . . . . . 22

2.6 Energy of a Strained Crystal . . . . . 22

2.7 Navier's Wave Equation . . . . . 24

2.7.1 Translational Equation of Motion . . . . . 24

2.7.2 Rotational Equation of Motion . . . . . 27

2.8 Piezoelectricity . . . . . 28

2.8.1 Quasi-Static Approximation . . . . . 31

2.9 Effects of Symmetry on Crystal Properties . . . . . 32

2.10 Thermal Effects . . . . . 36

2.11 Microscopic Origin of Elasticity, Piezoelectricity and Thermal Expansion . . 37

2.11.1 Elasticity . . . . . 38

2.11.2 Piezoelectricity . . . . . 38

**3 Equations of Motion For a Transversely Isotropic Piezoelectric Solid Cylinder 41**

3.1 Introduction . . . . . 41

3.2 Geometry and Coordinates used to Describe the System . . . . . 42

3.3 Method 1: Derivation of Equations of Motion via Navier's Equation and Gauss' law. . . . . 43

3.4 Method 2: Derivation of Equations of Motion via Hamilton's Variational Principle. . . . . 52

**4 Analytic Solutions for the Equations of Motion of the Cylinder and Numerical Results for a Sample PZT-4 rod 59**

4.1 Introduction . . . . . 59

4.2 Analytic Solutions of the Equations of Motion for the Piezoelectric Cylinder 61

4.3 Frequency Equation . . . . . 68

4.4 Non-axisymmetrical Wave Propagation in a Free Transversely Isotropic Non-piezoelectric Solid Cylinder. . . . . 71

4.5 Numerical results . . . . . 77

4.6 Discussion on the Artifacts . . . . . 95

**5 Conclusion** **113**

**Appendices**

**A Dispersion Curves Displayed by Honarvar et al via their Novel Method of Solving the Dispersion Relation** **118**

**Bibliography** **121**

# List of Figures


2.1 (a) Tensile strains $S_{11}$ and $S_{22}$. (b) Shear strains $S_{12}$ and $S_{21}$ [1] . . . . . 17

2.2 An infinitesimal cube surrounding point O showing stress components . . . . 19

2.3 A rectangular infinitesimal element acted on by inhomogeneous stresses [2] . 25

2.4 A rectangular infinitesimal element acted on by inhomogeneous stresses [2] . 27

2.5 Tetrahedral structure of zincblende, ZnS. Only part of unit cell is shown. Size of circles has no relation to size of ions [3] . . . . . 39

3.1 Infinitely long solid cylinder. . . . . 43

3.2 Infinitesimal volume element in cylindrical coordinates; situated in a stressed body. For clarity the stress triads on the rear faces have been indicated with curves originating from the faces concerned. . . . . 44

4.1 Dispersion curves for the flexural modes of a homogeneous isotropic aluminium solid cylinder by Mirsky's model ($m = 1$). . . . . 79

4.2 Dispersion curves for the flexural modes of a homogeneous isotropic aluminium solid cylinder by Honavar et al's model [4] ($m = 1$). . . . . 80

4.3 Dispersion curves for the flexural modes of a homogeneous transversely isotropic glass/epoxy fiber-reinforced composite solid cylinder by Mirsky's model ($m = 1$). 81

4.4 Dispersion curves for the flexural modes of a homogeneous transversely isotropic glass/epoxy fiber-reinforced composite solid cylinder by Honavar et al's model and produced from reference [4] ($m = 1$). . . . . 82

4.5 Dispersion curves for the flexural modes of a homogeneous transversely isotropic cobalt solid cylinder by Mirsky's model ($m = 1$). . . . . 83

4.6 Dispersion curves for the flexural modes of a homogeneous transversely isotropic cobalt solid cylinder by Honarvar et al's model and produced from reference [4] ($m = 1$). . . . . 84

4.7 Dispersion curves for the flexural modes of a homogeneous transversely isotropic glass/epoxy fiber-reinforced composite solid cylinder by Mirsky's model ($m = 1$) and making use of the sign function. . . . . 85

4.8 Dispersion curves for the flexural modes of a homogeneous transversely isotropic cobalt solid cylinder by Mirsky's model ($m = 1$) and making use of the sign function. . . . . 86

4.9 Dispersion curves for the flexural modes of a homogeneous transversely isotropic PZT-4 solid cylinder without electromecanical coupling by Mirsky's model ($m = 1$). . . . . 87

4.10 Dispersion curves for the flexural modes of a homogeneous transversely isotropic PZT-4 solid cylinder with $e_{ij} \cdot 0.001$ and $D_r|_a = 0$, ($m = 1$). . . . . 90

4.11 Dispersion curves for the flexural modes of a homogeneous transversely isotropic PZT-4 solid cylinder with $e_{ij} \cdot 0.001$ and $\phi|_a = 0$, ($m = 1$) . . . . . 91

4.12 Dispersion curves for the flexural modes of a homogeneous transversely isotropic PZT-4 solid cylinder with $e_{ij} \cdot 1$ and $D_r|_a = 0$, ($m = 1$). . . . . 92

4.13 Dispersion curves for the flexural modes of a homogeneous transversely isotropic PZT-4 solid cylinder with $e_{ij} \cdot 1$ and $\phi|_a = 0$, ($m = 1$) . . . . . 93

4.14 A 3D plot of $|\xi_1|$ projected unto the $k$-$\omega$ plane ($m = 1$). . . . . 97

4.15 A 3D plot of $|\xi_2|$ projected unto the $k$-$\omega$ plane ($m = 1$). . . . . 98

4.16 A 3D plot of $|\xi_3|$ projected unto the $k$-$\omega$ plane ($m = 1$). . . . . 99

4.17 A 3D plot of $|\lambda|$ projected unto the $k$-$\omega$ plane ($m = 1$). . . . . 100

4.18 A surface plot of $\log(|V|)$ projected unto the $k$-$\omega$ plane ($m = 1$). . . . . 102

4.19 A 3D plot of $\log(|B_3)|$ projected unto the $k$-$\omega$ plane ($m = 1$). . . . . 104

4.20 Dispersion curves for the flexural modes of a homogeneous isotropic aluminium solid cylinder by Mirsky's model ($m = 1$), with artifacts removed. . . . . 105

4.21 Dispersion curves for the flexural modes of a homogeneous transversely isotropic glass/epoxy fiber-reinforced composite solid cylinder by Mirsky's model ($m = 1$), with artifacts removed. . . . . 106

4.22 Dispersion curves for the flexural modes of a homogeneous transversely isotropic cobalt solid cylinder by Mirsky's model ($m = 1$), with artifacts removed. . . 107

4.23 Dispersion curves for the flexural modes of a homogeneous transversely isotropic PZT-4 solid cylinder without electromecanical coupling by Mirsky's model ($m = 1$), with artifacts removed. . . . . 108

4.24 Dispersion curves for the flexural modes of a homogeneous transversely isotropic PZT-4 solid cylinder with $e_{ij} \cdot 0.001$ and $D_r|_a = 0$, ($m = 1$), with artifacts removed. . . . . 109

4.25 Dispersion curves for the flexural modes of a homogeneous transversely isotropic PZT-4 solid cylinder with $e_{ij} \cdot 0.001$ and $\phi|_a = 0$, ($m = 1$), with artifacts removed. . . . . 110

4.26 Dispersion curves for the flexural modes of a homogeneous transversely isotropic PZT-4 solid cylinder with $e_{ij} \cdot 1$ and $D_r|_a = 0$, ($m = 1$), with artifacts removed.111

4.27 Dispersion curves for the flexural modes of a homogeneous transversely isotropic PZT-4 solid cylinder with $e_{ij} \cdot 1$ and $\phi|_a = 0$, $(m = 1)$, with artifacts removed. 112

# List of Tables

4.1 The material constants for a PZT-4 rod, aluminium, glass/epoxy and cobalt [4]. . . . . 77

# Chapter 1

# Introduction

## 1.1 Elastic Wave Phenomena and Piezoelectricity

Generally, waves can occur whenever a system is disturbed from its equilibrium state and when the disturbance can travel or propagate from one region of the system to another [5]. Waves can be classified into four main groups, namely: mechanical waves, electromagnetic waves, quantum mechanical wave functions and gravitational waves.

Mechanical waves are governed by Newton's laws and require a material medium for their propagation; electromagnetic, quantum mechanical and gravitational waves on the other hand do not require a material medium for their propagation and are based on the laws of electromagnetism (Maxwell's equations), quantum mechanics and the general theory of relativity. In this dissertation we are going to focus on a specific type of mechanical wave known as an elastic wave.

There are four main characteristics common to all kinds of mechanical waves [5, 6]: firstly, the existence of a mechanical wave in a disturbed medium relies on two main properties: inertia and a restoring force, which tends to restore the system to its undisturbed configuration; for the specific case of an elastic wave, it is dependent on the inertia and the elastic restoring

forces of the medium (in other words, inertia and elasticity of the medium). Secondly, the medium itself does not travel through space as the wave propagates; its individual particles undergo back-and-forth motions around their equilibrium positions. Instead, what travels is the overall pattern of the disturbance. Thirdly, mechanical work needs to be done on the system in order to disturb it from equilibrium; the resulting energy gained by the system, is transported by the wave motion from one region of the medium to another. Hence, these waves transport energy but not matter. Finally, the disturbance travels through the medium at a specific speed, which depends on the mechanical properties of the medium. In this dissertation, we study only travelling waves as opposed to standing waves, which do not propagate energy from one region of the medium to the other and result from interference of travelling waves moving in opposite directions in a medium.

We can understand qualitatively the cause of wave propagation in a perfectly elastic solid medium (a medium which returns to its original shape and size, upon removal of the applied forces causing the deformation) if we picture the interatomic forces in the solid as springs (i.e. a three dimensional array of a spring mass system) [5]. To generate an elastic wave in the medium, work has to be done on the material by some external force; the material becomes deformed (we assume that no rigid body motion of the material develops) as the individual atoms and molecules are forced from their equilibrium positions by differing amounts depending on the position of an atom in the system, resulting in an increase in the potential energy of the system. Both the force required to achieve a given deformation and the resulting mechanical displacement depends on the structure and bonding of the material. When the external force is removed, the "spring forces" act as restoring forces which accelerate the atoms back to their equilibrium positions. Nevertheless, maximum kinetic energy is attained at this point, and because of inertia, the atoms then overshoot leading to a reconversion of kinetic energy to potential energy as the material deforms in the opposite direction [7, 5]. Because, the oscillating atoms in the solid are coupled by the "springs", there will be a continuous transfer of energy between atoms (a fundamental behaviour of coupled oscillators) leading to the wave motion [8]. In the study of elastic waves, the elastic

medium is considered as a continuum, rather than a discrete array of atoms as described above [7, 6]. The particles in this case are really infinitesimal elements of the medium made up of many atoms. Thus, the theory of elastic waves deals with macroscopic phenomena [6]. Structure at the microscopic level becomes important only if it affects the macroscopic properties associated with the elastic wave. From here onwards, the use of the word particle should be associated with an infinitesimal element of the medium.

In the preceding paragraph, it is evident that the propagation of elastic waves results in time varying vibrations and deformations in the material medium. Therefore, to describe mathematically the vibrations and hence wave propagation, we need to define quantitatively the particle displacements, material deformation, and the elastic restoring forces together with any other forces associated with the deformations and which influences the dynamics of the system [6].

In a perfectly elastic medium, the particle motions and deformations are defined by the particle displacement and strain fields $u(\boldsymbol{r}, t)$ and $S(\boldsymbol{r}, t)$ (the change in length per unit length) respectively; the strains are defined through the displacement field. The restoring forces acting between neighbouring particles are defined through the stress field $\sigma(\boldsymbol{r}, t)$ (the force per unit area). Moreover, in a freely vibrating elastic medium the stresses are the only forces present. If the body is driven by an external agent, three kinds of excitation forces must be considered: body forces (a force per unit volume acting directly on the particles of the medium; e.g. gravity), body torques (a torque per unit volume acting directly on the particles of the medium; e.g. an electric field applied to a polarized medium) and surface forces acting on the boundary surface of a medium [6]. However, it has been shown that the body torques are balanced by shear stresses on the particles, otherwise there will be an infinite rotational acceleration about the centre of mass of the particle [2, 6]. The effect of body forces and torques is rarely significant and they are often neglected in traditional elastic wave problems.

Having explicitly defined the forces acting on the particles, we can then, via Newton's second

law, relate the acceleration of a particle to the elastic restoring force and the external driving forces (i.e. if applicable to the specific problem we are solving). This then leads to the governing equation of motion describing the wave motion in the medium. Moreover, if we consider only small deformations, then the stress becomes linearly proportional to the strain (where the constant of proportionality is an elastic modulus); a statement of Hooke's law. Consequently, in the absence of external driving forces, the equation of motion for the particles in the medium can be expressed entirely in terms of the displacement field in the medium.

In this dissertation, we will consider the specific case of harmonic waves (a simple case of the general class of periodic waves) where the particles of the medium oscillate with simple harmonic motion about their equilibrium positions; this is valid within the approximations of Hooke's law. This type of wave motion is different from the general case of a pulse; where a particle in the medium is brought back to its equilibrium position after the wave pulse has passed it. Moreover, harmonic waves are easier to analyse and any general disturbance be it periodic or a pulse can be expressed in terms of harmonic waves via Fourier series or Fourier transforms [8, 5]. A general expression for the displacement field of a harmonic travelling wave is

$$\boldsymbol{u}(\boldsymbol{r},t) = \boldsymbol{A}(\boldsymbol{r})e^{i(\omega t+\boldsymbol{k}\cdot\boldsymbol{r})}; \tag{1.1}$$

where $A(\boldsymbol{r})$ is the amplitude of the wave describing the maximum displacement of the particle at position $\boldsymbol{r}$ from the equilibrium position; $\omega = 2\pi f$ is the angular frequency and $f$ is the frequency of the oscillations i.e. the number of oscillations made by a particle in a second as the wave propagates in the medium; $|\boldsymbol{k}| = \frac{2\pi}{\lambda}$ is the wave number and $\lambda$ is the wave length of the wave which gives the distance between successive particles oscillating in phase. The direction of the vector $\boldsymbol{k}$ is the propagation direction of the phase of the wave. It has been shown that when the wavelength approaches the lattice spacing in a crystal lattice the wave then becomes sensitive to the discrete nature of the crystal, so that the continuum approximation then fails to describe the behaviour of the wave in this regime [7, 8]. This will not be of concern here since we will be considering only wavelengths much greater than the

interatomic spacing or characteristic microscale of the medium. The speed of propagation of the phase of the wave or the phase velocity, which is characteristic of all periodic waves [5], is given by:

$$v = \frac{\omega}{|\boldsymbol{k}|}; \tag{1.2}$$

and the group velocity (equal to velocity of propagation of the mechanical energy in a lossless media [9, 1]) is given as

$$v_g = \nabla_{\boldsymbol{k}} \omega(\boldsymbol{k}). \tag{1.3}$$

For a non dispersive elastic medium, the phase velocity $v$ is equal to the group velocity, $v_g$ and can also be expressed as a function of the elastic and inertia parameters of the medium [9, 5] as follows:

$$v = \sqrt{\frac{c}{\rho}}; \tag{1.4}$$

where $c$ is the elastic parameter (e.g. an elastic modulus, tension in a stretched string; both describing the restoring force) and $\rho$ is the inertia parameter (e.g. the density; a measure of the inertia of the medium). If the medium is dispersive or anisotropic, the phase velocity then becomes a function of the angular frequency (wave number) or direction of propagation in the medium respectively [9, 1] and the phase and group velocity are not in general equal. In any medium the relation between the angular frequency and the wave number magnitude is known as the dispersion relation.

If propagation of plane harmonic waves is assumed in an infinite elastic homogeneous, isotropic medium (i.e. properties are the same in every direction and do not vary with position), the particle displacements are given by Eqn.(1.1) except that $A(\boldsymbol{r})$ is now independent of $r$. When this particle displacement expression is substituted into the equation of motion (describing elastic waves); three orthogonal traveling wave solutions are obtained with particle displacements orthogonal to each other [7, 9, 1]. The displacement vector of one of these solutions is polarized (direction of particle displacement) in the direction of the wave vector (direction of propagation of phase of the wave), and it is known as a longitudinal wave mode. The other two modes with polarization of the displacement vectors perpendicular to

the wave vector are known as transverse wave modes and have the same phase velocities. The phase velocity of the longitudinal mode is greater than that of the transverse mode [9, 1]. A similarly assumed harmonic wave solution for an anisotropic medium (i.e. properties are not the same in every direction), leads to the famous Christoffel equations [6] for an anisotropic media (a system of linear homogeneous equation in the particle displacement components). The solution of the Christoffel equations leads as well, to three travelling wave modes with orthogonal particle displacements fields. In this case, the polarizations of the modes are in general not exactly parallel or perpendicular to $\boldsymbol{k}$; so we have one pure or quasi longitudinal mode and two pure or quasi transverse modes. The velocities of the two transverse modes are not in general equal as in the case of an isotropic medium. It is worth mentioning that these modes in an infinite medium are completely decoupled from each other and only interact when they encounter a boundary surface, a consequence of needing to satisfy the physical boundary conditions.

The travelling wave modes in infinite media discussed above are referred to as bulk wave modes; while guided wave modes, which is the subject of this dissertation are modes that require a boundary for their existence, for example Rayleigh waves at surfaces, interfacial waves and Lamb waves in plates [9]. It is worth mentioning that properties of wave propagation in the bulk of a semi-infinite medium (i.e away from the surface) are the same as bulk wave modes. Consequently, for all practical purposes, wave modes in plates can be considered as bulk wave modes in a semi-infinite medium providing the wavelength of excitation is small compared to the dimensions of the structure [9]. So in other words, a bulk wave mode is one that travels in the bulk of the material away from any boundary surface.

Bulk and guided wave modes, though fundamentally different, are governed by the same equations of motion. Mathematically, the difference between them is the absence of boundary conditions to be satisfied by a bulk wave in an infinite medium, whereas guided wave solutions must satisfy certain boundary conditions, since they require a boundary for their existence [9]. Moreover, unlike the finite number of modes that are solutions to a bulk wave problem

(i.e. longitudinal and transverse wave modes), there exist an infinite number of modes in the solution of certain guided wave problems; for example, in a plate and a rod (that is a finite body can support an infinite number of guided wave modes) [9]. Basically, guided waves in structures like plates (Lamb waves) and rods result from the superposition of the fundamental longitudinal and transverse wave modes in infinite media as they become coupled at the boundary surface, followed by interference as they propagate within the rod or plate [10, 9].

So far in the discussion on elastic wave phenomena, the only fundamental physical variables needed for its description are purely mechanical i.e. the displacement, strain and the stress field plus an external driving agent in the case of a driven system. If the material possesses the additional property of piezoelectricity, then electrical parameters, like the electric field and the electric displacement then enter into the analysis for the propagation of elastic wave in the material. By definition, a piezoelectric material (which is inherently anisotropic) is one exhibiting two main characteristics [3]:

- When subjected to a mechanical stimulus (e.g. a pressure wave or bending stress) a piezoelectric material will develop an electric field within it.
- The effect is reversible, i.e. the application of an electric field across the material results in mechanical strain.

A basic requirement for a material to be piezoelectric is the lack of a centre of symmetry in the material [2, 6]. Consequently, only materials belonging to specific crystal classes demonstrate the piezoelectric effect (i.e. all those lacking inversion symmetry with the exception of the class 432). Examples of piezoelectric materials include quartz, rochelle salt, barium titanate, ammonium dihydrogen, and lead zirconium titanate (PZT) [3] etc. Because of the above mentioned characteristics, materials exhibiting piezoelectric effect are used extensively in modern technology as transducers; for example, in microphones, and vibrating-sensing elements for converting a mechanical strain into an electrical signal; and

in sonic and ultrasonic transducers, headphones, loudspeakers in which a mechanical output is derived from and electrical signal input; just to mention a few [3].

The coupling between mechanical and electric variables in piezoelectric material alters the dynamics of a piezoelectric material during the propagation of a wave in the material. For example, the presence of a strain field in an elastic piezoelectric material generates an electric field in the material; this electric field in turn alters the strain and stress fields. As a result, the stress field that enters the dynamical equation describing the elastic wave is changed, leading to a modification of the wave modes propagating in a piezoelectric material [11, 6].

Now, that we have given an overview of the concept of wave phenomena and the related effect of piezoelectricity, the interesting question is what has been done so far with regards to analytic solutions to the wave equation for guided waves in rods and specifically piezoelectric rods? (this is the subject of this dissertation).

The problem of wave propagation in systems with cylindrical geometry has been analysed by a number of investigators. While the systems considered so far have been both isotropic and anisotropic in nature, a relatively larger literature exists for isotropic materials. The first investigator of waves in a solid cylinder was Pochhammer in 1876, who provided an exact solution for the propagation of free waves in an isotropic solid cylinder [9]; Other investigators on the subject can be found in standard texts such as Achenbach [12], Graff [13], and Rose [9]. For cylinders composed of anisotropic material, Cree [14] may have been the first investigator of axisymmetric waves in an anisotropic bar. Much later, Mirsky [15] investigated the more general problem of non-axisymmetric wave propagation in traversely isotropic circular hollow and solid cylinders. Other contributors to the subject are Berliner and Solecki [14], Honarvar et al [4], Frazer [16], Armenakas and Reitz [17]; just to name a few.

In the above mentioned investigations, no piezoelectric effect was included. Perhaps because it was thought that cylindrical geometry including piezoelectric effect, leads to intractable algebraic complications in attempting to obtain exact solutions [10]. However, there exist

some literature on the subject, though little that deals with exact and approximate solutions of waves in piezoelectric rods. For example, Paul [18] examined vibrations of circular cylindrical shells, Winkel et al [19] solved the problem of waves in a single infinite clad rod, Nayfeh et al [10] analysed waves in layered piezoelectric rods and their composites and Wei et al [20] examined the propagation of waves in a piezoelectric rod of 6mm symmetry. It should be noted that all the above researchers have considered only axisymmetric waves.

So, following from what has been done so far in the subject, we proceed in this dissertation to solve the problem of non-axisymmetric waves in piezoelectric cylinders of transversely isotropic material. We make use of the continuum theory of elasticity and linear eletromechanical coupling of the electric and elastic variables. Our approach parallels that of Mirsky [15] and Berliner and Solecki [14]. The 3-dimensional equations of elastodynamics together with Gauss' law are solved in terms of four displacement and three electric potentials, each satisfying the Helmholtz's equation as opposed to three displacement potentials in the case of Mirsky and Berliner, who did not take into account piezoelectricity. Imposing the allowed mechanical and electrical boundary conditions satisfied by the proposed solution on the surface of the cylinder, leads to the characteristic or dispersion equation (i.e. equation expressing the functional relationship between $\omega$ and $|\boldsymbol{k}|$) in determinantal form of the fourth order. We then proceed to obtain numerical solutions of the characteristic equation for a sample material i.e. PZT-4, followed by a plot of dispersion curves describing the propagating non-axisymmetric modes in the solid cylinder.

Studying the propagation of non-axisymmetric modes in a piezoelectric rod can find application in ultrasonic non-destructive evaluation (NDE) for defect characterisation and sizing studies [9] in rods. This is because, reflected echoes from defects in rod are generally non-axisymmetric in nature; thus, understanding the physical characteristics of these modes is required for these kind of applications. Moreover, a wave structure analysis (i.e. studying how the displacement, stress, and energy vary across the thickness of the rod [9, 21]) carried out on the wave modes, can guide us in the selection of modes in applications involving wa-

ter loading to minimise energy leakage; for example selecting a mode which has very small radial component of displacement on the surface of a rod will minimise energy loss to the surrounding water.

## 1.2 Preview

We start off in chapter 2 by discussing the concepts of elastodynamics and piezoelectricity, in which fundamental topics like strain, stress, Hooke's law, Navier's governing wave equation and quasistatic approximation (in a piezoelectric material) are presented. A good understanding of these concepts is necessary for the study of elastic waves in piezoelectric materials. Then in chapter 3, we make use of the fundamental equations developed in chapter 2 to derive the equations of motion for a homogeneous, piezoelectric solid cylinder of transversely isotropic material and the associated physical boundary conditions. We will accomplish this via two methods: firstly, by making use of Navier's dynamical equations, Gauss's law and the constitutive equations for the material and secondly, through the more elegant Hamilton's variational principle which also leads to the allowed boundary conditions of the system. We then in chapter 4, present analytic solutions to the equations of motion developed in chapter 3 by making use of four displacement and three electric potentials. We also present the characteristic equation in determinantal form, which results from the application of the allowed physical boundary conditions derived in chapter 3. In order to test the correctness of our model, we also develop the characteristic equation for the simpler problem of non-axisymmetrical wave propagation in a solid cylinder possessing transversely isotropic symmetry already solved by Mirsky [15] , Berliner et al [14] and Honarvar et al [4]. Lastly, in that chapter we present numerical results for the already derived characteristic equations through dispersion curves for the piezoelectric and non-piezoelectric models using the following sample materials: PZT-4 rod, and aluminium(isotropic), cobalt, glass/epoxi fiber-reinforced composite and PZT-4 (with electromechanical coupling absent) cylinders respectively. Finally, in chapter 5 we give a summary of what has been accomplished and

possible future problems which are based on the work in this dissertation.

# Chapter 2

# Elastodynamics and Piezoelectricity

## 2.1 Introduction

In elastodynamics, we are concerned with the dynamical behaviour of elastic bodies resulting from an imbalance of forces in an infinitesimal element of the material; which results in accelerations of the element [2]. In the absence of dissipative mechanisms, the energy is conserved through the elastic and inertia properties of the material. The concepts at the heart of linear elastodynamics are: strain, stress and Hooke's law [1] from which we are able to develop the equations of motion for an elastic material; known as the Navier's wave equation.

Moreover, in certain dielectric materials, the elastic variables of stress and strain become coupled with electric variables, such as the electric field and electric displacement vector. For example, an applied electric field in such a material results in a strain and a reversal in the direction of the field reverses the strain. As a result, the elastodynamic equations of motion become modified; this phenomenon is referred to as piezoelectricity [11].

Therefore, in this section we begin by describing the concepts of strain, stress, Hooke's law, Voigt notation (to simplify operations involving crystal properties), and elastic potential en-

ergy due to elastic deformations; followed by the development of the Navier's wave equation; after which we discuss the concept of piezoelectricity. We will also consider the effect of crystal symmetry on the physical properties of a crystal, for example elastic constants; and examine briefly the role of thermal energy in solving elastodynamic problems. Lastly, we give a short discussion on the microscopic origin of elasticity, piezoelectricity and thermal expansion. The derivations in this section will be purely in the Cartesian coordinate system. A good treatment of the fundamental concepts in elastodynamics can be found in the following texts [2], [6], [22] and [1]; and the discussions below are based heavily on these texts.

## 2.2 Strain

Whenever forces are exerted on a real elastic body, it undergoes deformations in the form of a change of shape or volume. In discussing deformations of real bodies we make the following assumptions [22, 1]:

1. Rigid body motions do not constitute deformation of the body
2. Only small deformations and displacements are considered; such as those permitted by the linear theory of elasticity. Also, we assume a continuous variation of the displacement over the volume of the body.

Lets consider an arbitrary point $\boldsymbol{p}$ in the body. In its undeformed configuration, the position vector of point $\boldsymbol{p}$ is $\boldsymbol{x}$ with respect to some Cartesian axes. After a deformation, point $\boldsymbol{p}$ is displaced to a new point with position vector $\boldsymbol{X}$. Hence, the displacement of point $\boldsymbol{p}$ is

$$\boldsymbol{u}(\boldsymbol{x}) = \boldsymbol{X}(\boldsymbol{x}) - \boldsymbol{x}. \tag{2.1}$$

For a distortion to occur, the distance between point $\boldsymbol{p}$ and a neighbouring point say $\boldsymbol{p}'$ at $\boldsymbol{x} + \delta\boldsymbol{x}$ should change after the deformation [6, 1]. Let the square of distance between the

points $\boldsymbol{p}$ and $\boldsymbol{p}'$ before and after the deformation be $\delta l^2$ and $\delta L^2$ respectively; expressed as

$$\begin{aligned}\delta l^2 &= |\boldsymbol{x} + \delta\boldsymbol{x} - \boldsymbol{x}|^2 \\ &= \delta x_1^2 + \delta x_2^2 + \delta x_3^2 \end{aligned} \tag{2.2}$$

and

$$\delta L^2 = |\boldsymbol{X}(\boldsymbol{x} + \boldsymbol{\delta x}) - \boldsymbol{X}(\boldsymbol{x})|^2. \tag{2.3}$$

$\boldsymbol{X}(\boldsymbol{x})$ in Eqn.(2.1) is clearly a continuous function of $\boldsymbol{x}$, since we have assumed that the displacement field is continuous. Therefore, we can expand $\boldsymbol{X}$ in a Taylor series about $\boldsymbol{p}$ [1]; so that we have

$$\boldsymbol{X}(\boldsymbol{x} + \boldsymbol{\delta x}) - \boldsymbol{X}(\boldsymbol{x}) = \delta x_i \frac{\partial \boldsymbol{X}}{\partial x_i}. \tag{2.4}$$

Where we make little error in discarding higher order terms; $i = 1, 2, 3$ and we make use of the Einstein summation convention. Eqn.(2.4) can further be expanded as

$$\boldsymbol{X}(\boldsymbol{x} + \boldsymbol{\delta x}) - \boldsymbol{X}(\boldsymbol{x}) = \delta x_i \frac{\partial X_1}{\partial x_i}\hat{i} + \delta x_i \frac{\partial X_2}{\partial x_i}\hat{j} + \delta x_i \frac{\partial X_3}{\partial x_i}\hat{k}. \tag{2.5}$$

Therefore,

$$\begin{aligned}\delta L^2 &= |\boldsymbol{X}(\boldsymbol{x} + \boldsymbol{\delta x}) - \boldsymbol{X}(\boldsymbol{x})|^2 \\ &= \left(\delta x_i \frac{\partial X_1}{\partial x_i}\right)^2 + \left(\delta x_i \frac{\partial X_2}{\partial x_i}\right)^2 + \left(\delta x_i \frac{\partial X_3}{\partial x_i}\right)^2;\end{aligned}$$

which can be expressed simply as

$$\delta L^2 = \frac{\partial X_k}{\partial x_i}\frac{\partial X_k}{\partial x_j}\delta x_i \delta x_j.$$

So, the change in the square of the separation becomes

$$\begin{aligned}\delta L^2 - \delta l^2 &= \frac{\partial X_k}{\partial x_i}\frac{\partial X_k}{\partial x_j}\delta x_i \delta x_j - \delta x_i \delta x_i \\ &= \frac{\partial X_k}{\partial x_i}\frac{\partial X_k}{\partial x_j}\delta x_i \delta x_j - \delta x_i \delta x_j \delta_{ij} \\ &= \left(\frac{\partial X_k}{\partial x_i}\frac{\partial X_k}{\partial x_j} - \delta_{ij}\right)\delta x_i \delta x_j \\ &= 2\eta_{ij}\delta x_i \delta x_j.\end{aligned}$$

where

$$\eta_{ij} = \frac{1}{2}\left(\frac{\partial X_k}{\partial x_i}\frac{\partial X_k}{\partial x_j} - \delta_{ij}\right). \tag{2.6}$$

$\eta_{ij}$ is called the Langrangian strain [1] and $\delta_{ij}$ is the kronecker delta. Eqn.(2.6) can further be simplified as follows:

From Eqn.(2.1), we have

$$X_k = u_k + x_k. \tag{2.7}$$

This implies that

$$\begin{aligned}
\eta_{ij} &= \frac{1}{2}\left(\frac{\partial X_k}{\partial x_i}\frac{\partial X_k}{\partial x_j} - \delta_{ij}\right) \\
&= \frac{1}{2}\left(\left(\frac{\partial u_k}{\partial x_i} + \frac{\partial x_k}{\partial x_i}\right)\left(\frac{\partial u_k}{\partial x_j} + \frac{\partial x_k}{\partial x_j}\right) - \delta_{ij}\right) \\
&= \frac{1}{2}\left(\left(\frac{\partial u_k}{\partial x_i} + \delta_{ki}\right)\left(\frac{\partial u_k}{\partial x_j} + \delta_{kj}\right) - \delta_{ij}\right) \\
&= \frac{1}{2}\left(\frac{\partial u_k}{\partial x_i}\frac{\partial u_k}{\partial x_j} + \frac{\partial u_k}{\partial x_i}\delta_{kj} + \frac{\partial u_k}{\partial x_j}\delta_{ki} + \delta_{ki}\delta_{kj} - \delta_{ij}\right) \\
&= \frac{1}{2}\left(\frac{\partial u_k}{\partial x_i}\frac{\partial u_k}{\partial x_j} + \frac{\partial u_j}{\partial x_i} + \frac{\partial u_i}{\partial x_j}\right).
\end{aligned} \tag{2.8}$$

For small deformations and hence small displacement gradients (i.e. $|\frac{\partial u_i}{\partial x_j}| << 1$), the product terms can be dropped i.e

$$\frac{\partial u_k}{\partial x_i}\frac{\partial u_k}{\partial x_j} \approx 0.$$

and $\eta_{ij}$ reduces to $S_{ij}$, i.e.

$$\eta_{ij} \approx S_{ij} = \frac{1}{2}\left(\frac{\partial u_i}{\partial x_j} + \frac{\partial u_j}{\partial x_i}\right); \tag{2.9}$$

where $S_{ij}$ is known as the infinitesimal strain. It is obvious from Eqn.(2.6) that the nine components $\eta_{ij}$ and hence $S_{ij}$ constitute a second- rank tensor called the strain tensor; since they relate linearly the components of a second rank tensor $\delta x_i \delta x_j$ and a zero-rank tensor $\delta L^2 - \delta l^2$ [2]. Also, from Eqn.(2.9) we observe that $S_{ij} = S_{ji}$; hence, $S_{ij}$ is a symmetric tensor and requires only six independent components for its specification.

The strain tensor, $S_{ij}$ can also be represented in matrix form as follows [6]:

$$S = \frac{1}{2}\left([\mathcal{E}] + [\tilde{\mathcal{E}}]\right); \tag{2.10}$$

where $[\mathcal{E}]$ and $[\tilde{\mathcal{E}}]$ are the matrix representations of the displacement gradient tensor $\mathcal{E}_{ij}$ and its transpose respectively. $\mathcal{E}_{ij}$ is defined as

$$\mathcal{E}_{ij} = \frac{\partial u_i}{\partial x_j}; \tag{2.11}$$

and it connects the differential displacement $\mathrm{d}\boldsymbol{u}$ for any two neighbouring particles in the deformed body to their equilibrium displacement $\mathrm{d}\boldsymbol{x}$; i.e.

$$\mathrm{d}u_i = \mathcal{E}_{ij}\mathrm{d}x_j. \tag{2.12}$$

In matrix form Eqn.(2.12) is expressed as follows [6]:

$$\begin{bmatrix} \mathrm{d}u_1 \\ \mathrm{d}u_2 \\ \mathrm{d}u_3 \end{bmatrix} = \begin{bmatrix} \frac{\partial u_1}{\partial x_1} & \frac{\partial u_1}{\partial x_2} & \frac{\partial u_1}{\partial x_3} \\ \frac{\partial u_2}{\partial x_1} & \frac{\partial u_2}{\partial x_2} & \frac{\partial u_2}{\partial x_3} \\ \frac{\partial u_3}{\partial x_1} & \frac{\partial u_3}{\partial x_1} & \frac{\partial u_3}{\partial x_1} \end{bmatrix} \begin{bmatrix} \mathrm{d}x_1 \\ \mathrm{d}x_2 \\ \mathrm{d}x_3 \end{bmatrix}, \tag{2.13}$$

and

$$[\mathcal{E}] = \begin{bmatrix} \frac{\partial u_1}{\partial x_1} & \frac{\partial u_1}{\partial x_2} & \frac{\partial u_1}{\partial x_3} \\ \frac{\partial u_2}{\partial x_1} & \frac{\partial u_2}{\partial x_2} & \frac{\partial u_2}{\partial x_3} \\ \frac{\partial u_3}{\partial x_1} & \frac{\partial u_3}{\partial x_1} & \frac{\partial u_3}{\partial x_1} \end{bmatrix}. \tag{2.14}$$

From matrix algebra Eqn.(2.10) is the symmetric part of the matrix $[\mathcal{E}]$ [6]. Hence, in the approximation of small displacements the strain tensor is the symmetric part of the displacement gradient tensor. We will make use of Eqn.(2.10) to develop the strain-displacement relations in cylindrical coordinates in the next chapter.

The meaning of the strain components are illustrated with the help of Fig.(2.1). The components $S_{ii}$, as shown in Fig.(2.1 (a)); corresponds to a change in length per unit length in the $x_1, x_2$ and $x_3$ directions. These are by definition equal to the engineering tensile strains. The off diagonal components for example, $S_{12}$ shown in Fig.(2.1 (b)), correspond to a unit shear distortion; which reduces the angle between two perpendicular planes e.g $x_1x_3$ and

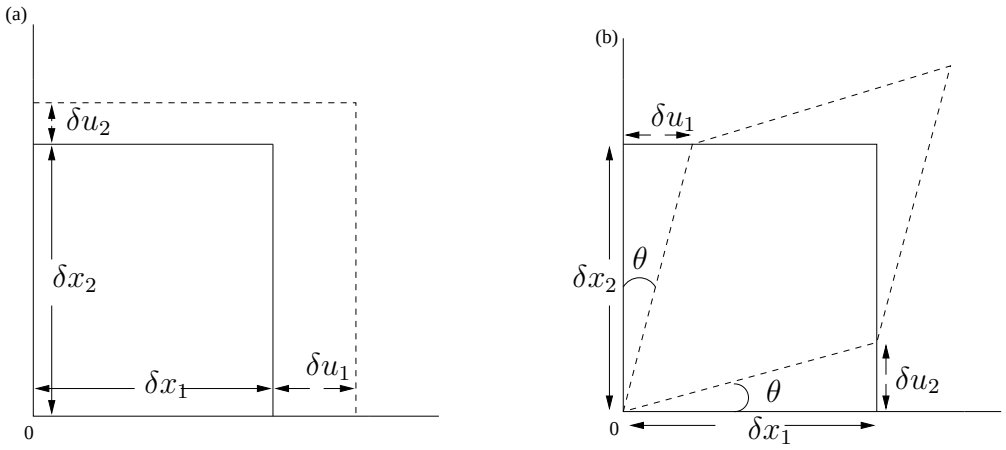


Figure 2.1: (a) Tensile strains $S_{11}$ and $S_{22}$. (b) Shear strains $S_{12}$ and $S_{21}$ [1]

$x_2x_3$ shown in Fig.(2.1 (b)) by $2\theta = 2S_{12}$. The engineering shear strain, $\gamma_{12}$, by definition is $\gamma_{12} = 2S_{12}$; which is just the reduction in angle [1, 2, 22].

It is worth noting that, the strain tensor as defined in Eqn.(2.9) is a field tensor i.e. can vary from point to point in a body (homogeneous or inhomogeneous) and also depends on time; analogous to an applied electric field. This is different from a material tensor (e.g the electric permittivity ), which is constant for a given homogeneous material and whose form is restricted by the inherent symmetry of the material [1, 2].

Also, given the six independent components of $S_{ij}$, we can obtain the elongation of a linear element in any given direction and the deformation in the angle between any two of such elements is as follows [22]

$$\begin{aligned} S &= S_{xx}l^2 + S_{yy}m^2 + S_{zz}n^2 + S_{xy}lm + S_{xz}ln + S_{xy}mn \\ S' &= S_{xx}l'^2 + S_{yy}m'^2 + S_{zz}n'^2 + S_{xy}l'm' + S_{xz}l'n' + S_{xy}m'n' \\ \cos(rr') &= (ll' + mm' + nn')\,(1 - S - S') + 2\,(S_{xx}ll' + S_{yy}mm' + S_{zz}nn') \\ &\quad S_{yz}\,(mn' + m'n) + S_{xz}\,(nl' + n'l) + S_{xy}\,(lm' + l'm)\,. \end{aligned} \tag{2.15}$$

Where $S$ and $S'$ are the unit elongations of linear elements with direction cosines $(l, m, n)$ and $(l', m'n')$ respectively, and $\cos(rr')$ represents the cosine of the angle between the two elements after deformation.

In summary, the strain tensor $S_{ij}$, is a symmetric 2-rank tensor field, which describes the deformations due to applied stresses in a continuous body. In the next chapter, we will express the strain tensor in terms of displacements in cylindrical coordinates; as derived in standard elasticity textbooks.

## 2.3 Stress

A body is said to be in a state of "stress" whenever one part of the body exerts forces on adjacent parts of the body; and vice versa. for example, when a body responds and reacts to external forces applied on it [2]. The strength of the forces acting in a body can be characterised in terms of a "stress"; which is the force per unit area acting on the surface of an infinitesimal element in the body due to adjacent elements; and it is short range. There can also be a body force, which is the force per unit volume acting throughout the body on all its elements and it is a long range force; for example, gravity etc [6, 2].

To accurately describe the state of stress in a real 3-dimensional stressed body, we need to define a "stress tensor" at each point of the body. To do this, lets consider an infinitesimal cube in a given body centered at the origin of a Cartesian coordinate system; with sides parallel to the axis as shown in Fig.(2.2). Lets further, for the moment, make the following assumptions [2]:

1. The state of stress in the body is homogeneous.
2. The cube is in static equilibrium.
3. No body forces or torques are present.

Without loss of generality, lets assume that the components of the forces per unit area acting across three planes of the cube, due to the surrounding material is as shown in Fig.(2.2). The forces on the remaining three planes not indicated are just equal and opposite to those

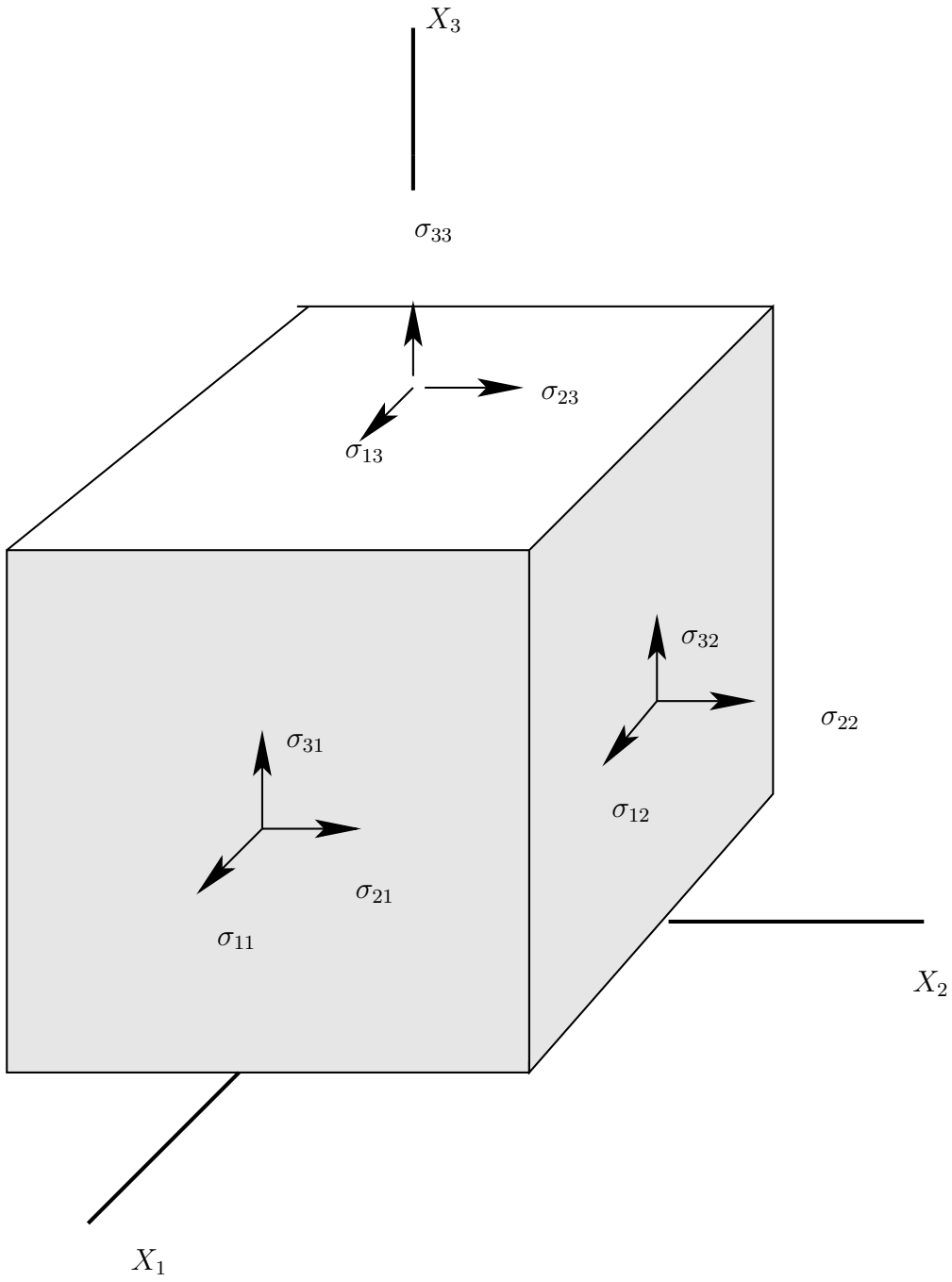


Figure 2.2: An infinitesimal cube surrounding point O showing stress components

of their opposite planes, since the state of stress is homogeneous [2]. The nine quantities [1]

$$\sigma_{ij} = \lim_{\delta A \to 0} \frac{\delta F^j{}_i}{\delta A} \quad i, j = 1, 2, 3; \tag{2.16}$$

where $\delta F_i^j$ is the $i$'th component of the force acting across the surface, with area $\delta A$ and with unit normal parallel to the $x_j$ direction, constitute the Cauchy stress tensor $\sigma_{ij}$ and completely specifies the state of stress in a given continuous body. The three diagonal components $\sigma_{ii}$, are called the normal stress components; with positive and negative $\sigma_{ii}$ being respectively tensile and compressional stresses, and the remaining six off-diagonal components $\sigma_{ij}$, $i \neq j$ are the shear components; with a positive and negative $\sigma_{ij}$ referring to a tendency for the component to rotate the cube anti-clockwise or clockwise.

Further restrictions are imposed on the stress tensor if static equilibrium of the cube is considered; where for moment balance $\sigma_{ij} = \sigma_{ji}$, implying that the stress tensor is symmetric and only six components are needed for its specification [2, 1]. Since the stress tensor is symmetric it can be referred to its principal axes, where $\sigma_{ij} = 0$ for $i \neq j$ and the $\sigma_{ii}$'s are referred to as principal stresses. With the above definition of the stress tensor, it is possible to obtain the force acting across any plane of arbitrary orientation that passes through the origin, using [22]

$$F_i = \sigma_{ij} n_j; \tag{2.17}$$

where $n_j$ are the direction cosines for the normal to the plane and $F_i$ are the components of the force on the plane. Eqn.(2.17) can be used to justify the assertion that the $\sigma_{ij}$'s constitute a 2-rank tensor, since they relate linearly the components of an area vector $n_j$ and a resultant force $F_i$ and thus obeys a tensor transformation law. Moreover, the stress tensor is a field tensor just as the strain tensor [2].

In summary, the stress tensor is a 2-rank symmetric tensor; which enables us to describe the distribution of forces acting on the surfaces of infinitesimal elements within a stressed body. It is worth noting that these mentioned characteristics of the stress tensor still hold, even when the assumptions of homogeneity, static equilibrium and absence of body forces

are removed as will be shown later when we derive the equations of motion in a continuous body. Break down of its symmetry will occur only in the presence of body torques [6, 2].

## 2.4 Hooke's Law

A solid body becomes strained, when subjected to stress. Provided the stress is below a certain limiting value, the elastic limit, the strains disappear when the stresses are removed and the solid is back to its original shape. Moreover, when the stresses and strains are small enough, we often find that the two are linearly related and the constant of proportionality is called an elastic modulus [5, 2]. This linear relation of stress and strain is called Hooke's law. The constitutive relation, expressing Hooke's law is [1, 2]

$$\sigma_{ij} = c_{ijkl} S_{kl}; \tag{2.18}$$

which upon inverting we obtain

$$S_{ij} = s_{ijkl} \sigma_{kl}. \tag{2.19}$$

The 81 $c_{ijkl}$ components are called the elastic stiffnesses of the material and are a measure of the resistance of the material to elastic deformation, and the $s_{ijkl}$ components are the elastic compliances and are a measure of the ease of deformation. From Eqn.(2.18) and (2.19), it is clear that the elastic stiffness and compliances form 4-rank material tensors that are inverses of each other [1]; i.e.

$$s_{ijkl} c_{klmn} = \delta_{im} \delta_{jn}. \tag{2.20}$$

Because there are only 6 independent components of stress and strain, it follows from Eqns.(2.18) and (2.19), that there are a maximum of 36 independent components of the elastic stiffness and compliance tensors i.e.

$$\begin{array}{rcccccl} c_{klmn} & = & c_{lkmn} & = & c_{klnm} & = & c_{lknm} \\ s_{klmn} & = & s_{lkmn} & = & s_{klnm} & = & s_{lknm} \end{array} \quad \text{and} \quad . \tag{2.21}$$

We will show in section(2.6), that they are further reduced to 21.

## 2.5 Voigt Contracted Notation

The stress, strain, elastic stiffness and compliance so far have been represented in full tensor subscript notation. But calculations involving these quantities are greatly simplified when the number of subscripts is reduced by making use of the Voigt contracted notation [1]. In the Voigt notation a pair of indices $ij$ is replaced with a single index $\alpha$ running from 1 to 6 as follows:

$$11 \rightarrow 1, \quad 22 \rightarrow 2, \quad 33 \rightarrow 3, \quad 23 \equiv 32 \rightarrow 4, \quad 31 \equiv 13 \rightarrow 5, \quad 12 \equiv 21 \rightarrow 6. \tag{2.22}$$

The correspondence between the tensor and reduced subscript representation is as follows:

$$S_{ij} \rightarrow n_\epsilon S_\alpha, \quad \sigma_{kl} \rightarrow \sigma_\beta, \quad c_{ijkl} \rightarrow c_{\alpha\beta}, \quad s_{ijkl} \rightarrow n_s s_{\alpha\beta}, \quad e_{ijk} \rightarrow n_f e_{i\alpha}; \tag{2.23}$$

where, $n_\epsilon = \frac{1}{2}$ if $\alpha > 3$, and is unity otherwise; $n_s = \frac{1}{4}$ if both $\alpha$ and $\beta > 3$, $n_s = \frac{1}{2}$ if either $\alpha$ or $\beta > 3$ and is unity otherwise [1]; and $e_{ijk}$ are the piezoelectric stress constants, which will be introduced in section (2.8); $n_f = \frac{1}{2}$ if $\alpha > 3$ and is otherwise unity [2].

In this reduced notation, the elastic stiffness, compliance and piezoelectric stress tensors can be represented in matrix form [2]; for example, the stress-strain relationship can be expressed as $\sigma = c\epsilon$, where $\sigma$ is a $6 \times 1$ matrix, c is $6 \times 6$, and $\epsilon$ is $6 \times 1$ [9]. However, the components in their reduced subscript notation do not constitute tensors; i.e. do not transform as tensors [2, 6].

## 2.6 Energy of a Strained Crystal

When a crystal is deformed elastically, work $W$ is done on the crystal which is stored as elastic potential energy [1, 2]. We derive below the expression for the elastic potential energy per unit volume due to strains resulting from applied stresses on the surface of the crystal. let's consider the cube of unit volume having same configuration as the cube in Fig.(2.2). Suppose that the strain component $S_1$ is increased to $S_1 + \mathrm{d}S_1$, while the other strain components

remain unchanged. The two faces perpendicular to $0x_1$ will move outwards by amounts $\frac{1}{2}\mathrm{d}S_1$, while the other four plane faces just get enlarged with the position of their centres fixed; so that the work done on these four faces is zero. Therefore, the work done by the normal stress components on the faces perpendicular to $0x_1$ is given by $2\sigma_1.\frac{1}{2}\mathrm{d}S_1 = \sigma_1\mathrm{d}S_1$. Similar expressions can be obtained for the strain components $S_2$ and $S_3$, respectively.

Now let's suppose that the cube is sheared by making the two faces perpendicular to $0x_2$ move in opposite directions parallel to $0x_3$, so that the strain component $S_4$ is increased to $S_4 + \mathrm{d}S_4$. For small strains and cube with sides of unit length, the centres of the faces perpendicular to $0x_2$ each move a distance $\frac{1}{2}\mathrm{d}S_4$. So, the work done by the component of stress $\sigma_4$ on these faces is $2\sigma_4.\frac{1}{2}\mathrm{d}S_4 = \sigma_4\mathrm{d}S_4$. The expressions for the work done due to the strain components $S_5$ and $S_6$ are obtained in a similar way. So, for a situation in which all the strain components are present, we have

$$\mathrm{d}W = \sigma_\alpha \mathrm{d}S_\alpha \quad (\alpha = 1, 2, ..., 6). \tag{2.24}$$

By making use of Hooke's law, Eqn.(2.24) becomes

$$\mathrm{d}W = c_{\alpha\beta}S_\beta \mathrm{d}S_\alpha \quad (\alpha, \beta = 1, 2, ..., 6). \tag{2.25}$$

On integrating, Eqn.(2.25) from an initial unstrained state of the cube to the final state $S_\alpha$; the work done per unit volume is

$$W = \int c_{\alpha\beta}S_\beta \mathrm{d}S_\alpha = \frac{1}{2}c_{\alpha\beta}S_\beta S_\alpha \quad (\alpha, \beta = 1, 2, ..., 6). \tag{2.26}$$

This work is stored as recoverable elastic potential energy $U$ per unit volume i.e.

$$U = \frac{1}{2}c_{\alpha\beta}S_\beta S_\alpha \quad (\alpha, \beta = 1, 2, ..., 6). \tag{2.27}$$

From Eqn.(2.27), the stress $\sigma_\alpha$ and the elastic stiffness $c_{\alpha\beta}$ is given by the first and second derivative of $U$ with respect to the strains $S_\alpha$ and $S_\beta$ respectively, i.e.

$$\sigma_\alpha = \frac{\partial U}{\partial S_\alpha}, \tag{2.28}$$

$$c_{\alpha\beta} = \frac{\partial}{\partial S_\beta}\left(\frac{\partial U}{\partial S_\alpha}\right). \tag{2.29}$$

From Eqn.(2.29), we observe that the order of the derivative is immaterial (because $U$, $\sigma_i$'s and $c_{ij}$'s are assumed to be continuous in the material); therefore,

$$c_{\alpha\beta} = c_{\beta\alpha}. \tag{2.30}$$

It is evident from Eqn.(2.30), that the elastic stiffness matrix is symmetrical about the diagonal. Consequently, there can be at most 21 (instead of 36) independent matrix elastic constants $c_{\alpha\beta}$, necessary to describe the most general anisotropic material. The presence of symmetry in a crystal, leads to further reduction in the number of independent elastic stiffness matrix constants; this effect will be discussed further in the section(2.9). It follows from the relationship between the $s_{\alpha\beta}$'s and $c_{\alpha\beta}$'s that

$$s_{\alpha\beta} = s_{\beta\alpha}. \tag{2.31}$$

## 2.7 Navier's Wave Equation

In this section, we derive the wave equation for an ideal elastic medium; also known as the Navier's wave equation as derived in [2]. To accomplish this, we consider the response of a continuous body to a non uniform distributed stress field, and a uniform distribution of body forces and torques; which when applied to the specific case of an ideal elastic medium, leads to Navier's equation.

Intuitively, from Newton's second law, we should expect a linear plus an angular acceleration for any infinitesimal element in our medium of interest. However, we will show that only linear accelerations are possible for such an element (as before we do not consider rigid body translations and rotations).

### 2.7.1 Translational Equation of Motion

Let's consider the rectangular infinitesimal element shown in Fig.(2.3) centered at the origin of the coordinate system; with edges parallel to the $0x_i\,(i = 1, 2, 3)$ axes and of lengths $\delta x_1$,

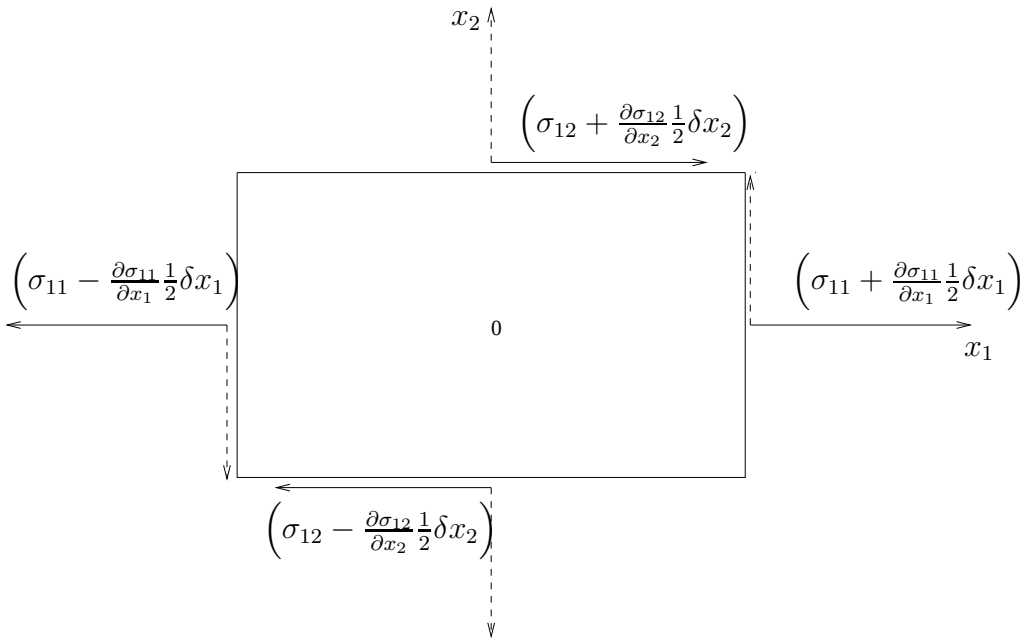


Figure 2.3: A rectangular infinitesimal element acted on by inhomogeneous stresses [2]

$\delta x_2$, $\delta x_3$ [2]. Lets obtain the equation of motion in the $0x_1$ direction given that the stress at the centre is $\sigma_{11}$; and for simplicity let the average stresses on the two faces perpendicular to $0x_1$ and $0x_2$ be as indicated in Fig.(2.3).

Thus, the resultant force in the $0x_1$ direction, acting on the faces normal to $0x_1$ is

$$-\left(\sigma_{11} - \frac{\partial\sigma_{11}}{\partial x_1}\frac{1}{2}\delta x_1\right)\delta x_2\delta x_3 + \left(\sigma_{11} + \frac{\partial\sigma_{11}}{\partial x_1}\frac{1}{2}\delta x_1\right)\delta x_2\delta x_3 = \frac{\partial\sigma_{11}}{\partial x_1}\delta x_1\delta x_2\delta x_3.$$

Following the same argument for the faces normal to $0x_2$ and $0x_3$, the resultant forces in the $0x_1$ direction are respectively:

$$\frac{\partial\sigma_{12}}{\partial x_2}\delta x_1\delta x_2\delta x_3 \quad \text{and} \quad \frac{\partial\sigma_{13}}{\partial x_3}\delta x_1\delta x_2\delta x_3.$$

Let's suppose the presence of a body force, with component $F_1$, in the $0x_1$ direction. Therefore, the equation of motion in the $0x_1$ direction becomes

$$\frac{\partial\sigma_{11}}{\partial x_1}\delta x_1\delta x_2\delta x_3 + \frac{\partial\sigma_{12}}{\partial x_2}\delta x_1\delta x_2\delta x_3 + \frac{\partial\sigma_{13}}{\partial x_3}\delta x_1\delta x_2\delta x_3 + F_1\delta x_1\delta x_2\delta x_3 = m\ddot{u}_1. \tag{2.32}$$

Dividing Eq.(2.32) by $\delta x_1 \delta x_2 \delta x_3$, we obtain finally

$$\frac{\partial \sigma_{11}}{\partial x_1} + \frac{\partial \sigma_{12}}{\partial x_2} + \frac{\partial \sigma_{13}}{\partial x_3} + F_1 = \rho \ddot{u}_1. \tag{2.33}$$

where $\rho$ is the mass density. Similarly, the equation of motion in the $0x_2$ and $0x_3$ directions are respectively

$$\frac{\partial \sigma_{21}}{\partial x_1} + \frac{\partial \sigma_{22}}{\partial x_2} + \frac{\partial \sigma_{23}}{\partial x_3} + F_2 = \rho \ddot{u}_2, \tag{2.34}$$

$$\frac{\partial \sigma_{31}}{\partial x_1} + \frac{\partial \sigma_{32}}{\partial x_2} + \frac{\partial \sigma_{33}}{\partial x_3} + F_3 = \rho \ddot{u}_3. \tag{2.35}$$

The three equations derived above can be expressed via a single equation, using the subscript summation convention as follows:

$$\frac{\partial \sigma_{ij}}{\partial x_j} + F_i = \rho \ddot{u}_i. \tag{2.36}$$

Eq.(2.36) is the translational equation of motion for an infinitesimal element in a continuous body. Due to deformations, the element's volume changes; leading to first order changes in the mass density of the element. However, these changes are ignored in the approximation of Hooke's law [6]. For an ideal elastic body; and by making use of Hooke's law and the strain-displacement relations in Eqs.(2.18) and (2.9), we obtain

$$\frac{1}{2} c_{ijkl} \left( \frac{\partial^2 u_k}{\partial x_j x_l} + \frac{\partial^2 u_l}{\partial x_j x_k} \right) + F_i = \rho \ddot{u}_i; \tag{2.37}$$

which is referred to as the Navier's wave equation for a general ideal elastic and anisotropic material.

The Navier's equation in an infinite isotropic elastic medium, admits three plane wave modes; with polarization of displacement vectors being either parallel or normal to the direction of propagation of the wave i.e longitudinal and transverse modes respectively; with the two transverse modes having the same phase velocity. For an anisotropic media, Navier's equation admits three mutually orthogonally polarized modes; with one of the modes being either longitudinal or quasi-longitudinal and the other two being either transverse or quasi-transverse [9, 1].

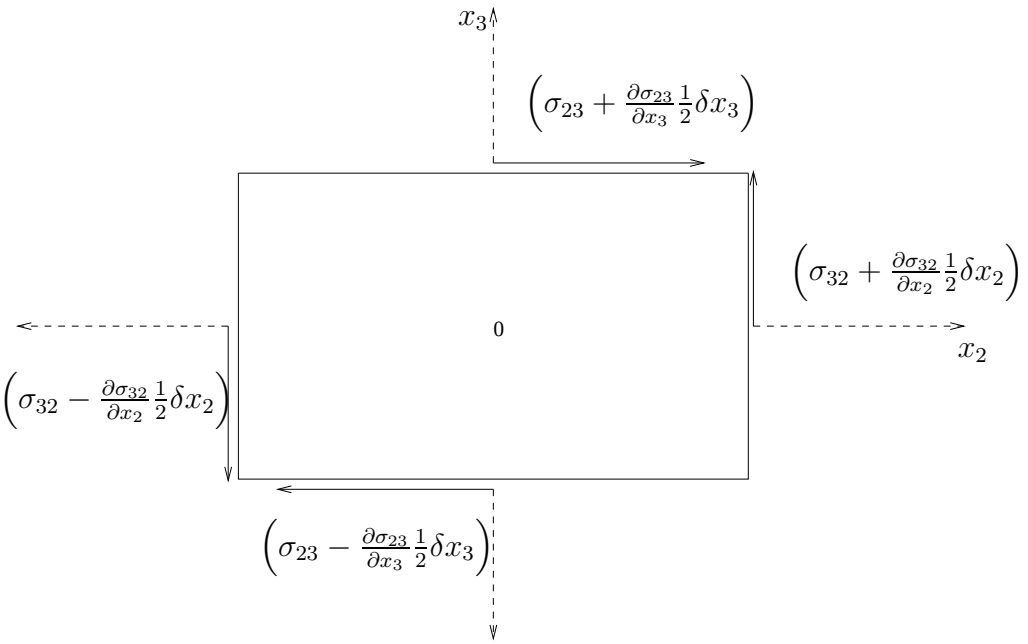


Figure 2.4: A rectangular infinitesimal element acted on by inhomogeneous stresses [2]

### 2.7.2 Rotational Equation of Motion

Firstly, lets consider the rotational equation of motion about the $0x_1$ axis. The components of stress, tending to cause such a rotation are shown in Fig.(2.4) [2]. The resultant anti-clockwise moment exerted on the element about $0x_1$ due to the shear stresses indicated in the figure on the faces perpendicular to $0x_2$ is

$$\left(\sigma_{32} - \frac{\partial\sigma_{32}}{\partial x_2}\frac{1}{2}\delta x_2\right)\delta x_1\delta x_3\frac{1}{2}\delta x_2 + \left(\sigma_{32} + \frac{\partial\sigma_{32}}{\partial x_2}\frac{1}{2}\delta x_2\right)\delta x_1\delta x_3\frac{1}{2}\delta x_2 = \sigma_{32}\delta x_1\delta x_2\delta x_3.$$

Similarly, the clockwise moment about $0x_1$ due to the shear stresses on faces perpendicular to $0x_3$ is

$$-\sigma_{23}\delta x_1\delta x_2\delta x_3.$$

Also, there are contributions to the angular acceleration about $0x_1$ from the normal forces on the faces of the element indicated in Fig.(2.4), since the resultant average stresses shown do not occur exactly at the center of the faces (it occurs rather at a stress weighted average position), due to the inhomogeneous nature of the stress. However, their lever arms are small

in comparison to those of the shear stresses calculated above and hence can be neglected [2]. Thus, the equation of motion about $0x_1$ is

$$(\sigma_{32} - \sigma_{23})\,\delta x_1 \delta x_2 \delta x_3 + G_1 \delta x_1 \delta x_2 \delta x_3 = I_1 \ddot{\theta}_1; \tag{2.38}$$

where $I_1$ is the moment of inertia about axis $0x_1$; $\ddot{\theta}_1$ is the angular acceleration of the element about axis $0x_1$, and $G_1$ is the component of the body-torque per unit volume in the $0x_1$ direction. Because $I_1$ is of the order of $\rho\delta x^5$ [6, 2]; as the element become infinitesimally small, $\ddot{\theta}_1$ increases without bound as $\frac{1}{\delta x^2}$ which is physically not possible for any real continuous material, unless

$$\sigma_{32} - \sigma_{23} + G_1 = 0. \tag{2.39}$$

In like manner, the equations of motion about $0x_2$ and $0x_3$ are respectively

$$\sigma_{13} - \sigma_{31} + G_2 = 0, \tag{2.40}$$

and

$$\sigma_{21} - \sigma_{12} + G_3 = 0. \tag{2.41}$$

In the absence of body torques, which may result from the presence of an electric, magnetic or gravitational field in the material, we then can deduce from Eqns.(2.39), (2.40) and (2.41) that

$$\sigma_{ij} = \sigma_{ji}. \tag{2.42}$$

Eqn.(2.42) implies that the stress tensor is symmetric only in the absence of body-torques.

## 2.8 Piezoelectricity

In certain dielectric crystals, the application of mechanical stress produces an electric polarization; which is proportional to the stress. If the crystal is isolated, this polarization results in a potential difference across the crystal, and if the crystal is short circuited, a flow of charge will result. Conversely, the application of an electric field in certain directions in

the crystal results in a mechanical strain (distortion). This reciprocal relationship is known as the piezoelectric effect [3, 6]. The phenomenon of generation of an electric polarization under a mechanical stress is referred to as the direct piezoelectric effect, and the mechanical strain resulting from an electric field is known as the converse piezoelectric effect.

The piezoelectric effect can only occur in crystal structures that lack a center of symmetry; with the exception of point symmetry group 432 (because of the presence of other crystallographic symmetry elements [23]). So, out of the 32 crystal classes 20 allow piezoelectricity. The direct and converse effect, can be represented quantitatively by the constitutive relations in a material as follows [6]:

$$\begin{aligned} P_i &= \epsilon_0 \chi^{\sigma}_{ij} E_j + d_{ijk}\sigma_{jk} \\ S_{ij} &= d_{kij} E_k + s^{E}_{ijkl}\sigma_{kl} \end{aligned} \tag{2.43}$$

In the above equations $i$,$j$,$k$,$l$ = 1,2,3; $\sigma_{kl}$, $S_{ij}$, $P_i$, and $E_j$ are respectively the stress, strain, electric polarisation and electric field; $s^{E}_{ijkl}$ are the elastic compliances at constant electric field; $\epsilon_0$ is the permittivity of free space; $\chi^{\sigma}_{ij}$ are the dielectric susceptibility constants at constant stress and $d_{ijk}$ are the piezoelectric strain constants.

In most engineering applications problems, the independent electrical variable is taken to be the electric displacement,

$$D_i = \epsilon_0 E_i + P_i. \tag{2.44}$$

The above equation implies that

$$P_i = D_i - \epsilon_0 E_i \tag{2.45}$$

substituting the expression for $P_i$ into Eqn.(2.43), we obtain the following:

$$\begin{aligned} D_i &= \epsilon_0 \chi^{\sigma}_{ij} E_j + \epsilon_0 E_i + d_{ijk}\sigma_{jk} \\ &= \epsilon_0 \chi^{\sigma}_{ij} E_j + \epsilon_0 \delta_{ij} E_j + d_{ijk}\sigma_{jk} \\ &= \epsilon_0 \left(\chi^{\sigma}_{ij} + \delta_{ij}\right) E_j + d_{ijk}\sigma_{jk} \\ &= \epsilon^{\sigma}_{ij} E_j + d_{ijk}\sigma_{jk} \end{aligned} \tag{2.46}$$

where $\epsilon_{ij}^{\sigma}$ is the permittivity at constant stress. Therefore, the constitutive equations (2.43) becomes

$$D_i = \epsilon_{ij}^{\sigma} E_j + d_{ijk}\sigma_{jk}, \tag{2.47}$$

$$S_{jk} = d_{ijk}E_i + s_{jklm}^{E}\sigma_{lm}. \tag{2.48}$$

In some problems [11, 6] and in this dissertation it is more convenient to use strain rather than stress as the independent variable. This is achieved as follows:
Multiplying Eqn.(2.48) by the stiffness constant, $c_{nojk}^{E}$ (i.e. the elastic stiffness constant at constant electric field) we obtain

$$c_{nojk}^{E} S_{jk} = c_{nojk}^{E} d_{ijk} E_i + \sigma_{no}. \tag{2.49}$$

from the above equation the stress component $\sigma_{no}$ is

$$\sigma_{no} = -e_{noi}E_i + c_{nojk}^{E} S_{jk}; \tag{2.50}$$

where $e_{noi} = d_{ijk}c_{nojk}^{E}$ is the piezoelectric stress constant. Changing the subscript $no$ to $lm$ and $i$ to $s$ in Eqn.(2.50) and substituting the resulting expression for stress into Eqn.(2.47), we obtain the following:

$$\begin{aligned} D_i &= \epsilon_{is}^{\sigma} E_s + d_{ilm}\left(-e_{lms}E_s + c_{lmjk}^{E}S_{jk}\right) \\ &= \epsilon_{is}^{\sigma} E_s - d_{ilm}e_{lms}E_s + d_{ilm}c_{lmjk}^{E}S_{jk} \\ &= \left(\epsilon_{is}^{\sigma} - d_{ilm}e_{lms}\right)E_s + d_{ilm}c_{lmjk}^{E}S_{jk} \\ &= \epsilon_{is}^{S}E_s + e_{ijk}S_{jk} \end{aligned} \tag{2.51}$$

where $\epsilon_{is}^{S} = \epsilon_{is}^{\sigma} - d_{ilm}e_{lms}$ is the permittivity at constant strain and $e_{ijk} = d_{ilm}c_{lmjk}^{E}$, since $c_{lmjk} = c_{jklm}$. Therefore, the final form of the piezoelectric constitutive relations with the stress and electric displacement as the dependent variables are

$$\begin{aligned} \sigma_{lm} &= c_{lmjk}^{E}S_{jk} - e_{lmi}E_i, \\ D_i &= e_{ijk}S_{jk} + \epsilon_{is}^{S}E_s. \end{aligned} \tag{2.52}$$

The permittivity tensor in Eqn.(3.14) is symmetric [2] and has six independent components. Also, from the constitutive equations, we observe that the piezoelectric stress tensor is symmetric with respect to the indices $jk$ and thus is specified by 18 independent components [2]. We will show later that the existence of material symmetry can further reduce the number of independent permittivity and piezoelectric stress constants.

From Eqn.(3.14), we observe that the electric and elastic fields are not independent as is the case with a non piezoelectric material. Thus, a strain field accompanying an acoustic field in a piezoelectric medium modifies and or generates an electric field; which in turn changes the stress field as described by Eqn.(3.14). Thus, the material appears elastically more stiffened or less depending on the nature of the coupling. From [6], it is shown that there exist 5 plane wave solutions in an infinite piezoelectric media; which is a combination of the following wave types: quasi-acoustic, quasi-electromagnetic (hybrid waves containing both electric and acoustic fields; with velocities slightly less than a pure acoustic mode and higher than a pure electromagnetic mode respectively), pure acoustic, pure electromagnetic, and stiffened acoustic fields. These 5 solutions are obtained by solving both Maxwell's equations for the electromagnetic fields and Navier's equation for the acoustic fields in addition to the constitutive equation for the selected material.

### 2.8.1 Quasi-Static Approximation

The coupling that results in the generation of a quasi-acoustic and quasi-electromagnetic waves is very small for most materials (except for very few exception for guided waves [6]) leading to corrections of acoustic velocities of the order of $\frac{v^2}{c^2}$ [11] ($v$ and $c$ are the acoustic and electromagnetic phase velocities respectively); which is very small, because $c$ is of the order of $10^5$ greater than $v$. So, in solving wave propagation problems in a piezoelectric material, the time varying electric field resulting from an acoustic field, is often assumed to have zero curl, so as not to be able to generate a magnetic field; and moreover, can be expressed as the gradient of a scalar potential [6, 11]. This electric field's phase velocity is of the order

of an acoustic field, and is referred to as a quasi-static electric field. This approximation is referred to as the quasi-static approximation. When the quasi-static approximation is made, acoustic waves become decoupled from electromagnetic waves, and quasi-acoustic and electromagnetic modes become pure modes. Also some elastic constants become stiffened, resulting in stiffened acoustic modes. This phenomenon is known as piezoelectric stiffening. For plane wave solutions, stiffened elastic constants are expressed as [11]

$$c_{ijlm} = c^{E}_{ijlm} + \frac{e_{ijr} n_r e_{lms} n_s}{\epsilon^{s}_{pq} n_p n_q}; \tag{2.53}$$

where the second term in Eqn.(2.53) is what is responsible for the stiffening, and the subscripted $n$'s represent components of the wave normal. The size of this term relative to the $c_{ijlm}$ determines the relative changes to the phase velocity and other properties of the wave, for example, phonon focusing [11] and plane wave reflection characteristics at a boundary [24]. It is worth mentioning that, Eqn.(2.53) is valid only for plane wave modes in an infinite medium. Piezoelectric stiffening in certain materials is pronounced, for example, lithium niobate and Rochelle salt and leads to changes in acoustic velocities of more than 20 percent in some directions; whereas in others the coupling is small and can be neglected [1]. It is worth mentioning that when the quasi-static approximation is made, we are left with just the Navier's equation and Gauss' law to solve for the unknown quantities comprising of the displacements and the electric potential.

## 2.9 Effects of Symmetry on Crystal Properties

Every crystal has some degree of symmetry added to the inherent translational symmetry. These additional symmetries are often described in terms of symmetry elements (for example, a rotation axis, and a mirror plane) with their associated operations; which when applied to the crystal transforms the crystal to itself. The operations of the symmetry elements into which the symmetry of any crystal lattice can be analyzed, are often divided into two major types [6]:

1. The translational symmetry operations which moves the crystal as a whole.

2. The point symmetry operations which leave at least one point of the crystal unchanged after its application.

A given symmetry element can have a combination of both operations. Symmetry elements that are used to describe the symmetries of any crystal lattice have been grouped into unique combinations called space groups. The operation of each element or a succession of elements in the group must transform the crystal lattice into itself. It has been found that there exist only 230 essentially different space groups that occur in nature [2]. Nevertheless, it has been observed that the characteristic symmetry displayed by the macroscopic properties of a crystal are point symmetry operations [2]; this is because the relative positions of symmetry elements in the crystal structure are ignored when studying the symmetries of macroscopic properties of crystals; only the orientations of the elements are important. Moreover, crystal properties like the elastic stiffness relate the stress and strain at a point, hence necessitating the use of point symmetry operations to describe its symmetry characteristics [2, 6]. The symmetry elements with point symmetry operations are: center of symmetry, mirror plane, 1, 2, 3, 4- or 6-fold rotation axes, 1, 2, 3, 4- or 6-fold rotation inversion axes. The possible combinations of macroscopic symmetry elements are called point groups and there exist just 32 different crystallographic point groups. Crystals are divided into 32 crystal classes according to the point groups. It is worth noting that, the symmetry operations associated with the symmetry elements are described with respect to the standard Cartesian crystal axes [6]. Moreover, the 32 crystal classes are traditionally organized into seven groups referred to as crystal systems. Members of a particular system are required to have a characteristic symmetry element common to all members of the group. These crystal systems are: triclinic, monoclinic, orthorhombic, tetragonal, trigonal, hexagonal (transversely isotropic) and cubic. It is then natural for one to ask; what is the relation between the symmetry elements of a crystal and those of its macroscopic properties? The answer to this question was given by Neumann, well expressed in his postulate referred to as Neumann's principle; which can be

stated a follows [2]:

"The symmetry elements of any physical property of a crystal must include the symmetry elements of the point group of the crystal".

In other words, the point group is a subgroup of the symmetry group of the crystal property. It is clear from the above postulate that a physical property can have inherent symmetries independent of the symmetry of the crystal. For example, the elastic stiffness tensor is centrosymmetric (i.e. has a centre of symmetry) but the crystal lattice say for example, a piezoelectric crystal will lack a centre of symmetry. Therefore, what effect does crystal symmetries have on the components of the tensors representing physical properties? To answer this question, two general arguments can be used [6]: firstly, by a purely intuitive physical argument, for example, if two directions are symmetrically equivalent in a crystal then identical stresses in these directions will lead to the same amount of strain. This implies that certain compliance constants are equal [6]. Secondly, by application of Neumann's principle, where if the crystal is symmetric under the application of a particular symmetry operation; in other words transformation of the coordinate axes, then we expect the components of the tensor representing the physical property to remain unchanged after the transformation. The second method is more systematic and has the advantage of ensuring that every possible relation between the components of the tensor have been obtained which is very challenging to arrive at by the first method [2]. A general outline of the second method is as follows:

- Determine the crystallographic point group of the crystal.
- Choose a set of symmetry elements that fully generate the point group of the crystal i.e. the generators of the point group.
- Choose a set of coordinate axes, most preferably the standard coordinate axes used in texts on crystallography and then transform the axes and tensor by each of the generators of the group.
- Obtain relationships between corresponding components of the tensor in the old and

new coordinate systems; since they are expected to be equal (e.g., $c'_{mnop} = -c_{ijkl}$, implying that $c_{ijkl} = 0$).

Examples of this procedure applied to a variety tensors representing physical properties of crystals can be found in classic texts like [6] and [2]. The result of the above procedure is that the number of independent components of the tensor needed to describe the physical properties of the crystal is greatly reduced. For example, the number of independent elastic constants for the seven crystal systems, range from 21 for triclinic (with minimum symmetry) to 3 for the cubic system. It is worth mentioning that, the number of independent elastic constants happen to be the same for all classes in a given system; however, this is not the case for other crystal properties for example, the piezoelectric moduli, where the number of independent components vary from class to class within a given system [6, 2].

In this dissertation the crystal class in the transversely isotropic system we are interested in, is the $6mm$; and the tensors of interest to us are $c_{ijkl}$, $e_{ijk}$ and $\epsilon_{ij}$ and have 5, 3, and 2 independent components respectively [10]. A full representation in matrix form using the Voigt notation of the above mentioned physical parameters of interest to us are as follows [10]:

$$c^E_{ab} = \begin{bmatrix} c^E_{11} & c^E_{12} & c^E_{13} & 0 & 0 & 0 \\ c^E_{12} & c^E_{11} & c^E_{13} & 0 & 0 & 0 \\ c^E_{13} & c^E_{13} & c^E_{33} & 0 & 0 & 0 \\ 0 & 0 & 0 & c^E_{55} & 0 & 0 \\ 0 & 0 & 0 & 0 & c^E_{55} & 0 \\ 0 & 0 & 0 & 0 & 0 & c^E_{66} \end{bmatrix}; \tag{2.54}$$

where $2c^E_{66} = \left(c^E_{11} - c^E_{12}\right)$ and $a, b = 1, 2, ..., 6$;

$$e_{ia} = \begin{bmatrix} 0 & 0 & 0 & 0 & e_{15} & 0 \\ 0 & 0 & 0 & e_{15} & 0 & 0 \\ e_{15} & e_{31} & e_{33} & 0 & 0 & 0 \end{bmatrix}, \tag{2.55}$$

$$\epsilon_{ij}^{S} = \begin{bmatrix} \epsilon_{11}^{S} & 0 & 0 \\ 0 & \epsilon_{11}^{S} & 0 \\ 0 & 0 & \epsilon_{33}^{S} \end{bmatrix}. \tag{2.56}$$

Therefore; we are indeed grateful for the effect of symmetry which by reducing the number of independent constants needed to describe physical properties of crystals, greatly simplifies algebraic manipulations involving these quantities.

## 2.10 Thermal Effects

Many physical properties of materials are temperature dependent, including mechanical properties like the density and elastic constants. So, it is often important to understand the relationship between the temperature and material properties, so as to gain optimal responses of materials in different technological applications [5]. Here we give a brief qualitative description on the effects of temperature in the dynamics of elastic bodies.

Generally, the elasticity of a material depends on the state of deformation, for example, metals will soften and polymers may stiffen as strains approach the state of material failure. In like manner, when a material gains heat and its temperature rises, it becomes strained; for example, either by contracting and becoming stiffer or expanding and becoming less stiff, depending on whether the material has a negative (quite rare) or positive thermal expansion coefficient. As a result, the elastic constants either increases or decreases. Moreover, the density of the material either decreases or increases. A quantitative discussion of the variation of the elastic constants with temperature uses the machinery of thermodynamics; the case for solids can be found in [25]. It is then, evident that the bulk wave phase velocities of propagating wave modes in such materials will be affected, since the general expression for such velocities is $\sqrt{\frac{c}{m}}$; where c stands for an elastic parameter and m for an inertia parameter.

On the other hand, when a material is compressed or stretched mechanically, it undergoes a change in temperature or entropy. Moreover, in vibration problems this stretching and

compressions occur so fast that there is very little heat conduction; as a result from the second law of thermodynamics the process can be considered as approximately adiabatic and isentropic. However, in a strict sense the process is irreversible and can be considered to be only adiabatic process. Consequently, the elastic constants used in vibration problems when ambient conditions of temperature are constant, are the adiabatic (isentropic) elastic moduli [1] and [6].

Also, before an elastic vibration is initiated in a material, there are inherent thermal vibrations also known as phonons. Nevertheless, in most wave propagation problems, these vibrations are not taken into account. This is because, in traditional mechanical wave propagation problems, we do not study motions of individual particles but rather an infinitesimal element of the material composed of millions of atoms; which is the subject of continuum mechanics. In such an element, the thermal vibrations of the individual particles are random and as a result can be averaged out in the direction of wave propagation. These thermal vibrations, however, will become significant if there is a temperature gradient in the material in the direction of wave propagation due to the presence of a source of heat. Therefore, for most purposes we do not consider thermal effects in elastic wave propagation problems as the ambient conditions of temperature are assumed constant.

## 2.11 Microscopic Origin of Elasticity, Piezoelectricity and Thermal Expansion

In this section, we give a qualitative description of the microscopic origin of elasticity (stiffness constants $c_{ijkl}$), piezoelectricity (the piezoelectricity moduli $e_{ijk}$) and thermal expansion (coefficients of thermal expansion $\alpha_{ij}$).

### 2.11.1 Elasticity

The origin of the elastic properties of materials can be understood by observing that in a crystal lattice, the constituent atoms are held together mainly by electrostatic interactions, since the magnetic and gravitational interactions are considered to be small in comparison to the electrostatic interactions. The nature and strength of the interaction is determined by the distribution of the valence and other electrons and the atomic nuclei [7]. If we suppose that the crystal is in its equilibrium configuration (most stable state i.e. minimum potential energy) and at absolute zero; and also neglects the zero point quantum mechanical vibrations. In this case neighbouring atoms will exert zero forces on each other due to balance of net attractive and repulsive contributions of the electrostatic interaction. However, if an atom is displaced from its equilibrium position, the potential energy of the system will change from its minimum value and the system becomes unstable. As a result, a force develops (which is a functions of the displacement of the particle from its equilibrium position) to restore the displaced atom to its equilibrium position and hence the crystal's original configuration. For small displacements (i.e. when Hooke's law is obeyed), the restoring force is proportional to the displacement; and the constant of proportionality is a measure of the elastic stiffness of the material (i.e. of similar order of magnitude) [7, 8].

### 2.11.2 Piezoelectricity

We can understand qualitatively the microscopic origin of piezoelectric effect by considering, for example, the cubic crystal zincblende (ZnS) depicted in Fig.(2.5) [3]. The positively charged Zn ions are located at the center of a regular tetrahedron $ABCD$ and with corners occupied by the negatively charged sulfur ions. If a shear stress is applied in the $xy$ plane of this system, the edges $AB$ and $CD$ of the tetrahedron will be elongated and shortened respectively. Consequently, as evident from the figure, the zinc ion will be displaced upwards along the z axis, thus giving rise to an electric dipole moment. The dipole moments arising from different octahedra, making up the unit cells will sum up because they all have the

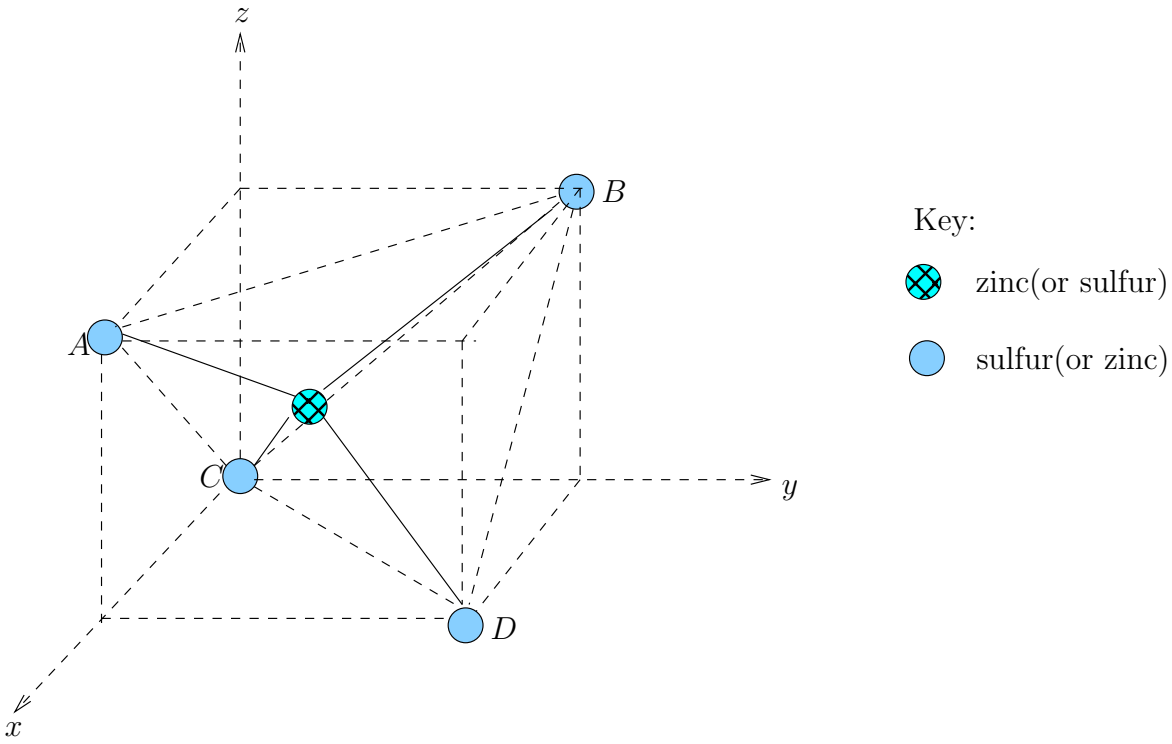


Figure 2.5: Tetrahedral structure of zincblende, ZnS. Only part of unit cell is shown. Size of circles has no relation to size of ions [3]

.

same orientation with respect to the axes $x$, $y$, $z$ . This is the direct piezoelectric effect.

Conversely, if a uniform electric field is applied parallel to the z axis, the zinc ion will be displaced upwards and the sulfur ions downwards, and the material will become strained. Clearly, if the direction of the field is reversed the displacements of the particles will be such as to reverse the strain. In this case, we have the converse piezoelectric effect.

**Thermal Expansion**

Thermal expansion can be understood qualitatively on a molecular bases, if we picture the inter-atomic forces between the atoms in a solid as springs. Supposing that the atoms are at rest at absolute zero (though this is impossible from quantum mechanics, as there are always zero point motions); when the solid is heated, the atoms gain energy leading to vibrations about their equilibrium positions. As the temperature increases, the amplitude of the vibrations also increase. If Hooke's law is assumed, no thermal expansion will occur because the particles are considered to oscillate harmonically about their equilibrium position, so that the average separation between atoms (molecules) remains the same [7]. Moreover, in this regime the inter-atomic forces and their associated potential energies are symmetric about the equilibrium position. However, for real materials Hooke's law is valid only for small amplitudes of vibration of the particles. Thus, as the amplitude of vibrations increases, the inter-atomic forces and their associated potential energies cease to be symmetric about the equilibrium position and in most cases behave as springs that are easier to stretch than to compress [5]. Consequently, the average distance between atoms (molecules) increases. Therefore, every dimension of the material increases.

# Chapter 3

# Equations of Motion For a Transversely Isotropic Piezoelectric Solid Cylinder

## 3.1 Introduction

In this section, we develop the equations of motion for a transversely isotropic piezoelectric cylinder based on the following assumptions and approximations:

- The linear theory of elasticity.
- Linear electromechanical coupling.
- Axial polarization.
- Quasi-static approximation of the electric field.
- The material is homogeneous and absence of free charges.
- We neglect thermal effects and body forces.

- Absence of damping forces.

We will achieve this by two independent methods: Firstly, by making use of Navier's equation, Gauss' law, the constitutive relations for the material under investigation and the strain-displacement relations; and secondly, via Hamilton's variational principle.

The first approach stated above, is used in countless guided wave problems that include plates, multilayer and tubes and has the setback of physically imposed boundary conditions, which are quite challenging to arrive at [9]. The second method on the other hand, based on Hamilton's variational principle is straightforward and more elegant than the first, and has the added advantage of leading to the allowed boundary conditions of the system depending on the geometry; this is not surprising as Hamilton's principle is more fundamental than Newton's second law on which the first method is based.

On this note, we begin this section with a description of the geometry of the model, followed by the derivation of the equations of motion, by the first and second methods stated above. The derivations made here will be purely in cylindrical coordinate system, the natural geometry for the problem.

## 3.2 Geometry and Coordinates used to Describe the System

The geometry of the system is depicted in Fig.(3.1) and the parameters $r$, $\theta$, and $z$ are the radial, angular and axial coordinates, while $u$, $v$, and $w$ are respectively the radial, tangential and axial displacement components. The cylinder is considered to be extended infinitely in the axial direction.

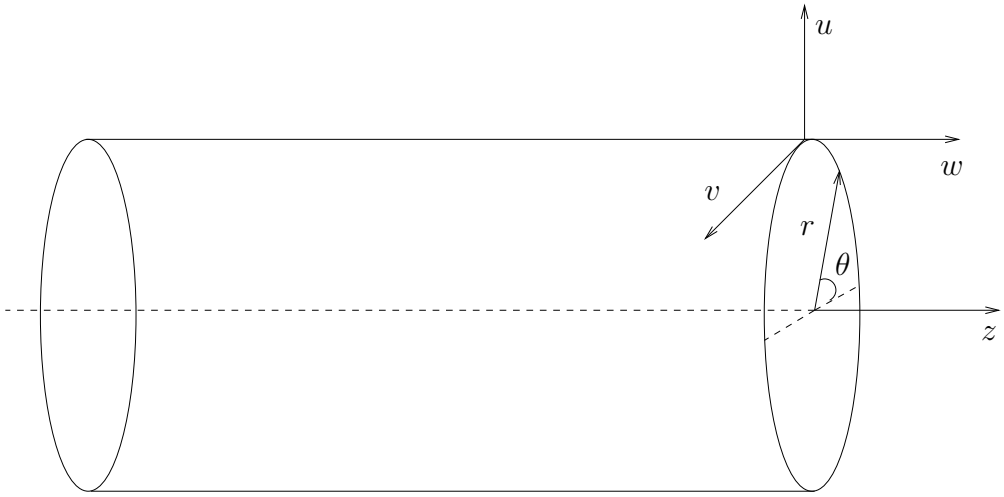


Figure 3.1: Infinitely long solid cylinder.

## 3.3 Method 1: Derivation of Equations of Motion via Navier's Equation and Gauss' law.

In this section, we derive the equations of motion of the cylinder by making use of Navier's equation, Gauss' law, the constitutive relations, the strain-mechanical displacement and electric field-electric potential relations. The above mentioned field equations, satisfied in the piezoelectric cylinder will be presented, based on the assumptions and approximation of the model. Moreover, they will be expressed purely in cylindrical coordinates, the natural geometry of the system.

1. Navier's Equation (in cylindrical coordinates): loosely following Timoshenko's [22] 2D approach, we have carried out the detailed 3D derivation in cylindrical coordinates, making use of the infinitesimal volume element depicted in Fig.(3.2). This element is located in a body with inhomogeneous stress distribution and homogeneous body force distribution, which we will later drop. Because of curvature associated with the element, the following remarks are crucial in the development of this equation:

    - Firstly, because of the curvature, the traction forces in the tangential direction

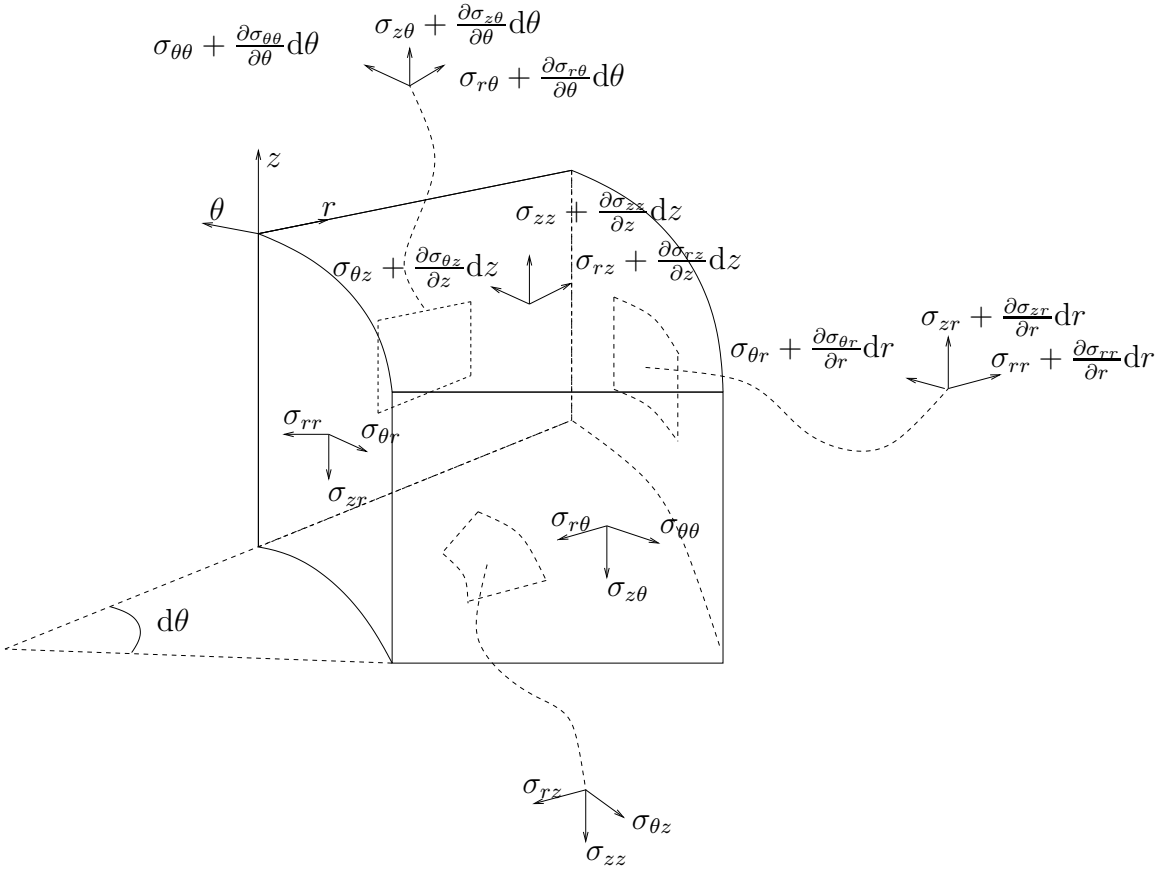


Figure 3.2: Infinitesimal volume element in cylindrical coordinates; situated in a stressed body. For clarity the stress triads on the rear faces have been indicated with curves originating from the faces concerned.

need to be compared relative to the same point.

- The tractions $-\sigma_{\theta\theta}\mathrm{d}r\mathrm{d}z$ and $\left(\sigma_{\theta\theta}+\frac{\partial\sigma_{\theta\theta}}{\partial\theta}\mathrm{d}\theta\right)\mathrm{d}r\mathrm{d}z$ have radial components of $-\sigma_{\theta\theta}\sin(\frac{\mathrm{d}\theta}{2})\mathrm{d}r\mathrm{d}z$ and $\left(\sigma_{\theta\theta}+\frac{\partial\sigma_{\theta\theta}}{\partial\theta}\mathrm{d}\theta\right)\sin(\frac{\mathrm{d}\theta}{2})\mathrm{d}r\mathrm{d}z$ respectively (i.e. with comparisons made relative to the bisector of the angle $\mathrm{d}\theta$); which may be expressed simply as $-\sigma_{\theta\theta}\frac{\mathrm{d}\theta}{2}\mathrm{d}r\mathrm{d}z$ and $\left(\sigma_{\theta\theta}+\frac{\partial\sigma_{\theta\theta}}{\partial\theta}\mathrm{d}\theta\right)\frac{\mathrm{d}\theta}{2}\mathrm{d}r\mathrm{d}z$. It is worth mentioning that the tangential components of these tractions are approximately equal to the magnitude of the tractions since $\cos(x)\approx 1$ for infinitesimal $x$.

- Similarly, contributions to the traction forces in the tangential direction are $\sigma_{r\theta}\frac{\mathrm{d}\theta}{2}\mathrm{d}r\mathrm{d}z$ and $\left(\sigma_{r\theta}+\frac{\partial\sigma_{r\theta}}{\partial\theta}\mathrm{d}\theta\right)\frac{\mathrm{d}\theta}{2}\mathrm{d}r$.

Summing up forces in the radial direction, including the body force per unit volume $R$, we obtain the radial equation of motion as follows:

$$\begin{aligned}&\left(\sigma_{rr}+\frac{\partial\sigma_{rr}}{\partial r}\mathrm{d}r\right)(r+\mathrm{d}r)\,\mathrm{d}\theta\mathrm{d}z-\sigma_{rr}r\mathrm{d}\theta\mathrm{d}z-\left(\sigma_{\theta\theta}+\frac{\partial\sigma_{\theta\theta}}{\partial\theta}\mathrm{d}\theta\right)\frac{\mathrm{d}\theta}{2}\mathrm{d}r\mathrm{d}z \\ &-\sigma_{\theta\theta}\frac{\mathrm{d}\theta}{2}\mathrm{d}r\mathrm{d}z+\left(\sigma_{r\theta}+\frac{\partial\sigma_{r\theta}}{\partial\theta}\mathrm{d}\theta\right)\mathrm{d}r\mathrm{d}z-\sigma_{r\theta}\mathrm{d}r\mathrm{d}z \\ &+\left(\sigma_{rz}+\frac{\partial\sigma_{rz}}{\partial z}\mathrm{d}z\right)r\mathrm{d}r\mathrm{d}\theta-\sigma_{rz}r\mathrm{d}r\mathrm{d}\theta+Rr\mathrm{d}r\mathrm{d}\theta\mathrm{d}z=m\ddot{u}.\end{aligned} \tag{3.1}$$

Simplifying Eqn.(3.1) leads to

$$\begin{aligned}&\frac{\sigma_{rr}}{\partial r}r\mathrm{d}r\mathrm{d}\theta\mathrm{d}z+\sigma_{rr}\mathrm{d}r\mathrm{d}\theta\mathrm{d}z+\frac{\sigma_{r\theta}}{\partial\theta}\mathrm{d}r\mathrm{d}\theta\mathrm{d}z \\ &+\frac{\sigma_{rz}}{\partial z}r\mathrm{d}r\mathrm{d}\theta\mathrm{d}z-\sigma_{\theta\theta}\mathrm{d}r\mathrm{d}\theta\mathrm{d}z+Rr\mathrm{d}r\mathrm{d}\theta\mathrm{d}z=m\ddot{u}.\end{aligned} \tag{3.2}$$

Dividing Eqn.(3.2) through by $r\mathrm{d}r\mathrm{d}\theta\mathrm{d}z$, we obtain

$$\frac{\partial\sigma_{rr}}{\partial r}+\frac{1}{r}\frac{\partial\sigma_{\theta r}}{\partial\theta}+\frac{\partial\sigma_{zr}}{\partial z}+\frac{\sigma_{rr}-\sigma_{\theta\theta}}{r}+R=\rho\ddot{u}; \tag{3.3}$$

where $\rho$ is the mass density of the material. Similarly, by summing forces in the tangential direction we obtain the equation of motion in the tangential direction as

follows:

$$\left(\sigma_{\theta\theta}+\frac{\partial\sigma_{\theta\theta}}{\partial\theta}\mathrm{d}\theta\right)\mathrm{d}r\mathrm{d}z-\sigma_{\theta\theta}\mathrm{d}r\mathrm{d}z+\left(\sigma_{r\theta}+\frac{\partial\sigma_{r\theta}}{\partial r}\mathrm{d}r\right)(r+\mathrm{d}r)\,\mathrm{d}\theta\mathrm{d}z \tag{3.4}$$
$$+\left(\sigma_{r\theta}+\frac{\partial\sigma_{r\theta}}{\partial\theta}\mathrm{d}\theta\right)\frac{\mathrm{d}\theta}{2}\mathrm{d}r\mathrm{d}z+\sigma_{r\theta}\frac{\mathrm{d}\theta}{2}\mathrm{d}r\mathrm{d}z-\sigma_{r\theta}r\mathrm{d}\theta\mathrm{d}z$$
$$+\left(\sigma_{z\theta}+\frac{\partial\sigma_{z\theta}}{\partial z}\mathrm{d}z\right)r\mathrm{d}r\mathrm{d}\theta-\sigma_{z\theta}r\mathrm{d}r\mathrm{d}\theta+Sr\mathrm{d}r\mathrm{d}\theta\mathrm{d}z=m\ddot{v};$$

where $S$ is the is the body force per unit volume in the tangential direction. Further simplification of Eqn.(3.4) leads to

$$\frac{\partial\sigma_{\theta\theta}}{\partial\theta}\mathrm{d}r\mathrm{d}\theta\mathrm{d}z+\frac{\partial\sigma_{r\theta}}{\partial r}r\mathrm{d}r\mathrm{d}\theta\mathrm{d}z+\sigma_{r\theta}\mathrm{d}r\mathrm{d}\theta\mathrm{d}z \tag{3.5}$$
$$+\frac{\partial\sigma_{z\theta}}{\partial z}r\mathrm{d}r\mathrm{d}\theta\mathrm{d}z+\sigma_{r\theta}\mathrm{d}r\mathrm{d}\theta\mathrm{d}z+Sr\mathrm{d}r\mathrm{d}\theta\mathrm{d}z=m\ddot{v}.$$

Dividing Eqn.(3.5) through by $r\mathrm{d}r\mathrm{d}\theta\mathrm{d}z$, we obtain

$$\frac{\partial\sigma_{r\theta}}{\partial r}+\frac{1}{r}\frac{\partial\sigma_{\theta\theta}}{\partial\theta}+\frac{\partial\sigma_{z\theta}}{\partial z}+\frac{2\sigma_{r\theta}}{r}+S=\rho\ddot{v}. \tag{3.6}$$

Finally, by summing forces in the $z$ (axial) direction we obtain the equation of motion in the axial direction as follows:

$$\left(\sigma_{rz}+\frac{\sigma_{rz}}{\partial r}\mathrm{d}r\right)(r+\mathrm{d}r)\,\mathrm{d}\theta\mathrm{d}z-\sigma_{rz}r\mathrm{d}\theta\mathrm{d}z-\sigma_{z\theta}\mathrm{d}r\mathrm{d}z \tag{3.7}$$
$$+\left(\sigma_{z\theta}+\frac{\sigma_{z\theta}}{\partial\theta}\mathrm{d}\theta\right)\mathrm{d}r\mathrm{d}z+\left(\sigma_{zz}+\frac{\sigma_{zz}}{\partial z}\mathrm{d}z\right)r\mathrm{d}r\mathrm{d}\theta$$
$$-\sigma_{zz}r\mathrm{d}r\mathrm{d}\theta+Qr\mathrm{d}r\mathrm{d}\theta\mathrm{d}z=m\ddot{w}; \tag{3.8}$$

where $Q$ is the body force per unit volume in the $z$ direction. After simplification of Eqn.(3.8) we obtain

$$\frac{\partial\sigma_{rz}}{\partial r}r\mathrm{d}r\mathrm{d}\theta\mathrm{d}z+\frac{\partial\sigma_{z\theta}}{\partial\theta}\mathrm{d}r\mathrm{d}\theta\mathrm{d}z+\sigma_{rz}\mathrm{d}r\mathrm{d}\theta\mathrm{d}z \tag{3.9}$$
$$+\frac{\partial\sigma_{zz}}{\partial z}r\mathrm{d}r\mathrm{d}\theta\mathrm{d}z+Qr\mathrm{d}r\mathrm{d}\theta\mathrm{d}z=m\ddot{w}.$$

Similarly, dividing Eqn.(3.9) by $r\mathrm{d}r\mathrm{d}\theta\mathrm{d}z$ we obtain

$$\frac{\partial\sigma_{rz}}{\partial r}+\frac{1}{r}\frac{\partial\sigma_{\theta z}}{\partial\theta}+\frac{\partial\sigma_{zz}}{\partial z}+\frac{\sigma_{rz}}{r}+Q=\rho\ddot{w}. \tag{3.10}$$

Therefore, in the absence of body forces the Navier's equations of motion (a statement Newton's second law) for the cylinder are [15]:

$$\frac{\partial \sigma_{rr}}{\partial r} + \frac{1}{r}\frac{\partial \sigma_{\theta r}}{\partial \theta} + \frac{\partial \sigma_{zr}}{\partial z} + \frac{\sigma_{rr} - \sigma_{\theta\theta}}{r} = \rho \ddot{u}, \tag{3.11a}$$

$$\frac{\partial \sigma_{r\theta}}{\partial r} + \frac{1}{r}\frac{\partial \sigma_{\theta\theta}}{\partial \theta} + \frac{\partial \sigma_{z\theta}}{\partial z} + \frac{2\sigma_{r\theta}}{r} = \rho \ddot{v}, \tag{3.11b}$$

$$\frac{\partial \sigma_{rz}}{\partial r} + \frac{1}{r}\frac{\partial \sigma_{\theta z}}{\partial \theta} + \frac{\partial \sigma_{zz}}{\partial z} + \frac{\sigma_{rz}}{r} = \rho \ddot{w}. \tag{3.11c}$$

2. Gauss' law in the material with no free charges:

   The coordinate independent form of Gauss' law in the absence of free charges is $\boldsymbol{\nabla} \cdot \boldsymbol{D} = 0$; where $\boldsymbol{D}$ is the electric displacement vector. To obtain the corresponding equation in cylindrical coordinates, we make use of the general expression in curvilinear systems for the divergence of a vector, which is as follows [26]:

$$\boldsymbol{\nabla} \cdot \boldsymbol{A} = \frac{1}{h_1 h_2 h_3}\left[\frac{\partial (h_2 h_3 A_1)}{\partial q_1} + \frac{\partial (h_1 h_3 A_2)}{\partial q_2} + \frac{\partial (h_1 h_2 A_3)}{\partial q_3}\right]; \tag{3.12}$$

   where the $q_i$'s are any general curvilinear coordinates; the $h_i$'s are the scale factors for the given curvilinear system defined as $h_i = |\frac{\partial \boldsymbol{r}}{\partial q_i}|$ ($\boldsymbol{r}$ is the position vector of a general point). So, for the specific case of cylindrical coordinates, $q_1 = r$, $q_2 = \theta$, and $q_3 = z$; also $h_1 = 1$, $h_2 = r$ and $h_3 = 1$ [26]. Therefore, Gauss' law is expressed in cylindrical coordinates as follows:

$$\frac{\partial D_r}{\partial r} + \frac{1}{r}D_r + \frac{1}{r}\frac{\partial D_\theta}{\partial \theta} + \frac{\partial D_z}{\partial z} = 0. \tag{3.13}$$

3. The coupled constitutive equations satisfied by the system [1]: The constitutive relations for the material in cylindrical coordinates, are the same as those expressed in Cartesian coordinate in the previous chapter. This is because the cylinder system is transversely isotropic, and as the name implies is isotropic in the plane perpendicular to the axis. Hence, the constitutive relations remain unchanged for a transformation from the former Cartesian coordinate system to the present cylindrical coordinate system.

So the constitutive relations satisfied by the system are:

$$\sigma_{ij} = c^E_{ijkl} S_{kl} - e_{ijk} E_k : \tag{3.14a}$$

$$D_r = e_{klr} S_{kl} + \epsilon^S_{rk} E_k. \tag{3.14b}$$

In the above equations $i$,$j$,$k$,$l$ = 1,2,3 (which is also synonymous with $r$, $\theta$, $z$); $\sigma_{ij}$, $S_{kl}$, $D_r$ and $E_k$ are respectively the stress, strain, electric displacement and electric field; $c^E_{ijkl}$ are the elastic constants at constant electric field; $\epsilon^S_{rk}$ are the dielectric constants at constant strain and $e_{ijk}$ are the piezoelectric stress constants (the coupling coefficients are constants since we are dealing with a homogeneous system).

4. The strain-mechanical displacement relations of elasticity: As stated in the previous chapter the strain tensor is the symmetric part of the displacement gradient. So deriving the expression for the displacement gradient in cylindrical coordinates, will lead easily to the expression for the strain in cylindrical coordinates. In coordinate independent notation the differential displacement is defined as [6]

$$\mathrm{d}\boldsymbol{u} = \boldsymbol{\nabla u} \cdot \mathrm{d}\boldsymbol{r}; \tag{3.15}$$

where $\boldsymbol{\nabla u}$ is the displacement gradient. Nabla, $\boldsymbol{\nabla}$ and the differetial, $\mathrm{d}\boldsymbol{r}$ in general curvilinear coordinate are expresses as [26]

$$\boldsymbol{\nabla} = \frac{1}{h_i}\left(\frac{\partial}{\partial q_i}\right)\hat{\boldsymbol{q}}_i, \tag{3.16}$$

and

$$\mathrm{d}\boldsymbol{r} = \frac{\partial \boldsymbol{r}}{\partial q_i}\mathrm{d}q_i = \mathrm{d}q_i h_i \hat{\boldsymbol{q}}_i; \tag{3.17}$$

where the $\hat{\boldsymbol{q}}_i$'s are the basis vectors in a general curvilinear coordinate system; the $q_i$'s and $h_i$'s are as defined previously. In the special case of cylindrical coordinate systems, Nabla, $\boldsymbol{\nabla}$ and the differetial, $\mathrm{d}\boldsymbol{r}$ are

$$\boldsymbol{\nabla} = \frac{\partial}{\partial r}\hat{\boldsymbol{r}} + \frac{1}{r}\frac{\partial}{\partial \theta}\hat{\boldsymbol{\theta}} + \frac{\partial}{\partial z}\hat{\boldsymbol{z}}, \tag{3.18}$$

and

$$\mathrm{d}\boldsymbol{r} = \mathrm{d}r\hat{\boldsymbol{r}} + r\mathrm{d}\theta\hat{\boldsymbol{\theta}} + \mathrm{d}z\hat{\boldsymbol{z}}. \tag{3.19}$$

Therefore, from Eqns.(3.15), (3.18) and (3.19) the differential displacement in cylindrical coordinate takes the form [6]

$$\mathrm{d}\boldsymbol{u} = \frac{\partial \boldsymbol{u}}{\partial r}\mathrm{d}r + \frac{1}{r}\frac{\partial \boldsymbol{u}}{\partial \theta}\left(r\mathrm{d}\theta\right) + \frac{\partial \boldsymbol{u}}{\partial z}\mathrm{d}z. \tag{3.20}$$

In Eqn.(3.20), $\boldsymbol{u} = u\hat{\boldsymbol{r}}+v\hat{\boldsymbol{\theta}}+w\hat{\boldsymbol{z}}$. Substituting this expression for $\boldsymbol{u}$ back into Eqn.(3.20) and remembering that the unit vectors $\hat{\boldsymbol{r}}$ and $\hat{\boldsymbol{\theta}}$ are dependent on the coordinate $\theta$ (i.e. $\frac{\partial \hat{\boldsymbol{r}}}{\partial \theta} = \hat{\boldsymbol{\theta}}$ and $\frac{\partial \hat{\boldsymbol{\theta}}}{\partial \theta} = -\hat{\boldsymbol{r}}$); gives

$$\begin{aligned}\mathrm{d}\boldsymbol{u} = &\left(\frac{\partial u}{\partial r}\mathrm{d}r + \left(\frac{1}{r}\frac{\partial u}{\partial \theta} - \frac{v}{r}\right)r\mathrm{d}\theta + \frac{\partial u}{\partial z}\mathrm{d}z\right)\hat{\boldsymbol{r}} \qquad (3.21)\\ &+ \left(\frac{\partial v}{\partial r}\mathrm{d}r + \left(\frac{1}{r}\frac{\partial v}{\partial \theta} + \frac{u}{r}\right)r\mathrm{d}\theta + \frac{\partial v}{\partial z}\mathrm{d}z\right)\hat{\boldsymbol{\theta}}\\ &+ \left(\frac{\partial w}{\partial r}\mathrm{d}r + \left(\frac{1}{r}\frac{\partial w}{\partial \theta}\right)r\mathrm{d}\theta + \frac{\partial w}{\partial z}\mathrm{d}z\right)\hat{\boldsymbol{z}}. \qquad (3.22)\end{aligned}$$

Eqn.(3.22) can be written in matrix form as follows:

$$\begin{bmatrix} \mathrm{d}u \\ \mathrm{d}v \\ \mathrm{d}w \end{bmatrix} = \begin{bmatrix} \frac{\partial u}{\partial r} & \frac{1}{r}\frac{\partial u}{\partial \theta} - \frac{v}{r} & \frac{\partial u}{\partial z} \\ \frac{\partial v}{\partial r} & \frac{1}{r}\frac{\partial v}{\partial \theta} + \frac{u}{r} & \frac{\partial v}{\partial z} \\ \frac{\partial w}{\partial r} & \frac{1}{r}\frac{\partial w}{\partial \theta} & \frac{\partial w}{\partial z} \end{bmatrix} \begin{bmatrix} \mathrm{d}r \\ r\mathrm{d}\theta \\ \mathrm{d}z \end{bmatrix}. \tag{3.23}$$

From Eqn.(3.23), we deduce that the matrix representation of the displacement gradient in cylindrical coordinates is [6]

$$\boldsymbol{\nabla u} \rightarrow \begin{bmatrix} \frac{\partial u}{\partial r} & \frac{1}{r}\frac{\partial u}{\partial \theta} - \frac{v}{r} & \frac{\partial u}{\partial z} \\ \frac{\partial v}{\partial r} & \frac{1}{r}\frac{\partial v}{\partial \theta} + \frac{u}{r} & \frac{\partial v}{\partial z} \\ \frac{\partial w}{\partial r} & \frac{1}{r}\frac{\partial w}{\partial \theta} & \frac{\partial w}{\partial z} \end{bmatrix}. \tag{3.24}$$

Since by definition, the strain tensor is the symmetric part of the displacement gradient; it follows that the strain matrix in cylindrical coordinates is defined as [6]

$$\boldsymbol{S} = \frac{1}{2}\left(\boldsymbol{\nabla u} + \tilde{\boldsymbol{\nabla}}\boldsymbol{u}\right). \tag{3.25}$$

Therefore, from Eqn.(3.25), it is easily shown that the components of the strain tensor

(strain-displacement relations) in cylindrical coordinates are as follows [12]:

$$\begin{aligned} S_{rr} &= \frac{\partial u}{\partial r}, \quad S_{\theta\theta} = \frac{1}{r}\left(u + \frac{\partial v}{\partial \theta}\right), \\ S_{zz} &= \frac{\partial w}{\partial z}, \quad S_{rz} = \frac{1}{2}\left(\frac{\partial w}{\partial r} + \frac{\partial u}{\partial z}\right), \\ S_{r\theta} &= \frac{1}{2r}\left(\frac{\partial u}{\partial \theta} - v\right) + \frac{1}{2}\frac{\partial v}{\partial r}, \quad S_{z\theta} = \frac{1}{2}\left(\frac{\partial v}{\partial z} + \frac{1}{r}\frac{\partial w}{\partial \theta}\right). \end{aligned} \tag{3.26}$$

5. Due to the quasi-static approximation, the electric field generated by the strain field can be expressed as a gradient of a scalar potential i.e.

$$\boldsymbol{E} = -\boldsymbol{\nabla}\phi; \tag{3.27}$$

where $\phi$ is the electric potential. When Eqn.(3.27) is expanded in cylindrical coordinates, the components of $\boldsymbol{E}$ are given as follows:

$$E_r = -\frac{\partial \phi}{\partial r}, \quad E_\theta = -\frac{1}{r}\frac{\partial \phi}{\partial \theta}, \quad E_z = -\frac{\partial \phi}{\partial z}. \tag{3.28}$$

For completeness, the matrix representation of the material constants used in the constitutive relations are, as stated in the previous chapter are given below [10]:

$$c_{ab}^E = \begin{bmatrix} c_{11}^E & c_{12}^E & c_{13}^E & 0 & 0 & 0 \\ c_{12}^E & c_{11}^E & c_{13}^E & 0 & 0 & 0 \\ c_{13}^E & c_{13}^E & c_{33}^E & 0 & 0 & 0 \\ 0 & 0 & 0 & c_{55}^E & 0 & 0 \\ 0 & 0 & 0 & 0 & c_{55}^E & 0 \\ 0 & 0 & 0 & 0 & 0 & c_{66}^E \end{bmatrix}; \tag{3.29}$$

where $2c_{66}^E = \left(c_{11}^E - c_{12}^E\right)$ and $a, b = 1, 2, ..., 6$;

$$e_{ia} = \begin{bmatrix} 0 & 0 & 0 & 0 & e_{15} & 0 \\ 0 & 0 & 0 & e_{15} & 0 & 0 \\ e_{15} & e_{31} & e_{33} & 0 & 0 & 0 \end{bmatrix}, \tag{3.30}$$

$$\epsilon_{ij}^{S} = \begin{bmatrix} \epsilon_{11}^{S} & 0 & 0 \\ 0 & \epsilon_{11}^{S} & 0 \\ 0 & 0 & \epsilon_{33}^{S} \end{bmatrix}. \tag{3.31}$$

Making use of the above matrices, the constitutive equations can be obtained by expanding the matrix product below [27]

$$\left[\begin{array}{c} D_1 \\ D_2 \\ D_3 \\ \hline \sigma_1 \\ \sigma_2 \\ \sigma_3 \\ \sigma_4 \\ \sigma_5 \\ \sigma_6 \end{array}\right] = \left[\begin{array}{ccc|cccccc} \epsilon_{11}^{S} & 0 & 0 & 0 & 0 & 0 & 0 & e_{15} & 0 \\ 0 & \epsilon_{11}^{S} & 0 & 0 & 0 & 0 & e_{15} & 0 & 0 \\ 0 & 0 & \epsilon_{33}^{S} & e_{15} & e_{31} & e_{33} & 0 & 0 & 0 \\ \hline 0 & 0 & -e_{31} & c_{11}^{E} & c_{12}^{E} & c_{13}^{E} & 0 & 0 & 0 \\ 0 & 0 & -e_{31} & c_{12}^{E} & c_{11}^{E} & c_{13}^{E} & 0 & 0 & 0 \\ 0 & 0 & -e_{33} & c_{13}^{E} & c_{13}^{E} & c_{33}^{E} & 0 & 0 & 0 \\ 0 & -e_{15} & 0 & 0 & 0 & 0 & c_{55}^{E} & 0 & 0 \\ -e_{15} & 0 & 0 & 0 & 0 & 0 & 0 & c_{55}^{E} & 0 \\ 0 & 0 & 0 & 0 & 0 & 0 & 0 & 0 & c_{66}^{E} \end{array}\right] \left[\begin{array}{c} E_1 \\ E_2 \\ E_3 \\ \hline S_1 \\ S_2 \\ S_3 \\ S_4 \\ S_5 \\ S_6 \end{array}\right]. \tag{3.32}$$

Thus, in expanded form the constitutive relations are expressed as follows:

$$\sigma_1 = c_{11}^{E} S_1 + c_{12}^{E} S_2 + c_{13}^{E} S_3 - e_{31} E_3, \tag{3.33a}$$

$$\sigma_2 = c_{12}^{E} S_1 + c_{11}^{E} S_2 + c_{13}^{E} S_3 - e_{31} E_3, \tag{3.33b}$$

$$\sigma_3 = c_{13}^{E} \left(S_1 + S_2\right) + c_{33}^{E} S_3 - e_{33} E_3, \tag{3.33c}$$

$$\sigma_4 = c_{55}^{E} S_4 - e_{15} E_2, \quad \sigma_5 = c_{55}^{E} S_5 - e_{15} E_1, \quad \sigma_6 = c_{66}^{E} S_6, \tag{3.33d}$$

$$D_1 = \epsilon_{11}^{S} E_1 + e_{15} S_5, \quad D_2 = \epsilon_{11}^{S} E_2 + e_{15} S_4, \tag{3.33e}$$

$$D_3 = \epsilon_{33}^{S} E_3 + e_{31} \left(S_1 + S_2\right) + e_{33} S_3. \tag{3.33f}$$

Hereafter, $c_{pq}^{E}$ and $\epsilon_{ij}^{s}$ will be denoted for convenience as $c_{pq}$ and $\epsilon_{ij}$ respectively.

Combining the field equations, the constitutive relations stated above and assuming harmonic solutions in time (because of Hook's law) and with the use of Maple's symbolic package, yields

the four coupled equations below:

$$c_{11}\left(\frac{\partial^2 u}{\partial r^2}+\frac{1}{r}\frac{\partial u}{\partial r}-\frac{1}{r^2}\frac{\partial v}{\partial \theta}-\frac{u}{r}\right)+c_{66}\left(\frac{1}{r}\frac{\partial^2 v}{\partial \theta \partial r}+\frac{1}{r^2}\frac{\partial^2 u}{\partial \theta^2}-\frac{1}{r^2}\frac{\partial v}{\partial \theta}\right)$$
$$+c_{44}\left(\frac{\partial^2 u}{\partial z^2}+\frac{\partial^2 w}{\partial z \partial r}\right)+c_{13}\frac{\partial^2 w}{\partial z \partial r}+e_{31}\frac{\partial^2 \phi}{\partial z \partial r}+\rho\omega^2 u=0, \tag{3.34a}$$

$$c_{66}\left(\frac{\partial^2 v}{\partial r^2}+\frac{1}{r^2}\frac{\partial u}{\partial \theta}-\frac{1}{r^2}v+\frac{1}{r}\frac{\partial^2 u}{\partial \theta \partial r}+\frac{1}{r}\frac{\partial v}{\partial r}\right)+c_{11}\left(\frac{1}{r^2}\frac{\partial^2 v}{\partial \theta^2}+\frac{1}{r^2}\frac{\partial u}{\partial \theta}\right)$$
$$+c_{44}\left(\frac{\partial^2 v}{\partial z^2}+\frac{1}{r}\frac{\partial^2 w}{\partial z \partial \theta}\right)+\frac{c_{12}}{r}\frac{\partial^2 u}{\partial \theta \partial r}+\frac{c_{13}}{r}\frac{\partial^2 w}{\partial z \partial \theta}+\frac{e_{31}}{r}\frac{\partial^2 \phi}{\partial z \partial \theta}+\frac{e_{15}}{r}\frac{\partial^2 \phi}{\partial z \partial \theta}+\rho\omega^2 v=0, \tag{3.34b}$$

$$c_{44}\left(\frac{1}{r}\frac{\partial^2 v}{\partial z \partial \theta}+\frac{1}{r^2}\frac{\partial^2 w}{\partial \theta^2}+\frac{\partial^2 u}{\partial z \partial r}+\frac{\partial^2 w}{\partial r^2}+\frac{1}{r}\frac{\partial u}{\partial z}+\frac{1}{r}\frac{\partial w}{\partial r}\right)+c_{13}\left(\frac{\partial^2 u}{\partial z \partial r}+\frac{1}{r}\frac{\partial^2 v}{\partial z \partial \theta}+\frac{1}{r}\frac{\partial u}{\partial z}\right)$$
$$+c_{33}\frac{\partial^2 w}{\partial z^2}+\frac{e_{15}}{r}\frac{\partial \phi}{\partial r}+e_{15}\frac{\partial^2 \phi}{\partial r^2}+\frac{e_{15}}{r^2}\frac{\partial^2 \phi}{\partial \theta^2}+e_{33}\frac{\partial^2 \phi}{\partial z^2}+\rho\omega^2 w=0, \tag{3.34c}$$

$$e_{15}\left(\frac{1}{r}\frac{\partial^2 v}{\partial z \partial \theta}+\frac{1}{r^2}\frac{\partial^2 w}{\partial \theta^2}+\frac{\partial^2 u}{\partial z \partial r}+\frac{\partial^2 w}{\partial r^2}+\frac{1}{r}\frac{\partial u}{\partial z}+\frac{1}{r}\frac{\partial w}{\partial r}\right)+e_{31}\left(\frac{\partial^2 u}{\partial z \partial r}+\frac{1}{r}\frac{\partial^2 v}{\partial z \partial \theta}+\frac{1}{r}\frac{\partial u}{\partial z}\right)$$
$$+e_{33}\frac{\partial^2 w}{\partial z^2}+\epsilon_{11}\left(-\frac{\partial^2 \phi}{\partial r^2}-\frac{1}{r}\frac{\partial \phi}{\partial r}-\frac{1}{r^2}\frac{\partial^2 \phi}{\partial \theta^2}\right)-\epsilon_{33}\frac{\partial^2 \phi}{\partial z^2}=0. \tag{3.34d}$$

The above equations are the governing equations of motion for the system. Because we are solving a guided wave problem, these equations have to be supplemented by physically allowed boundary condition, so as to make the problem well posed. These boundary conditions will appear naturally, when we derive the equations of motion via Hamilton's variational principle.

## 3.4 Method 2: Derivation of Equations of Motion via Hamilton's Variational Principle.

Here we derive the equations of motion from Hamilton's variational principle. As already mentioned, this method has the advantage of leading naturally to the boundary conditions of the system. In order to use Hamiltons principle, we need to define the Lagrangian, $L$ of the system; and based on the assumptions on which the model is based, the Lagrangian is defined as follows [28]:

$$\tilde{L}=\tilde{K}-\tilde{U}+\tilde{W}, \tag{3.35}$$

where $\tilde{K}$ is the kinetic energy; $\tilde{U}$ the strain energy and $\tilde{W}$ the electric potential energy. The Lagrangian as defined above is exactly the same as that used by Nesbitt et al in [27], to model piezoelectric actuator dynamics for active structural control. The definitions of $\tilde{K}$, $\tilde{U}$ and $\tilde{W}$ for the cylinder are defined as follows:

$$\begin{aligned}
\tilde{K} &= \frac{\rho}{2}\int_{-\infty}^{\infty}\int_{0}^{2\pi}\int_{0}^{a}\left(\dot{u}^2+\dot{v}^2+\dot{w}^2\right) r\,\mathrm{d}r\mathrm{d}\theta\mathrm{d}z,\\
\tilde{U} &= \frac{1}{2}\int_{-\infty}^{\infty}\int_{0}^{2\pi}\int_{0}^{a}\left(\sigma_1 S_1+\sigma_2 S_2+\sigma_3 S_3+\sigma_6 S_6+\sigma_5 S_5+\sigma_4 S_4\right) r\,\mathrm{d}r\mathrm{d}\theta\mathrm{d}z,\\
\tilde{W} &= \frac{1}{2}\int_{-\infty}^{\infty}\int_{0}^{2\pi}\int_{0}^{a}\left(D_1 E_1+D_2 E_2+D_3 E_3\right) r\,\mathrm{d}r\mathrm{d}\theta\mathrm{d}z.
\end{aligned} \tag{3.36}$$

From Eqn.(3.36), we can express the kinetic, elastic and electric energy densities as follows:

$$\begin{aligned}
K &= K\left(\dot{u},\dot{v},\dot{w}\right),\\
U &= U\left(u,v,u'_r,v'_r,w'_r,u'_\theta,v'_\theta,w'_\theta,u'_z,v'_z,w'_z,\phi'_r,\phi'_\theta,\phi'_z\right),\\
W &= W\left(u,u'_r,w'_r,v'_\theta,w'_\theta,u'_z,w'_z,\phi'_r,\phi'_\theta,\phi'_z\right);
\end{aligned}$$

where $u'_r$ denotes derivative of $u$ with respect to $r$; with the other independent variables defined similarly. Therefore, the Lagrangian density can be expressed as a function of the following variables

$$L = L\left(u,v,\dot{u},\dot{v},\dot{w},u'_r,v'_r,w'_r,u'_\theta,v'_\theta,w'_\theta,u'_z,v'_z,w'_z,\phi'_r,\phi'_\theta,\phi'_z\right).$$

Lets define a new function, $L'$ to be the Lagrangian density multiplied by $r$; which will simplify our subsequent derivations. By making use of Maple's symbolic package, the following explicit expression for $L'$ has been obtained:

$$\begin{aligned}
L' = {} & \frac{\rho}{2}\left(\dot{u}^2+\dot{v}^2+\dot{w}^2\right) r+\frac{1}{2}\left(-\left(e_{15}\left(u'_z+w'_r\right)-\epsilon_{11}\phi'_r\right)\phi'_r-\frac{1}{r}\left(e_{15}\left(v'_z+\frac{w'_\theta}{r}\right)-\frac{\epsilon_{11}\phi'_\theta}{r}\right)\phi'_\theta\right.\\
& -\left(-\epsilon_{33}\phi'_z+e_{31}\left(u'_r+\frac{v'_\theta+u}{r}\right)+e_{33}w'_z\right)\phi'_z-\left(c_{11}u'_r+\frac{c_{12}\left(v'_\theta+u\right)}{r}+c_{13}w'_z+e_{31}\phi'_z\right)u'_r\\
& -\left(c_{13}\left(u'_r+\frac{v'_\theta+u}{r}\right)+c_{33}w'_z+e_{33}\phi'_z\right)w'_z-\left(c_{44}\left(v'_z+\frac{w'_\theta}{r}\right)+\frac{e_{15}\phi'_\theta}{r}\right)\left(v'_z+\frac{w'_\theta}{r}\right)\\
& -\left(c_{44}\left(u'_z+w'_r\right)+e_{15}\phi'_r\right)\left(u'_z+w'_r\right)-c_{66}\left(v'_r+\frac{u'_\theta-v}{r}\right)^2-\frac{\left(v'_\theta+u\right)}{r}\left(c_{13}w'_z+e_{31}\phi'_z\right)\\
& \left.-\frac{\left(v'_\theta+u\right)}{r}\left(c_{12}u'_r+\frac{c_{11}\left(v'_\theta+u\right)}{r}\right)\right) r.
\end{aligned} \tag{3.37}$$

The action, $A$ for the system is defined as

$$\begin{aligned} A &= \int_0^\tau \tilde{L}\mathrm{d}t \\ &= \int_0^\tau \int_{-\infty}^{\infty} \int_0^{2\pi} \int_0^a L' \,\mathrm{d}r\mathrm{d}\theta\mathrm{d}z\mathrm{d}t. \end{aligned} \tag{3.38}$$

According to Hamilton's variational principle, the action is stationary on the real (natural) motion of system; expressed mathematically as follows:

$$\delta A = 0 \quad \text{on a real trajectory.} \tag{3.39}$$

Let's perform a variation on $L'$;

$$\begin{aligned} \delta L' =& \frac{\partial L'}{\partial u}\delta u + \frac{\partial L'}{\partial v}\delta v + \frac{\partial L'}{\partial \dot{u}}\delta \dot{u} + \frac{\partial L'}{\partial \dot{v}}\delta \dot{v} + \frac{\partial L'}{\partial \dot{w}}\delta \dot{w} + \frac{\partial L'}{\partial u'_r}\delta u'_r + \\ & \frac{\partial L'}{\partial v'_r}\delta v'_r + \frac{\partial L'}{\partial w'_r}\delta w'_r + \frac{\partial L'}{\partial u'_\theta}\delta u'_\theta + \frac{\partial L'}{\partial v'_\theta}\delta v'_\theta + \frac{\partial L'}{\partial w'_\theta}\delta w'_\theta + \qquad (3.40) \\ & \frac{\partial L'}{\partial u'_z}\delta u'_z + \frac{\partial L'}{\partial v'_z}\delta v'_z + \frac{\partial L'}{\partial w'_z}\delta w'_z + \frac{\partial L'}{\partial \phi'_r}\delta \phi'_r + \frac{\partial L'}{\partial \phi'_\theta}\delta \phi'_\theta + \frac{\partial L'}{\partial \phi'_z}\delta \phi'_z; \qquad (3.41) \end{aligned}$$

where we have neglected higher order terms for small perturbations. We observe that

$$\frac{\partial L'}{\partial \dot{q}}\delta \dot{q} = \frac{\partial}{\partial t}\left(\frac{\partial L'}{\partial \dot{q}}\delta q\right) - \frac{\partial}{\partial t}\left(\frac{\partial L'}{\partial \dot{q}}\right)\delta q; \tag{3.42}$$

where $q = u, v, w$, and

$$\frac{\partial L'}{\partial q'_s}\delta q'_s = \frac{\partial}{\partial s}\left(\frac{\partial L'}{\partial q'_s}\delta q\right) - \frac{\partial}{\partial s}\left(\frac{\partial L'}{\partial q'_s}\right)\delta q; \tag{3.43}$$

where $s = r, \theta, z$ and $q'_s$ stands for derivatives of $q$ w.r.t $s$, and finally

$$\frac{\partial L'}{\partial \phi'_s}\delta \phi'_s = \frac{\partial}{\partial s}\left(\frac{\partial L'}{\partial \phi'_s}\delta \phi\right) - \frac{\partial}{\partial s}\left(\frac{\partial L'}{\partial \phi'_s}\right)\delta \phi. \tag{3.44}$$

Substituting Eqns.(3.42), (3.43) and (3.44), into (3.41) yields

$$\begin{aligned} \delta L' =& \frac{\partial}{\partial t}\left(\frac{\partial L'}{\partial \dot{u}}\delta u + \frac{\partial L'}{\partial \dot{v}}\delta v + \frac{\partial L'}{\partial \dot{w}}\delta w\right) + \frac{\partial}{\partial r}\left(\frac{\partial L'}{\partial u'_r}\delta u + \frac{\partial L'}{\partial v'_r}\delta v + \frac{\partial L'}{\partial w'_r}\delta w + \frac{\partial L'}{\partial \phi'_r}\delta \phi\right) \\ & + \frac{\partial}{\partial \theta}\left(\frac{\partial L'}{\partial u'_\theta}\delta u + \frac{\partial L'}{\partial v'_\theta}\delta v + \frac{\partial L'}{\partial w'_\theta}\delta w + \frac{\partial L'}{\partial \phi'_\theta}\delta \phi\right) + \frac{\partial}{\partial z}\left(\frac{\partial L'}{\partial u'_z}\delta u + \frac{\partial L'}{\partial v'_z}\delta v + \frac{\partial L'}{\partial w'_z}\delta w + \frac{\partial L'}{\partial \phi'_z}\delta \phi\right) \\ & - \Big[\frac{\partial}{\partial t}\left(\frac{\partial L'}{\partial \dot{u}}\right) + \frac{\partial}{\partial r}\left(\frac{\partial L'}{\partial u'_r}\right) + \frac{\partial}{\partial \theta}\left(\frac{\partial L'}{\partial u'_\theta}\right) + \frac{\partial}{\partial z}\left(\frac{\partial L'}{\partial u'_z}\right) - \frac{\partial L'}{\partial u}\Big]\delta u \qquad (3.45) \\ & - \Big[\frac{\partial}{\partial t}\left(\frac{\partial L'}{\partial \dot{v}}\right) + \frac{\partial}{\partial r}\left(\frac{\partial L'}{\partial v'_r}\right) + \frac{\partial}{\partial \theta}\left(\frac{\partial L'}{\partial v'_\theta}\right) + \frac{\partial}{\partial z}\left(\frac{\partial L'}{\partial v'_z}\right) - \frac{\partial L'}{\partial v}\Big]\delta v \\ & - \Big[\frac{\partial}{\partial t}\left(\frac{\partial L'}{\partial \dot{w}}\right) + \frac{\partial}{\partial r}\left(\frac{\partial L'}{\partial w'_r}\right) + \frac{\partial}{\partial \theta}\left(\frac{\partial L'}{\partial w'_\theta}\right) + \frac{\partial}{\partial z}\left(\frac{\partial L'}{\partial w'_z}\right)\Big]\delta w \\ & - \Big[\frac{\partial}{\partial r}\left(\frac{\partial L'}{\partial \phi'_r}\right) + \frac{\partial}{\partial \theta}\left(\frac{\partial L'}{\partial \phi'_\theta}\right) + \frac{\partial}{\partial z}\left(\frac{\partial L'}{\partial \phi'_z}\right)\Big]\delta \phi. \end{aligned}$$

Therefore, we have

$$\delta A = \delta \int_{-\infty}^{\infty}\int_{0}^{2\pi}\int_{0}^{a}\int_{0}^{\tau} L'\,\mathrm{d}r\mathrm{d}\theta\mathrm{d}t\mathrm{d}z$$

$$\begin{aligned}
\delta A = \int_{-\infty}^{\infty}\int_{0}^{2\pi}\int_{0}^{a}\int_{0}^{\tau}\Big[&\frac{\partial}{\partial z}\left(\frac{\partial L'}{\partial u'_z}\delta u + \frac{\partial L'}{\partial v'_z}\delta v + \frac{\partial L'}{\partial w'_z}\delta w + \frac{\partial L'}{\partial \phi'_z}\delta\phi\right)\\
&+ \frac{\partial}{\partial \theta}\left(\frac{\partial L'}{\partial u'_\theta}\delta u + \frac{\partial L'}{\partial v'_\theta}\delta v + \frac{\partial L'}{\partial w'_\theta}\delta w + \frac{\partial L'}{\partial \phi'_\theta}\delta\phi\right)\\
&+ \frac{\partial}{\partial r}\left(\frac{\partial L'}{\partial u'_r}\delta u + \frac{\partial L'}{\partial v'_r}\delta v + \frac{\partial L'}{\partial w'_r}\delta w + \frac{\partial L'}{\partial \phi'_r}\delta\phi\right)\\
&+ \frac{\partial}{\partial t}\left(\frac{\partial L'}{\partial \dot{u}}\delta u + \frac{\partial L'}{\partial \dot{v}}\delta v + \frac{\partial L'}{\partial \dot{w}}\delta w\right)\Big]\,\mathrm{d}t\mathrm{d}r\mathrm{d}\theta\mathrm{d}z
\end{aligned} \tag{3.46}$$

$$\begin{aligned}
&-\int_{-\infty}^{\infty}\int_{0}^{2\pi}\int_{0}^{a}\int_{0}^{\tau}\Big[\Big(\frac{\partial}{\partial t}\left(\frac{\partial L'}{\partial \dot{u}}\right) + \frac{\partial}{\partial r}\left(\frac{\partial L'}{\partial u'_r}\right) + \frac{\partial}{\partial \theta}\left(\frac{\partial L'}{\partial u'_\theta}\right) + \frac{\partial}{\partial z}\left(\frac{\partial L'}{\partial u'_z}\right) - \frac{\partial L'}{\partial u}\Big)\delta u\\
&+ \Big(\frac{\partial}{\partial t}\left(\frac{\partial L'}{\partial \dot{v}}\right) + \frac{\partial}{\partial r}\left(\frac{\partial L'}{\partial v'_r}\right) + \frac{\partial}{\partial \theta}\left(\frac{\partial L'}{\partial v'_\theta}\right) + \frac{\partial}{\partial z}\left(\frac{\partial L'}{\partial v'_z}\right) - \frac{\partial L'}{\partial v}\Big)\delta v\\
&+ -\Big(\frac{\partial}{\partial t}\left(\frac{\partial L'}{\partial \dot{w}}\right) + \frac{\partial}{\partial r}\left(\frac{\partial L'}{\partial w'_r}\right) + \frac{\partial}{\partial \theta}\left(\frac{\partial L'}{\partial w'_\theta}\right) + \frac{\partial}{\partial z}\left(\frac{\partial L'}{\partial w'_z}\right)\Big)\delta w\\
&+ \Big(\frac{\partial}{\partial r}\left(\frac{\partial L'}{\partial \phi'_r}\right) + \frac{\partial}{\partial \theta}\left(\frac{\partial L'}{\partial \phi'_\theta}\right) + \frac{\partial}{\partial z}\left(\frac{\partial L'}{\partial \phi'_z}\right)\Big)\delta\phi\Big]\,\mathrm{d}t\mathrm{d}r\mathrm{d}\theta\mathrm{d}z.
\end{aligned}$$

Let's call the first term of Eqn.(3.46) $\Pi_1$ and the second term $\Pi_2$. Clearly, Eqn.(3.46) is zero if in particular

$$\Pi_1 = 0 \quad \text{and} \quad \Pi_2 = 0. \tag{3.47}$$

The condition $\Pi_1 = 0$, leads to the boundary conditions of the problem and $\Pi_2 = 0$ leads to the equations of motion for the system; we demonstrate this assertion below.

The condition, $\Pi_2 = 0$, in Eqn.(3.47) will be satisfied for arbitrary $\delta u$, $\delta v$, $\delta w$ and $\delta\phi$ if and only if

$$\frac{\partial}{\partial t}\left(\frac{\partial L'}{\partial \dot{u}}\right) + \frac{\partial}{\partial r}\left(\frac{\partial L'}{\partial u'_r}\right) + \frac{\partial}{\partial \theta}\left(\frac{\partial L'}{\partial u'_\theta}\right) + \frac{\partial}{\partial z}\left(\frac{\partial L'}{\partial u'_z}\right) - \frac{\partial L'}{\partial u} = 0, \tag{3.48a}$$

$$\frac{\partial}{\partial t}\left(\frac{\partial L'}{\partial \dot{v}}\right) + \frac{\partial}{\partial r}\left(\frac{\partial L'}{\partial v'_r}\right) + \frac{\partial}{\partial \theta}\left(\frac{\partial L'}{\partial v'_\theta}\right) + \frac{\partial}{\partial z}\left(\frac{\partial L'}{\partial v'_z}\right) - \frac{\partial L'}{\partial v} = 0, \tag{3.48b}$$

$$\frac{\partial}{\partial t}\left(\frac{\partial L'}{\partial \dot{w}}\right) + \frac{\partial}{\partial r}\left(\frac{\partial L'}{\partial w'_r}\right) + \frac{\partial}{\partial \theta}\left(\frac{\partial L'}{\partial w'_\theta}\right) + \frac{\partial}{\partial z}\left(\frac{\partial L'}{\partial w'_z}\right) = 0, \tag{3.48c}$$

$$\frac{\partial}{\partial r}\left(\frac{\partial L'}{\partial \phi'_r}\right) + \frac{\partial}{\partial \theta}\left(\frac{\partial L'}{\partial \phi'_\theta}\right) + \frac{\partial}{\partial z}\left(\frac{\partial L'}{\partial \phi'_z}\right) = 0. \tag{3.48d}$$

The Eqns.(3.48), are the equations of motion for the cylinder system, which when simplified further, leads to our previous equations of motion obtained in Eqns.(3.34). For example, let us compare Eqns.(3.34d) and (3.48d). From the expression of $L'$ in Eqn.(3.37), and utilising Maple's symbolic package we obtain the following:

$$\begin{aligned}\frac{1}{r}\frac{\partial}{\partial r}\left(\frac{-\partial L'}{\partial \phi_r'}\right) &= \frac{1}{r}\frac{\partial}{\partial r}\big((u_z' + w_r')\, r e_{15} - \epsilon_{11}\phi_r' r\big) \\ &= \big(u_{z,r}'' + w_r'' + \frac{1}{r}\,(u_z' + w_r')\big)e_{15} - \left(\phi_r'' - \frac{1}{r}\phi_r'\right)\epsilon_{11};\end{aligned} \tag{3.49}$$

$$\begin{aligned}\frac{1}{r}\frac{\partial}{\partial \theta}\left(\frac{-\partial L'}{\partial \phi_\theta'}\right) &= \frac{1}{r}\frac{\partial}{\partial \theta}\left(\frac{(v_z' r + w_\theta')\, e_{15}}{r} - \frac{\epsilon_{11}\phi_\theta'}{r}\right) \\ &= \left(\frac{v_{z\theta}''}{r} + \frac{w_\theta''}{r^2}\right) e_{15} - \frac{\epsilon_{11}\phi_\theta''}{r^2};\end{aligned} \tag{3.50}$$

$$\begin{aligned}\frac{1}{r}\frac{\partial}{\partial z}\left(\frac{-\partial L'}{\partial \phi_z'}\right) &= \frac{1}{r}\frac{\partial}{\partial z}\big(e_{31}\,(u_r' r + v_\theta' + u) - \epsilon_{33}\phi_z' r + e_{33} w_z' r\big) \\ &= e_{31}\left(u_{rz}'' + \frac{v_{\theta z}''}{r} + \frac{u_z'}{r}\right) + e_{33} w_z'' - \epsilon_{33}\phi_z''.\end{aligned} \tag{3.51}$$

Substituting Eqns.(4.20), (3.50) and (4.21) into Eqn.(3.48d), we obtain

$$\begin{aligned}&\big(u_{zr}'' + w_r'' + \frac{1}{r}\,(u_z' + w_r') + \frac{v_{z\theta}''}{r} + \frac{w_\theta''}{r^2}\big)e_{15} + \left(u_{rz}'' + \frac{v_{\theta z}''}{r} + \frac{u_z''}{r}\right) e_{31} \\ &+ e_{33} w_z'' - \left(\phi_r'' + \frac{\phi_r'}{r} + \frac{\phi_\theta''}{r^2}\right)\epsilon_{11} - \epsilon_{33}\phi_z'' = 0.\end{aligned} \tag{3.52}$$

We can clearly see that Eqn.(4.22) is in perfect agreement with Eqn.(3.34d).

The condition, $\Pi_1 = 0$, leads to the following:

$$\begin{aligned}&\Pi_1 = 0 \Rightarrow \\ &\int_{-\infty}^{\infty}\int_0^{2\pi}\int_0^a\int_0^\tau \Big[\frac{\partial}{\partial z}\left(\frac{\partial L'}{\partial u_z'}\delta u + \frac{\partial L'}{\partial v_z'}\delta v + \frac{\partial L'}{\partial w_z'}\delta w + \frac{\partial L'}{\partial \phi_z'}\delta\phi\right) \\ &+ \frac{\partial}{\partial \theta}\left(\frac{\partial L'}{\partial u_\theta'}\delta u + \frac{\partial L'}{\partial v_\theta'}\delta v + \frac{\partial L'}{\partial w_\theta'}\delta w + \frac{\partial L'}{\partial \phi_\theta'}\delta\phi\right) \\ &+ \frac{\partial}{\partial r}\left(\frac{\partial L'}{\partial u_r'}\delta u + \frac{\partial L'}{\partial v_r'}\delta v + \frac{\partial L'}{\partial w_r'}\delta w + \frac{\partial L'}{\partial \phi_r'}\delta\phi\right) \\ &+ \frac{\partial}{\partial t}\left(\frac{\partial L'}{\partial \dot{u}}\delta u + \frac{\partial L'}{\partial \dot{v}}\delta v + \frac{\partial L'}{\partial \dot{w}}\delta w\right)\Big]\,\mathrm{d}t\mathrm{d}r\mathrm{d}\theta\mathrm{d}z = 0;\end{aligned} \tag{3.53}$$

Eqn.(3.53) then leads to

$$\left[\frac{\partial L'}{\partial u'_z}\delta u + \frac{\partial L'}{\partial v'_z}\delta v + \frac{\partial L'}{\partial w'_z}\delta w + \frac{\partial L'}{\partial \phi'_z}\delta\phi\right]_{z\to-\infty}^{z\to+\infty} + \left[\frac{\partial L'}{\partial u'_\theta}\delta u + \frac{\partial L'}{\partial v'_\theta}\delta v + \frac{\partial L'}{\partial w'_\theta}\delta w + \frac{\partial L'}{\partial \phi'_\theta}\delta\phi\right]_{\theta=0}^{\theta=2\pi}$$
$$+ \left[\frac{\partial L'}{\partial u'_r}\delta u + \frac{\partial L'}{\partial v'_r}\delta v + \frac{\partial L'}{\partial w'_r}\delta w + \frac{\partial L'}{\partial \phi'_r}\delta\phi\right]_{r=0}^{r=a} + \left[\frac{\partial L'}{\partial \dot{u}}\delta u + \frac{\partial L'}{\partial \dot{v}}\delta v + \frac{\partial L'}{\partial \dot{w}}\delta w\right]_{t=0}^{t=\tau} = 0. \quad (3.54)$$

Eqn.(3.54) can further be simplified by observing that from Hamilton's variational principle, $\delta u$, $\delta v$, $\delta w$, and $\delta\phi$ are zero at $t = 0$ and $t = \tau$. Also, from the geometry of our system; the points $\theta = 0$ and $\theta = 2\pi$ must be equal, since we assume a homogeneous circular cylinder of infinite length. Therefore, the second and fourth terms in Eqn.(3.54) are identically equal to zero. Thus, Eqn.(3.54) becomes

$$\left[\frac{\partial L'}{\partial u'_z}\delta u + \frac{\partial L'}{\partial v'_z}\delta v + \frac{\partial L'}{\partial w'_z}\delta w + \frac{\partial L'}{\partial \phi'_z}\delta\phi\right]_{z\to-\infty}^{z\to+\infty} + \left[\frac{\partial L'}{\partial u'_r}\delta u + \frac{\partial L'}{\partial v'_r}\delta v + \frac{\partial L'}{\partial w'_r}\delta w + \frac{\partial L'}{\partial \phi'_r}\delta\phi\right]_{r=0}^{r=a} = 0. \quad (3.55)$$

Eqn.(3.55) is satisfied for arbitrary variations of $u$, $v$, $w$ and $\phi$ if and only if the terms are individually equal to zero at both boundaries; i.e. $(-\infty, \infty)$ and $(0, a)$. However, we will not analyze the behavior of the first term in Eqn.(3.55), because it is analogous to a bulk wave problem where boundary conditions are not required. Rather, we will pursue the behavior of the second term at the boundaries $(0, a)$, which leads naturally to the allowed boundary conditions of the system. At $r = 0$ and $r = a$ from Eqn.(3.55), we have

$$\left.\frac{\partial L'}{\partial p'_r}\delta p\right|_0 = 0, \qquad \left.\frac{\partial L'}{\partial p'_r}\delta p\right|_a = 0 \quad \text{where} \quad p = u, v, w, \phi. \quad (3.56)$$

The conditions in the first term in Eqn.(3.56) will always be satisfied; since $\frac{\partial L'}{\partial p'_r}$ can be expressed in terms of Bessel's functions of the first kind, with orders greater than zero (a characteristics of guided wave solutions in rods [13, 9, 15]). But the condition in the second term of Eqn.(3.56) will be satisfied if either $p(a)$ is given an arbitrary value and $\left.\frac{\partial L'}{\partial p'_r}\right|_a = 0$; and vice versa. For example, without loss of generality, lets assume that $p(a)$ is arbitrary; in other words, we allow for free oscillations of the surface of the cylinder and also giving it an arbitrary electric potential. Therefore, we are left with the condition, $\left.\frac{\partial L'}{\partial p'_r}\right|_a = 0$; which when evaluated (with the use of Maple's symbolic package), we obtain the following familiar

expressions:

$$\left.\frac{\partial L'}{\partial u'_r}\right|_a = c_{11}u'_r + c_{12}\big[\frac{1}{r}\left(u + v'_\theta\right)\big] + c_{13}w'_z + e_{31}\phi'_z\Big|_a = \sigma_1|_a = 0, \tag{3.57a}$$

$$\left.\frac{\partial L'}{\partial v'_r}\right|_a = c_{66}\big[v'_r + \frac{1}{r}\left(u'_\theta - v\right)\big]\Big|_a = \sigma_6|_a = 0, \tag{3.57b}$$

$$\left.\frac{\partial L'}{\partial w'_r}\right|_a = c_{44}\left(u'_z + w'_r\right) + e_{15}\phi'_r|_a = \sigma_5|_a = 0, \tag{3.57c}$$

$$\left.\frac{\partial L'}{\partial \phi'_r}\right|_a = e_{15}\left(u'_z + w'_r\right) - \epsilon_{11}\phi'_r|_a = D_1|_a = 0. \tag{3.57d}$$

The Eqns.(3.57), are the boundary conditions of stresses and the electric displacement vector respectively at the surface $r = a$ of the cylinder in a vacuum, which agree nicely with those used in [10]. On the other hand, if the displacement vector component $D_1$, at the surface is arbitrary, while the electric potential $\phi$ is fixed to say zero for example (which is a physically plausible boundary condition for the given model system); then from Eqn.(3.56), the resulting boundary conditions are as follows:

$$\left.\frac{\partial L'}{\partial u'_r}\right|_a = c_{11}u'_r + c_{12}\big[\frac{1}{r}\left(u + v'_\theta\right)\big] + c_{13}w'_z + e_{31}\phi'_z\Big|_a = \sigma_1|_a = 0, \tag{3.58a}$$

$$\left.\frac{\partial L'}{\partial v'_r}\right|_a = c_{66}\big[v'_r + \frac{1}{r}\left(u'_\theta - v\right)\big]\Big|_a = \sigma_6|_a = 0, \tag{3.58b}$$

$$\left.\frac{\partial L'}{\partial w'_r}\right|_a = c_{44}\left(u'_z + w'_r\right) + e_{15}\phi'_r|_a = \sigma_5|_a = 0, \tag{3.58c}$$

$$\phi|_a = 0. \tag{3.58d}$$

So, we have obtained the equations of motion, together with the allowed physical boundary conditions of the piezoelectric solid cylinder, from a purely variational principle, saving us the challenge of figuring out the boundary conditions intuitively.

# Chapter 4

# Analytic Solutions for the Equations of Motion of the Cylinder and Numerical Results for a Sample PZT-4 rod

## 4.1 Introduction

In this chapter, we solve analytically the system of coupled partial differential equations developed in the previous chapter, that describes the propagation of non-axisymmetric elastic waves along the axis of a transversely isotropic piezoelectric solid cylinder. This system of equations will be solved in terms of four displacement and three electric potentials as opposed to three displacement potentials, first introduced by Mirsky [15]; this follows from the introduction of piezoelectric coupling in the cylinder.

After obtaining analytic solutions to the system of equations (though with arbitrary displacement amplitudes to be determined by application of boundary conditions), we will then

evaluate expressions for stress, electric displacement and electric potential by making use of the mechanical displacement component solutions already obtained. The mechanical and electrical boundary conditions satisfied by the stress components and the electric displacement vector component (or electric potential) are then imposed. This will lead to an algebraic system of linear homogeneous equations in terms of unknown displacement amplitudes. For nontrivial solutions of the system, we require the determinant of the coefficient matrix to be zero, which leads to the dispersion relation for the system. We then proceed as described above to develop the dispersion relation in determinantal form for the simpler problem of non-axisymmetric wave propagation in a non-piezoelectric cylinder. This will serve as a test to our model when the piezoelectric coupling approaches zero. The dispersion relations for the piezoelectric and non-piezoelectric models are then solved numerically for the sample piezoelectric material, PZT-4 and for the following transversely isotropic and isotropic materials: PZT-4 (with electromechanical coupling absent), aluminium (isotropic), cobalt and glass/epoxi fiber-reinforced composite cylinder. Resulting dispersion curves are then presented with two and four straight lines, which are artifacts combined with the allowed propagating wave modes for the non-piezoelectric and piezoelectric models respectively. We will then proceed with discussions of the results obtained (dispersion curves). Finally, we provide a discussion on the artifacts, to account for their existence and how they can be removed from the dispersion curves.

In this chapter we made use of the symbolic package of Maple to derive some additional complicated equations. We also performed a dimensional analysis check on these equations after typing them in Mathcad and this dissertation to ensure that no error has been made. The physical parameters and their dimensions used in this section are given below:

$$\begin{array}{ccccc} \sigma_{ij} = \frac{M}{T^2 L}, & S_{ij} = \frac{L}{L} & E = \frac{ML}{T^2 Q}, & D = \frac{Q}{L^2}, & \epsilon_{ij} = \frac{Q^2 T^2}{ML^3} \\ e_{ijk} = \frac{Q}{L^2}, & u,\, v,\, w = L, & \phi = \frac{ML^2}{T^2 Q}, & \varphi = L^2 & \omega = \frac{1}{T} \\ \psi = L^2, & T = \frac{ML^2}{T^2 Q}, & \mu = \frac{M}{T^2 Q}, & \eta = \frac{1}{L} & k = \frac{1}{L} \\ \xi = \frac{1}{L}, & a = \frac{1}{L^2}, & b = \frac{1}{L^4}, & c = \frac{1}{L^6}; & \end{array} \tag{4.1}$$

where $L$ = Length; $M$ = Mass; $T$ = Time; and $Q$ = Charge.

## 4.2 Analytic Solutions of the Equations of Motion for the Piezoelectric Cylinder

To obtain propagation of harmonic waves along the $z$-axis in the cylinder, we assume as Mirsky did [4] that the displacement vector field, $\boldsymbol{U}$ in the cylinder can be expressed in terms of two displacement potentials, $\varphi\,(r,\theta,z,t)$ and $\psi\,(r,\theta,z,t)$ as follows:

$$\boldsymbol{U} = \bar{\boldsymbol{\nabla}}\varphi e^{i(\omega t+kz)} + \boldsymbol{\nabla}\times(\psi e^{i(\omega t+kz)}\hat{e}_z) + \eta\varphi e^{i(\omega t+kz)}\hat{e}_z; \tag{4.2}$$

where $\bar{\boldsymbol{\nabla}} \equiv \frac{\partial}{\partial r}\hat{e}_r + \frac{1}{r}\frac{\partial}{\partial\theta}\hat{e}_\theta$; $\omega$ is the angular frequency, $k$ the axial wave number and $\eta$ is an unknown parameter to be determined later in the analysis. When Eqn.(4.2) is expanded, the displacement components $u$, $v$ and $w$ are expressed as follows [15]:

$$\begin{aligned} u\,(r,\theta,z,t) &= \left[\varphi_r + \frac{1}{r}\psi_\theta\right] e^{i(\omega t+kz)}, \\ v\,(r,\theta,z,t) &= \left[\frac{1}{r}\varphi_\theta - \psi_r\right] e^{i(\omega t+kz)}, \\ w\,(r,\theta,z,t) &= \eta\varphi e^{i(\omega t+kz)}. \end{aligned} \tag{4.3}$$

The subscript denotes partial derivative with respect to the designated variable. From the piezoelectric constitutive relations, we expect the electric potential to have the same phase dependence as the displacement field. Therefore, we define the electric potential as

$$\phi(r,\theta,z,t) = T(r,\theta)e^{i(\omega t+kz)}. \tag{4.4}$$

Substituting Eqn.(4.3) and (4.4) into Eqns.(3.34) and using Maple's symbolic package with further rearrangements, we obtain the following equations of motion for the displacement

and electric potentials:

$$\frac{\partial}{\partial r}\Big\{c_{11}\nabla^2\varphi + \big(\rho\omega^2 - k^2c_{44} + i\eta k(c_{13}+c_{44})\varphi\big) + ik(e_{15}+e_{31})T\Big\} + \frac{1}{r}\frac{\partial}{\partial\theta}\Big\{c_{66}\nabla^2\psi + (\rho\omega^2 - k^2c_{44})\psi\Big\} = 0, \tag{4.5a}$$

$$\frac{1}{r}\frac{\partial}{\partial\theta}\Big\{c_{11}\nabla^2\varphi + \big(\rho\omega^2 - k^2c_{44} + i\eta k(c_{13}+c_{44})\varphi\big) + ik(e_{15}+e_{31})T\Big\} - \frac{\partial}{\partial r}\Big\{c_{66}\nabla^2\psi + (\rho\omega^2 - k^2c_{44})\psi\Big\} = 0, \tag{4.5b}$$

$$\Big\{ik(c_{13}+c_{44}) + \eta c_{44}\Big\}\nabla^2\varphi + (\rho\omega^2 - k^2c_{33})\eta\varphi + e_{15}\nabla^2T - e_{33}k^2T = 0, \tag{4.5c}$$

$$\Big\{ik(e_{31}+e_{15}) + \eta e_{15}\Big\}\nabla^2\varphi - k^2e_{33}\eta\varphi - \epsilon_{11}\nabla^2T + \epsilon_{33}k^2T = 0; \tag{4.5d}$$

where

$$\nabla^2 = \frac{\partial^2}{\partial r^2} + \frac{1}{r}\frac{\partial}{\partial r} + \frac{1}{r^2}\frac{\partial^2}{\partial\theta^2}$$

is the two-dimensional laplacian operator in cylindrical coordinates.

The first two equations of the system of Eqns.(4.5) are satisfied if in particular

$$c_{66}\nabla^2\psi + (\rho\omega^2 - k^2c_{44})\psi = 0, \tag{4.6}$$

$$c_{11}\nabla^2\varphi + \big(\rho\omega^2 - k^2c_{44} + i\eta k(c_{13}+c_{44})\big)\varphi + ik(e_{15}+e_{31})T = 0. \tag{4.7}$$

We observe that we have 3 coupled equations in $\varphi$ and $T$ i.e Eqns.(4.5c), (4.5d) and (4.7) and an independent one in $\psi$ i.e Eqn.(4.6). We now seek values of the constant $\eta$ which will make the 3 equations in $\varphi$ and $T$ consistent; we achieve this by assuming that $\varphi$ and $T$ satisfy the Helmholtz's equations [14]

$$\left.\begin{array}{rcrcl} \nabla^2\varphi & + & \xi^2\varphi & = & 0 \\ \nabla^2 T & + & \xi^2 T & = & 0 \end{array}\right\} \rightarrow \quad \left\{\begin{array}{rcl} \nabla^2\varphi & = & -\xi^2\varphi \\ \nabla^2 T & = & -\xi^2 T \end{array}\right. . \tag{4.8}$$

Substituting Eqn.(4.8) into Eqns.(4.7), (4.5c) and (4.5d), we obtain the following algebraic

equations in $\varphi$ and $T$

$$i\eta k(c_{13}+c_{44})\varphi + ik(e_{15}+e_{31})T - \xi^2 c_{11}\varphi + (\rho\omega^2 - k^2 c_{44})\varphi = 0, \tag{4.9}$$

$$\Big(\big\{ik(c_{13}+c_{44}) + \eta c_{44}\big\}\xi^2 - (\rho\omega^2 - k^2 c_{33})\eta\Big)\varphi + (\xi^2 e_{15} - k^2 e_{33})T = 0, \tag{4.10}$$

$$\Big(-\big\{ik(e_{31}+e_{15}) + \eta e_{15}\big\}\xi^2 - k^2 e_{33}\eta\Big)\varphi + (\xi^2\epsilon_{11} + k^2\epsilon_{33})T = 0. \tag{4.11}$$

From Eqn.(4.11), $T$ can be expressed as

$$\begin{aligned} T &= \frac{\big(\eta k^2 e_{33} + \xi^2\big[(\eta+ik)e_{15} + ike_{31}\big]\big)\,\varphi}{\epsilon_{11}\xi^2 + \epsilon_{33}k^2} \\ &= \mu\varphi; \end{aligned} \tag{4.12}$$

where

$$\mu = \frac{\big(\eta k^2 e_{33} + \xi^2\big[(\eta+ik)e_{15} + ike_{31}\big]\big)}{\epsilon_{11}\xi^2 + \epsilon_{33}k^2}.$$

Substituting Eqn.(4.12) into Eqns.(4.9) and (4.10) and dividing through by $\varphi$, we obtain

$$\big(ik(c_{13}+c_{44}) + \eta c_{44}\big)\xi^2 - (\rho\omega^2 - k^2 c_{33})\eta + (\xi^2 e_{15} - k^2 e_{33})\frac{\big(\eta k^2 e_{33} + \xi^2\big[(\eta+ik)e_{15} + ike_{31}\big]\big)}{\epsilon_{11}\xi^2 + \epsilon_{33}k^2} = 0, \tag{4.13}$$

$$i\eta k(c_{13}+c_{44}) - \xi^2 c_{11} + (\rho\omega^2 - k^2 c_{44}) + ik(e_{15}+e_{31})\frac{\big(\eta k^2 e_{33} + \xi^2\big[(\eta+ik)e_{15} + ike_{31}\big]\big)}{\epsilon_{11}\xi^2 + \epsilon_{33}k^2} = 0. \tag{4.14}$$

Solving for $\eta$ in both Eqns.(4.13) and (4.14), by using Maple's symbolic package, we obtain

$$\eta = \frac{-i}{k}\left(\begin{array}{c} \xi^4 c_{11}e_{15} + \xi^2\Big[k^2\big(e_{33}c_{11} - e_{15}c_{13} \\ -e_{31}\,(c_{13}+c_{44})\big] - \rho\omega^2 e_{15}\Big] + e_{33}k^2\left(k^2 c_{44} - \rho\omega^2\right) \\ \hline k^2\Big[e_{33}\,(c_{13}+c_{44}) - c_{33}\,(e_{15}+e_{31})\Big] \\ -\xi^2\,(c_{44}e_{31} - c_{13}e_{15}) + \rho\omega^2(e_{31}+e_{15}) \end{array}\right), \tag{4.15}$$

$$\eta = \left(\begin{array}{c} \Big(\xi^2 k^2\big[\epsilon_{11}c_{44} + e_{31}^2 + e_{15}^2 + 2e_{15}e_{31} + \epsilon_{33}c_{11}\big] \\ +k^4\epsilon_{33}c_{44} + \xi^4\epsilon_{11}c_{11} - \rho\omega^2\left(k^2\epsilon_{33} + \xi^2\epsilon_{11}\right)\Big) \\ \hline ik\Big(k^2\big[e_{33}(e_{15}+e_{31}) + \epsilon_{33}(c_{13}+c_{44})\big] \\ +\xi^2\big[e_{15}(e_{15}+e_{31}) + \epsilon_{11}(c_{13}+c_{44})\big]\Big) \end{array}\right). \tag{4.16}$$

Subtracting Eqn.(4.16) from (4.15) and dividing by $i(e_{15}+e_{31})$ (again using marple's symbolic package), we obtain a sixth order polynomial equation in $\xi$ given by

$$\begin{aligned}
&c_{11}\left(e_{15}^2+\epsilon_{11}c_{44}\right)\xi^6+\left(-2e_{15}k^2c_{13}e_{31}-2e_{15}^2k^2c_{13}-\rho\omega^2\epsilon_{11}c_{44}\right.\\
&-e_{15}^2\rho\omega^2+\epsilon 11c_{11}k^2c_{33}-k^2c_{13}^2\epsilon_{11}+k^2c_{44}e_{31}^2-\epsilon_{11}c_{11}\rho\omega^2\\
&\left.-2k^2c_{13}\epsilon_{11}c_{44}+c_{11}k^2\epsilon_{33}c_{44}\right)\xi^4+\left(K^4e_{31}^2c_{33}-e_{15}^2K^2\rho\omega^2-k^4e_{33}^2c_{11}\right.\\
&-2k^4c_{13}\epsilon_{33}c_{44}-k^4c_{13}^2\epsilon_{33}+e_{15}^2k^4c_{33}-k^2e_{31}^2\rho\omega^2+\epsilon_{11}\rho^2\omega^4\\
&-\epsilon_{11}\rho\omega^2k^2c_{33}-\epsilon_{11}\rho\omega^2k^2c_{44}-k^2\epsilon_{33}c_{44}\rho\omega^2+2e_{15}k^4e_{31}c_{33}-2e_{15}k^2e_{31}\rho\omega^2\\
&\left.+\epsilon_{11}k^4c_{44}c_{33}-k^2\epsilon_{33}c_{11}\rho\omega^2+k^4\epsilon_{33}c_{11}c_{33}\right)\xi^2+k^2\left(k^2\epsilon_{33}c_{33}\right.\\
&\left.+k^2e_{33}^2-\epsilon_{33}\rho\omega^2\right)\left(k^2c_{44}-\rho\omega^2\right)=0.
\end{aligned}\tag{4.17}$$

Making a change of variable, $x=\xi^2$; Eqn.(4.17) can be expressed as a third order polynomial of the form

$$x^3+ax^2+bx+c=0;\tag{4.18}$$

where

$$\begin{aligned}
a=&\frac{-\rho\omega^2\left[e_{15}^2+\epsilon_{11}(c_{11}+c_{44})\right]+k^2\epsilon_{11}\left(c_{11}c_{33}-2c_{13}c_{44}-c_{13}^2\right)}{c_{11}\left(e_{15}^2+\epsilon_{11}c_{44}\right)}\\
&+\frac{k^2\left[c_{44}\left(e_{31}^2+\epsilon_{33}c_{11}\right)+2\left(e_{15}(c_{11}e_{33}-c_{13}e_{31})-c_{13}e_{15}^2\right)\right]}{c_{11}\left(e_{15}^2+\epsilon_{11}c_{44}\right)},\\
b=&\frac{\epsilon_{11}\rho^2\omega^4-k^2\rho\omega^2\left[\epsilon_{11}(c_{33}+c_{44})+\epsilon_{33}(c_{11}+c_{44})+(e_{15}+e_{31})^2+2e_{15}e_{33}\right]}{c_{11}\left(e_{15}^2+\epsilon_{11}c_{44}\right)}\\
&+\frac{k^4\left[c_{33}\left[(e_{15}+e_{31})^2+\epsilon 11c_{44}+\epsilon_{33}c_{11}\right]+e_{33}^2c_{11}-2c_{44}e_{31}e_{33}\right]}{c_{11}\left(e_{15}^2+\epsilon_{11}c_{44}\right)}\\
&-\frac{k^4\left[c_{13}^2\epsilon_{33}-2c_{13}\left[e_{33}(e_{15}+e_{31})+c_{44}\epsilon_{33}\right]\right]}{c_{11}\left(e_{15}^2+\epsilon_{11}c_{44}\right)},\\
c=&\frac{k^2\left[k^2c_{44}-\rho\omega^2\right]\left[k^2\left(c_{33}\epsilon_{33}+e_{33}^2\right)-\epsilon_{33}\rho\omega^2\right]}{c_{11}\left(e_{15}^2+\epsilon_{11}c_{44}\right)}.
\end{aligned}\tag{4.19}$$

In order to solve Eqn.(4.18), we make another change of variable, $x=y-\frac{a}{3}$, [29]; so that Eqn.(4.18) becomes

$$y^3+py+q=0;\tag{4.20}$$

where $p = -\frac{a^2}{3} + b$ and $q = 2\left(\frac{a}{3}\right)^3 - \frac{ab}{3} + c$.

The solutions of Eqn.(4.20), can be expressed in terms of variables $A$, $B$ and $Q$ defined as follows:

$$Q = \left(\frac{p}{3}\right)^3 + \left(\frac{q}{2}\right)^2, \quad A = \left(-\frac{q}{2} + \sqrt{Q}\right)^{\frac{1}{3}} \text{ and } \quad B = \left(-\frac{q}{2} - \sqrt{Q}\right)^{\frac{1}{3}}. \tag{4.21}$$

So that

$$y_1 = A + B; \quad y_{2,3} = -\frac{A+B}{2} \pm i\left(\frac{A-B}{2}\right)\sqrt{3}. \tag{4.22}$$

Hence, the solutions for $\xi$ are

$$\xi_1 = \pm\sqrt{A + B - \frac{a}{3}}, \tag{4.23}$$

$$\xi_2 = \pm\sqrt{-\frac{A+B}{2} - i\left(\frac{A-B}{2}\right)\sqrt{3} - \frac{a}{3}}, \tag{4.24}$$

$$\xi_3 = \pm\sqrt{-\frac{A+B}{2} + i\left(\frac{A-B}{2}\right)\sqrt{3} - \frac{a}{3}}. \tag{4.25}$$

We can now determine the values of the constants $\eta_1$, $\eta_2$, $\eta_3$ corresponding to the roots $\xi_1^2$, $\xi_2^2$ and $\xi_3^2$. Also, the potential functions $\varphi_1$, $\varphi_2$, $\varphi_3$, $T_1$, $T_2$, and $T_3$ corresponding to the roots $\xi_i^2$ $(i = 1, 2, 3)$ and $\psi$, each satisfy the Helmholtz's equations:

$$\nabla^2\varphi_i + \xi_i^2\varphi_i = 0, \tag{4.26}$$

$$\nabla^2 T_i + \xi_i^2 T_i = 0, \tag{4.27}$$

$$\nabla^2\psi + \lambda^2\psi = 0; \tag{4.28}$$

where $\lambda^2 = \frac{\rho\omega^2 - k^2 c_{44}}{c_{66}}$, $i = 1, 2, 3$ and $c_{66} = \frac{1}{2}(c_{11} - c_{12})$ as noted before.

Strictly speaking, we just have four independent equations to solve for the potentials instead of the above seven equations, as $T$ and $\psi$ are related through Eqn.(4.12). Thus, we have the following four independent equations:

$$\begin{aligned} \nabla^2\varphi_i \quad &+ \quad \xi_i^2\varphi_i \quad = 0, \\ \nabla^2\psi \quad &+ \quad \lambda^2\psi \quad = 0. \end{aligned} \tag{4.29}$$

Using the method of separation of variables [26], we look for solutions for $\varphi$ and $\psi$ of the form

$$\begin{aligned} \varphi_i(r,\theta) &= R_i(r)H_i(\theta), \\ \psi(r,\theta) &= F(r)G(\theta) \end{aligned} \tag{4.30}$$

Substituting the expression for $\varphi_i$ in Eqn.(4.30) into (4.26), we obtain the following:

$$H_i(\theta)\frac{\partial^2 R_i(r)}{\partial r^2} + \frac{H_i(\theta)}{r}\frac{\partial R_i(r)}{\partial r} + \frac{R_i(r)}{r^2}\frac{\partial^2 H_i(\theta)}{\partial \theta^2} + \xi_i^2 R_i(r)H_i(\theta) = 0. \tag{4.31}$$

Multiplying and dividing Eqn.(4.31) by $r^2$ and $R(r)H(\theta)$ respectively, leads to

$$\frac{r^2}{R_i(r)}\frac{\partial^2 R_i(r)}{\partial r^2} + \frac{r}{R_i(r)}\frac{\partial R_i(r)}{\partial r} + (r\xi_i)^2 + \frac{1}{H_i(\theta)}\frac{\partial^2 H_i(\theta)}{\partial \theta^2} = 0. \tag{4.32}$$

Eqn.(4.32) is made up of two terms, which are separately functions of $r$ and $\theta$ respectively. For Eqn.(4.32) to hold for all $r$ and $\theta$ in the domain of definition, the separate terms in (4.32) must be both constants; that is

$$\frac{r^2}{R_i(r)}\frac{\partial^2 R_i(r)}{\partial r^2} + \frac{r}{R_i(r)}\frac{\partial R_i(r)}{\partial r} + (r\xi_i)^2 = c_r; \tag{4.33}$$

and

$$\frac{1}{H_i(\theta)}\frac{\partial^2 H_i(\theta)}{\partial \theta^2} = c_\theta. \tag{4.34}$$

Therefore, from Eqn.(4.32), we have

$$c_r + c_\theta = 0. \tag{4.35}$$

From the geometry of the cylinder, we expect the solution to be periodic in $\theta$, repeating every $2\pi$. If this were not so, $H_i(\theta) \neq H_i(\theta + 2\pi)$ and $\varphi_i(r,\theta)$ would not be a single-valued function of the angle. So, for solutions with period of $2\pi$ in $\theta$ we expect $c_\theta$ to be a negative integer with zero inclusive; that is $c_\theta = -n^2 \leq 0$ $(n = 0, 1, 2, 3, ...)$. Therefore, Eqn.(4.34) becomes

$$\frac{1}{H_i(\theta)}\frac{\partial^2 H_i(\theta)}{\partial \theta^2} = -n^2. \tag{4.36}$$

Solving Eqn.(4.36), leads to an oscillating solution of the form

$$H_i(\theta) = A_i^1 \sin(n\theta) + B_i^1 \cos(n\theta);$$

where $A_i^1$ and $B_i^1$ are undetermined constants. Substituting the value of $c_\theta$ in Eqn.(4.35) and making use of $c_r$ in Eqn.(4.33), we obtain

$$\begin{aligned}
&\frac{r^2}{R_i(r)}\frac{\partial^2 R_i(r)}{\partial r^2} + \frac{r}{R_i(r)}\frac{\partial R_i(r)}{\partial r} + (r\xi_i)^2 - n^2 = 0 \\
&\frac{\partial^2 R_i(r)}{\partial r^2} + \frac{1}{r}\frac{\partial R_i(r)}{\partial r} + \left(\xi_i^2 - \frac{n^2}{r^2}\right) R_i(r) = 0 \\
&\frac{\partial^2 R_i(r)}{\partial (\xi_i r)^2} + \frac{1}{\xi_i r}\frac{\partial R_i(r)}{\partial (\xi_i r)} + \left(1 - \frac{n^2}{(\xi_i r)^2}\right) R_i(r) = 0. \qquad (4.37)
\end{aligned}$$

Lets, define a new variable $s = \xi_i r$ and a new function $R_i'(\xi_i r) = R_i(r)$. With these new quantities, Eqn.(4.37) becomes

$$\frac{\partial^2 R_i'(s)}{\partial s^2} + \frac{1}{s}\frac{\partial R_i'(s)}{\partial s} + \left(1 - \frac{n^2}{s^2}\right) R_i'(s) = 0. \qquad (4.38)$$

Eqn.(4.38) is the famous Bessel's equation of order $n$ whose solutions are well known. So, $R_i'(s)$ is expressed as

$$\begin{aligned}
R_i'(s) &= A_i^2 J_n(s) + B_i^2 Y_n(s); \\
R_i'(\xi_i r) &= A_i^2 J_n(\xi_i r) + B_i^2 Y_n(\xi_i r);
\end{aligned}$$

where $J_n(\xi_i r)$ and $Y_n(\xi_i r)$ are Bessel functions of the first and second kind respectively and $A_i^2$ and $B_i^2$ are undetermined constants; these functions are still used even when $\xi_i$ is complex. However, if $\xi_i^2 < 0$ (i.e. $\xi_i = i\xi_i'$ and $\xi_i'$ is real); then $R'(\xi_i r)$ becomes

$$R_i'(\xi_i r) = A_i^2 I_n(\xi_i' r) + B_i^2 K_n(\xi_i' r);$$

where $I_n(\xi_i' r)$ and $K_n(\xi_i' r)$ are the modified Bessel functions of the first and second kind respectively. For the problem at hand, where we are dealing with a solid cylinder, we discard solutions $Y_n(\xi_i r)$ and $K_n(\xi_i' r)$, due to their singular behaviour at the origin. Therefore, the final solution for $\varphi_i(r, \theta)$ is

$$\varphi_i(r, \theta) = A_i J_n(\xi_i r)\cos(n\theta) + B_i J_n(\xi_i r)\sin(n\theta); \qquad (4.39)$$

where the undetermined constants associated with the solutions of $H_i(\theta)$, have been absorbed into $A_i$ and $B_i$ respectively.

Similarly, the solution for $\psi(r,\theta)$ is

$$\psi(r,\theta) = A_4 J_n(\lambda r)\sin(n\theta) + B_4 J_n(\lambda r)\cos(n\theta). \tag{4.40}$$

However, for simplicity we let $\varphi_i(r,\theta)$ and $\psi(r,\theta)$ have the same $\theta$ dependence as in [14]. This will lead to the same functional dependence of $u, v$ and $w$ on $\theta$ as found in traditional non-axisymmetric guided wave problems in rods, and thus representing well the flexural nature of the waves [9]. Thus, $\varphi_i(r,\theta)$ and $\psi(r,\theta)$ are represented finally as

$$\begin{aligned} \varphi_i(r,\theta) &= A_i J_n(\xi_i r)\cos(n\theta), \quad i = 1,2,3, \\ \psi(r,\theta) &= A_4 J_n(\lambda r)\sin(n\theta). \end{aligned} \tag{4.41}$$

Therefore, in view of Eqn.(4.41), the final form of Eqns.(4.3) and (4.4) are

$$\begin{aligned} u\,(r,\theta,z,t) &= \left[\varphi_{1r} + \varphi_{2r} + \varphi_{3r} + \tfrac{1}{r}\psi_\theta\right] e^{i(\omega t + kz)}, \\ v\,(r,\theta,z,t) &= \left[\tfrac{1}{r}\left(\varphi_{1\theta} + \varphi_{2\theta} + \varphi_{3\theta}\right) - \psi_r\right] e^{i(\omega t + kz)}, \\ w\,(r,\theta,z,t) &= \left\{\eta_1\varphi_1 + \eta_2\varphi_2 + \eta_3\varphi_3\right\} e^{i(\omega t + kz)}, \\ \phi(r,\theta,z,t) &= \left\{T_1 + T_2 + T_3\right\} e^{i(\omega t + kz)}. \end{aligned} \tag{4.42}$$

## 4.3 Frequency Equation

In order to obtain the frequency (characteristic) equation, and hence complete the analytic formulation of the problem, we now impose the mechanical and electrical boundary conditions satisfied by the fields in the system. We impose the following boundary conditions as derived in the previous chapter (i.e. Eqns.(3.57) and (3.58)) and used by Nayfeh et al [10]:

$$\sigma_{rr} = \sigma_{r\theta} = \sigma_{rz} = 0 \quad \text{and} \quad D_r = 0 \quad \text{or} \quad \phi = 0 \quad \text{at} \quad r = r_o. \tag{4.43}$$

In [10] only the case with $D_r = 0$ was considered. By making use of the solutions in Eqn.(4.42) and the expressions for the stress and electric displacement fields in Eqns.(3.33), together with the boundary conditions above; we obtain an algebraic system of four linear homogeneous equations in the unknown amplitudes $A_i$ and $A_4$. For non trivial solutions of the system, we obtain the frequency equation in determinantal form as follows:

$$D_4 = 0; \tag{4.44}$$

where

$$D_4 = \begin{vmatrix} a_{11} & a_{12} & a_{13} & a_{14} \\ a_{21} & a_{22} & a_{23} & a_{24} \\ a_{31} & a_{32} & a_{33} & a_{34} \\ a_{41} & a_{42} & a_{43} & a_{44} \end{vmatrix}; \tag{4.45}$$

and

$$\begin{aligned}
a_{11} =& \left[\frac{m(m-1)}{r_o^2} - \xi_1^2\right] J_m(\xi_1, r_o) + \frac{\xi_1}{r_o} J_{m+1}(\xi_1, r_o) \\
&+ \frac{C_{12}}{C_{11} r_o} \left[\frac{m}{r_o} J_m(\xi_1, r_o) - \xi_1 J_{m+1}(\xi_1, r_o) - \frac{m^2}{r_o} J_m(\xi_1, r_o)\right] \\
&ik \left[\frac{C_{13}}{C_{11}} \eta_1 J_m(\xi_1, r_o) + \frac{e_{31}}{C_{11}} \mu_1 J_m(\xi_1, r_o)\right], \\
a_{12} =& \left[\frac{m(m-1)}{r_o^2} - \xi_2^2\right] J_m(\xi_2, r_o) + \frac{\xi_2}{r_o} J_{m+1}(\xi_2, r_o) \\
&+ \frac{C_{12}}{C_{11} r_o} \left[\frac{m}{r_o} J_m(\xi_2, r_o) - \xi_2 J_{m+1}(\xi_2, r_o) - \frac{m^2}{r_o} J_m(\xi_2, r_o)\right] \\
&ik \left[\frac{C_{13}}{C_{11}} \eta_2 J_m(\xi_2, r_o) + \frac{e_{31}}{C_{11}} \mu_2 J_m(\xi_2, r_o)\right], \\
a_{13} =& \left[\frac{m(m-1)}{r_o^2} - \xi_3^2\right] J_m(\xi_3, r_o) + \frac{\xi_3}{r_o} J_{m+1}(\xi_3, r_o) \\
&+ \frac{C_{12}}{C_{11} r_o} \left[\frac{m}{r_o} J_m(\xi_3, r_o) - \xi_3 J_{m+1}(\xi_3, r_o) - \frac{m^2}{r_o} J_m(\xi_3, r_o)\right] \\
&ik \left[\frac{C_{13}}{C_{11}} \eta_3 J_m(\xi_3, r_o) + \frac{e_{31}}{C_{11}} \mu_3 J_m(\xi_3, r_o)\right], \\
a_{14} =& \frac{m}{r_o} \left[\frac{m}{r_o} J_m(\lambda r_o) - \lambda J_{m+1}(\lambda r_o) - \frac{1}{r_o} J_m(\lambda r_o)\right] \\
&+ \frac{C_{12}}{C_{11} r_o} \left[\frac{m}{r_o} J_m(\lambda r_o)(1-m) - m\lambda J_{m+1}(\lambda r_o)\right],
\end{aligned}$$

$$
\begin{aligned}
a_{21} =& \frac{-m}{r_o}\left[\frac{m}{r_o}J_m(\xi_1,r_o)-\xi_1 J_{m+1}(\xi_1,r_o)-\frac{1}{r_o}J_m(\xi_1,r_o)\right] \\
& -\frac{1}{r_o}\left[\frac{m^2}{r_o}J_m(\xi_1,r_o)-m\xi_1 J_{m+1}(\xi_1,r_o)-\frac{m}{r_o}J_m(\xi_1,r_o)\right], \\
a_{22} =& \frac{-m}{r_o}\left[\frac{m}{r_o}J_m(\xi_2,r_o)-\xi_2 J_{m+1}(\xi_2,r_o)-\frac{1}{r_o}J_m(\xi_2,r_o)\right] \\
& -\frac{1}{r_o}\left[\frac{m^2}{r_o}J_m(\xi_2,r_o)-m\xi_2 J_{m+1}(\xi_2,r_o)-\frac{m}{r_o}J_m(\xi_2,r_o)\right], \\
a_{23} =& \frac{-m}{r_o}\left[\frac{m}{r_o}J_m(\xi_3,r_o)-\xi_3 J_{m+1}(\xi_3,r_o)-\frac{1}{r_o}J_m(\xi_3,r_o)\right] \\
& -\frac{1}{r_o}\left[\frac{m^2}{r_o}J_m(\xi_3,r_o)-m\xi_3 J_{m+1}(\xi_3,r_o)-\frac{m}{r_o}J_m(\xi_3,r_o)\right], \\
a_{24} =& \left[\lambda^2+\frac{m(m-1)}{{r_o}^2}\right]J_m(\lambda r_o)+\frac{\lambda}{r_o}J_{m+1}(\lambda r_o) \\
& -\frac{1}{r_o}\left[\frac{m^2}{r_o}J_m(\lambda,r_o)+\lambda J_{m+1}(\lambda r_o)-\frac{m}{r_o}J_m(\lambda,r_o)\right], \\
a_{31} =& \left[ik+\eta_1+\frac{e_{15}}{C_{44}}\mu_1\right]\left(\frac{m}{r_o}J_m(\xi_1,r_o)-\xi_1 J_{m+1}(\xi_1,r_o)\right), \\
a_{32} =& \left[ik+\eta_2+\frac{e_{15}}{C_{44}}\mu_2\right]\left(\frac{m}{r_o}J_m(\xi_2,r_o)-\xi_2 J_{m+1}(\xi_2,r_o)\right), \\
a_{33} =& \left[ik+\eta_3+\frac{e_{15}}{C_{44}}\mu_3\right]\left(\frac{m}{r_o}J_m(\xi_3,r_o)-\xi_3 J_{m+1}(\xi_3,r_o)\right), \\
a_{34} =& \frac{ikm}{r_o}J_m(\lambda,r_o);
\end{aligned}
$$

for $D_r|_{r_o}=0$, we have

$$
\begin{aligned}
a_{41} =& \left[ik+\eta_1+\frac{\epsilon_{11}}{e_{15}}\mu_1\right]\left(\frac{m}{r_o}J_m(\xi_1,r_o)-\xi_1 J_{m+1}(\xi_1,r_o)\right), \\
a_{42} =& \left[ik+\eta_2+\frac{\epsilon_{11}}{e_{15}}\mu_2\right]\left(\frac{m}{r_o}J_m(\xi_2,r_o)-\xi_2 J_{m+1}(\xi_2,r_o)\right), \\
a_{43} =& \left[ik+\eta_3+\frac{\epsilon_{11}}{e_{15}}\mu_3\right]\left(\frac{m}{r_o}J_m(\xi_3,r_o)-\xi_3 J_{m+1}(\xi_3,r_o)\right), \\
a_{44} =& \frac{ikm}{r_o}J_m(\lambda,r_o);
\end{aligned}
$$

and for $\phi|_{r_o} = 0$, the above coefficients become

$$\begin{aligned} a_{41} =& \mu_1 J_n(\xi_1 r_o), \\ a_{42} =& \mu_2 J_n(\xi_2 r_o), \\ a_{43} =& \mu_3 J_n(\xi_3 r_o), \\ a_{44} =& 0. \end{aligned}$$

In the above expressions, $m \equiv n$.

## 4.4 Non-axisymmetrical Wave Propagation in a Free Transversely Isotropic Non-piezoelectric Solid Cylinder.

In this section, we solve the problem of propagation of waves in a free transversely isotropic non-piezoelectric solid cylinder; as a means for numerically checking the results coming out of the piezoelectric cylinder calculations. The analytic solution to this problem is a simple case of the more general problem of propagation of waves in a hollow and fluid-loaded cylinder, already solved by Mirsky [15] and Berliner et al [14] respectively. Here, we follow Berliner's approach to obtain the analytic solution to the problem.

The field equations satisfied in the cylinder are [14]:

- Navier's equation:

$$\frac{\partial \sigma_{rr}}{\partial r} + \frac{1}{r}\frac{\partial \sigma_{\theta r}}{\partial \theta} + \frac{\partial \sigma_{zr}}{\partial z} + \frac{\sigma_{rr} - \sigma_{\theta\theta}}{r} = \rho \ddot{u}, \tag{4.46a}$$

$$\frac{\partial \sigma_{r\theta}}{\partial r} + \frac{1}{r}\frac{\partial \sigma_{\theta\theta}}{\partial \theta} + \frac{\partial \sigma_{z\theta}}{\partial z} + \frac{2\sigma_{r\theta}}{r} = \rho \ddot{v}, \tag{4.46b}$$

$$\frac{\partial \sigma_{rz}}{\partial r} + \frac{1}{r}\frac{\partial \sigma_{\theta z}}{\partial \theta} + \frac{\partial \sigma_{zz}}{\partial z} + \frac{\sigma_{rz}}{r} = \rho \ddot{w}. \tag{4.46c}$$

- The strain-displacement relations:

$$\begin{aligned} S_{rr} &= \frac{\partial u}{\partial r}, \quad S_{\theta\theta} = \frac{1}{r}\left(u + \frac{\partial v}{\partial \theta}\right), \\ S_{zz} &= \frac{\partial w}{\partial z}, \quad S_{rz} = \frac{1}{2}\left(\frac{\partial w}{\partial r} + \frac{\partial u}{\partial z}\right), \\ S_{r\theta} &= \frac{1}{2r}\left(\frac{\partial u}{\partial \theta} - v\right) + \frac{1}{2}\frac{\partial v}{\partial r}, \quad S_{z\theta} = \frac{1}{2}\left(\frac{\partial v}{\partial z} + \frac{1}{r}\frac{\partial w}{\partial \theta}\right). \end{aligned} \tag{4.47}$$

- The stress-strain constitutive relations:

$$\sigma_1 = c_{11}S_1 + c_{12}S_2 + c_{13}S_3, \tag{4.48a}$$

$$\sigma_2 = c_{12}S_1 + c_{11}S_2 + c_{13}S_3, \tag{4.48b}$$

$$\sigma_3 = c_{13}\left(S_1 + S_2\right) + c_{33}S_3, \tag{4.48c}$$

$$\sigma_4 = c_{55}S_4, \quad \sigma_5 = c_{55}S_5, \quad \sigma_6 = c_{66}S_6. \tag{4.48d}$$

$$\tag{4.48e}$$

By making use of the constitutive and strain-displacement relations, Navier's equation can be expressed in terms of the mechanical displacement components as follows:

$$\begin{aligned} &c_{11}\left(\frac{\partial^2 u}{\partial r^2} + \frac{1}{r}\frac{\partial u}{\partial r} - \frac{1}{r^2}\frac{\partial v}{\partial \theta} - \frac{u}{r}\right) + c_{66}\left(\frac{1}{r}\frac{\partial^2 v}{\partial \theta \partial r} + \frac{1}{r^2}\frac{\partial^2 u}{\partial \theta^2} - \frac{1}{r^2}\frac{\partial v}{\partial \theta}\right) \\ &+ c_{44}\left(\frac{\partial^2 u}{\partial z^2} + \frac{\partial^2 w}{\partial z \partial r}\right) + c_{13}\frac{\partial^2 w}{\partial z \partial r} + \rho\omega^2 u = 0; \end{aligned} \tag{4.49a}$$

$$\begin{aligned} &c_{66}\left(\frac{\partial^2 v}{\partial r^2} + \frac{1}{r^2}\frac{\partial u}{\partial \theta} - \frac{1}{r^2}v + \frac{1}{r}\frac{\partial^2 u}{\partial \theta \partial r} + \frac{1}{r}\frac{\partial v}{\partial r}\right) + c_{11}\left(\frac{1}{r^2}\frac{\partial^2 v}{\partial \theta^2} + \frac{1}{r^2}\frac{\partial u}{\partial \theta}\right) \\ &+ c_{44}\left(\frac{\partial^2 v}{\partial z^2} + \frac{1}{r}\frac{\partial^2 w}{\partial z \partial \theta}\right) + \frac{c_{12}}{r}\frac{\partial^2 u}{\partial \theta \partial r} + \frac{c_{13}}{r}\frac{\partial^2 w}{\partial z \partial \theta} + \rho\omega^2 v = 0; \end{aligned} \tag{4.49b}$$

$$\begin{aligned} &c_{44}\left(\frac{1}{r}\frac{\partial^2 v}{\partial z \partial \theta} + \frac{1}{r^2}\frac{\partial^2 w}{\partial \theta^2} + \frac{\partial^2 u}{\partial z \partial r} + \frac{\partial^2 w}{\partial r^2} + \frac{1}{r}\frac{\partial u}{\partial z} + \frac{1}{r}\frac{\partial w}{\partial r}\right) \\ &+ c_{13}\left(\frac{\partial^2 u}{\partial z \partial r} + \frac{1}{r}\frac{\partial^2 v}{\partial z \partial \theta} + \frac{1}{r}\frac{\partial u}{\partial z}\right) + c_{33}\frac{\partial^2 w}{\partial z^2} + \rho\omega^2 w = 0. \end{aligned} \tag{4.49c}$$

To decouple the above system of equations, we make use of the expressions below for the

displacement components as introduced by Berliner et al [14]:

$$\begin{aligned} u(r,\theta,z,t) &= \left[\varphi_r + \frac{1}{r}\psi_\theta\right] e^{i(\omega t+kz)}, \\ v(r,\theta,z,t) &= \left[\frac{1}{r}\varphi_\theta - \psi_r\right] e^{i(\omega t+kz)}, \\ w(r,\theta,z,t) &= \eta\varphi e^{i(\omega t+kz)}; \end{aligned} \tag{4.50}$$

where $\varphi$, $\psi$ and $\eta$ are as defined previously. Substituting the above expressions for the displacement components into the system of Eqns.(4.49), we obtain the resulting coupled equations in terms of the displacement potentials $\varphi$ and $\psi$:

$$\frac{\partial}{\partial r}\Big\{c_{11}\nabla^2\varphi + \big(\rho\omega^2 - k^2c_{44} + i\eta k(c_{13}+c_{44})\varphi\big)\Big\}$$
$$+ \frac{1}{r}\frac{\partial}{\partial\theta}\Big\{c_{66}\nabla^2\psi + (\rho\omega^2 - k^2c_{44})\psi\Big\} = 0; \tag{4.51a}$$
$$\frac{1}{r}\frac{\partial}{\partial\theta}\Big\{c_{11}\nabla^2\varphi + \big(\rho\omega^2 - k^2c_{44} + i\eta k(c_{13}+c_{44})\varphi\big)\Big\}$$
$$- \frac{\partial}{\partial r}\Big\{c_{66}\nabla^2\psi + (\rho\omega^2 - k^2c_{44})\psi\Big\} = 0; \tag{4.51b}$$
$$\Big\{ik(c_{13}+c_{44}) + \eta c_{44}\Big\}\nabla^2\varphi + (\rho\omega^2 - k^2c_{33})\eta\varphi = 0. \tag{4.51c}$$
$$\tag{4.51d}$$

where

$$\nabla^2 = \frac{\partial^2}{\partial r^2} + \frac{1}{r}\frac{\partial}{\partial r} + \frac{1}{r^2}\frac{\partial^2}{\partial\theta^2},$$

is the two-dimensional laplacian operator in cylindrical coordinates.

The first two equations of the system of Eqns.(4.51) are satisfied if in particular

$$c_{66}\nabla^2\psi + (\rho\omega^2 - k^2c_{44})\psi = 0, \tag{4.52}$$

$$c_{11}\nabla^2\varphi + \big(\rho\omega^2 - k^2c_{44} + i\eta k(c_{13}+c_{44})\big)\varphi = 0. \tag{4.53}$$

In order to obtain the value of $\eta$ which will make Eqn.(4.51c) and Eqn.(4.53) consistent, we assume that the displacement potential, $\varphi$ satisfies the Helmholtz's equation i.e.

$$\nabla^2\varphi + \xi^2\varphi = 0. \tag{4.54}$$

Eqn.(4.54) implies that

$$\nabla^2\varphi = -\xi^2\varphi. \tag{4.55}$$

Substituting Eqn.(4.55) into Eqns.(4.51c) and (4.53), we obtain the following:

$$-c_{11}\xi^2\varphi + \left(\rho\omega^2 - k^2c_{44} + i\eta k(c_{13}+c_{44})\right)\varphi = 0, \tag{4.56}$$

$$-\left(ik(c_{13}+c_{44}) + \eta c_{44}\right)\xi^2\varphi + (\rho\omega^2 - k^2c_{33})\eta\varphi = 0. \tag{4.57}$$

From Eqn.(4.57), $\eta$ is obtained easily and is given by

$$\eta = \frac{ik\xi^2(c_{13}+c_{44})}{\rho\omega^2 - k^2c_{33} - \xi^2c_{44}}. \tag{4.58}$$

Substituting for $\eta$ into Eqn.(4.56) and simplifying, we obtain the following quadratic expression in $\xi^2$:

$$\begin{aligned}&(c_{11}c_{44})(\xi^2)^2 - \left((c_{11}+c_{44})\rho\omega^2 + (c_{13}^2 + 2c_{13}c_{44} - c_{11}c_{33})k^2\right)\xi^2 \\ &+ (\rho\omega^2 - c_{33}k^2)(\rho\omega^2 - c_{44}k^2).\end{aligned} \tag{4.59}$$

By making use of the quadratic formula, the solutions for $\xi^2$ are

$$\begin{aligned}\xi_1^2 &= \tfrac{-B+\sqrt{B^2-4AC}}{2A}, \\ \xi_2^2 &= \tfrac{-B-\sqrt{B^2-4AC}}{2A};\end{aligned} \tag{4.60}$$

where

$$\begin{aligned}A &= (c_{11}c_{44}), \\ B &= -\left[(c_{11}+c_{44})\rho\omega^2 + (c_{13}^2 + 2c_{13}c_{44} - c_{11}c_{33})k^2\right], \\ C &= (\rho\omega^2 - c_{33}k^2)(\rho\omega^2 - c_{44}k^2).\end{aligned} \tag{4.61}$$

Hence, the expressions satisfied by the displacement potentials $\varphi$ and $\psi$ are:

$$\begin{aligned}\nabla^2\varphi_1 &+ \xi_1^2\varphi_1 = 0, \\ \nabla^2\varphi_2 &+ \xi_2^2\varphi_2 = 0, \\ \nabla^2\psi &+ q^2\psi = 0;\end{aligned} \tag{4.62}$$

where

$$q^2 = \frac{(\rho\omega^2 - c_{44}k^2)}{c_{66}} \quad \text{and} \quad c_{66} = \frac{1}{2}(c_{11} - c_{12}). \tag{4.63}$$

By making use of the method of separation of variables, the solutions to the displacement potentials are:

$$\begin{aligned} \varphi_i(r,\theta) = &\quad A_i J_n(\xi_i r)\cos(n\theta), \quad i = 1,2 \\ \psi(r,\theta) = &\quad A_3 J_n(qr)\sin(n\theta). \end{aligned} \tag{4.64}$$

From Eqn.(4.64) the displacement components $u$, $v$ and $w$ may now be expressed as follows:

$$\begin{aligned} u\,(r,\theta,z,t) &= \left[\varphi_{1r} + \varphi_{2r} + \tfrac{1}{r}\psi_\theta\right] e^{i(\omega t + kz)}, \\ v\,(r,\theta,z,t) &= \left[\tfrac{1}{r}\left(\varphi_{1\theta} + \varphi_{2\theta}\right) - \psi_r\right] e^{i(\omega t + kz)}, \\ w\,(r,\theta,z,t) &= \left\{\eta_1\varphi_1 + \eta_2\varphi_2\right\} e^{i(\omega t + kz)}; \end{aligned} \tag{4.65}$$

where $\eta_1$ and $\eta_2$ are functions of $\xi_1^2$ and $\xi_2^2$ respectively. In the absence of boundary and damping forces, the boundary conditions to the cylinder are

$$\sigma_{rr} = \sigma_{r\theta} = \sigma_{rz} = 0 \quad \text{at} \quad r = r_o. \tag{4.66}$$

Applying the above boundary conditions, we obtain an algebraic system of three linear homogeneous equations in the unknown amplitudes $A_i$ and $A_3$. For non trivial solutions of the system, we obtain the characteristic (frequency) equation in determinantal form as follows:

$$D_3 = 0; \tag{4.67}$$

where

$$D_3 = \begin{vmatrix} a_{11} & a_{12} & a_{13} \\ a_{21} & a_{22} & a_{23} \\ a_{31} & a_{32} & a_{33} \end{vmatrix}; \tag{4.68}$$

and

$$
\begin{aligned}
a_{11} =& \left[\frac{m(m-1)}{r_o^2} - \xi_1^2\right] J_m(\xi_1, r_o) + \frac{\xi_1}{r_o} J_{m+1}(\xi_1, r_o) \\
&+ \frac{C_{12}}{C_{11} r_o} \left[\frac{m}{r_o} J_m(\xi_1, r_o) - \xi_1 J_{m+1}(\xi_1, r_o) - \frac{m^2}{r_o} J_m(\xi_1, r_o)\right] \\
& ik \left[\frac{C_{13}}{C_{11}} \eta_1 J_m(\xi_1, r_o)\right], \\
a_{12} =& \left[\frac{m(m-1)}{r_o^2} - \xi_2^2\right] J_m(\xi_2, r_o) + \frac{\xi_2}{r_o} J_{m+1}(\xi_2, r_o) \\
&+ \frac{C_{12}}{C_{11} r_o} \left[\frac{m}{r_o} J_m(\xi_2, r_o) - \xi_2 J_{m+1}(\xi_2, r_o) - \frac{m^2}{r_o} J_m(\xi_2, r_o)\right] \\
& ik \left[\frac{C_{13}}{C_{11}} \eta_2 J_m(\xi_2, r_o)\right], \\
a_{13} =& \frac{m}{r_o} \left[\frac{m}{r_o} J_m(q, r_o) - q J_{m+1}(q, r_o) - \frac{1}{r_o} J_m(q, r_o)\right] \\
&+ \frac{C_{12}}{C_{11} r_o} \left[\frac{m}{r_o} J_m(q, r_o)(1-m) - mq J_{m+1}(q, r_o)\right], \\
\\
a_{21} =& \frac{-m}{r_o} \left[\frac{m}{r_o} J_m(\xi_1, r_o) - \xi_1 J_{m+1}(\xi_1, r_o) - \frac{1}{r_o} J_m(\xi_1, r_o)\right] \\
&- \frac{1}{r_o} \left[\frac{m^2}{r_o} J_m(\xi_1, r_o) - m\xi_1 J_{m+1}(\xi_1, r_o) - \frac{m}{r_o} J_m(\xi_1, r_o)\right], \\
a_{22} =& \frac{-m}{r_o} \left[\frac{m}{r_o} J_m(\xi_2, r_o) - \xi_2 J_{m+1}(\xi_2, r_o) - \frac{1}{r_o} J_m(\xi_2, r_o)\right] \\
&- \frac{1}{r_o} \left[\frac{m^2}{r_o} J_m(\xi_2, r_o) - m\xi_2 J_{m+1}(\xi_2, r_o) - \frac{m}{r_o} J_m(\xi_2, r_o)\right], \\
a_{23} =& \left[q^2 + \frac{m(m-1)}{{r_o}^2}\right] J_m(q, r_o) + \frac{q}{r_o} J_{m+1}(q, r_o) \\
&- \frac{1}{r_o} \left[\frac{m^2}{r_o} J_m(q, r_o) + q J_{m+1}(q, r_o) - \frac{m}{r_o} J_m(q, r_o)\right], \\
a_{31} =& [ik + \eta_1] \left(\frac{m}{r_o} J_m(\xi_1, r_o) - \xi_1 J_{m+1}(\xi_1, r_o)\right), \\
a_{32} =& [ik + \eta_2] \left(\frac{m}{r_o} J_m(\xi_2, r_o) - \xi_2 J_{m+1}(\xi_2, r_o)\right), \\
a_{33} =& \frac{ikm}{r_o} J_m(q, r_o).
\end{aligned}
$$

## 4.5 Numerical results

In this section, sample results of the dispersion relations Eqns.(4.67) and (4.44) are presented for waves with circumferential order m=1 in the following materials: PZT-4 composite, (with and without electromechanical coupling included), cobalt, glass/epoxi fiber-reinforced composite and aluminium rods. The physical parameters used in this section and their numerical values are listed in Table(4.1). The method used to solve the dispersion relation

| Material Constant | PZT-4 | Aluminium | Glass/epoxy | Cobalt | SI units |
|---|---|---|---|---|---|
| Radius ($a$) | 1 | 1 | 1 | 1 | $m$ |
| $\rho$ | $7.5 \cdot 10^3$ | $2.8 \cdot 10^3$ | $1.9 \cdot 10^3$ | $8.9 \cdot 10^3$ | $kgm^{-3}$ |
| $c_{11}$ | $13.9 \cdot 10^{10}$ | $11.03 \cdot 10^{10}$ | $1.98 \cdot 10^{10}$ | $29.5 \cdot 10^{10}$ | $Nm^{-2}$ |
| $c_{12}$ | $7.78 \cdot 10^{10}$ | $5.43 \cdot 10^{10}$ | $0.55 \cdot 10^{10}$ | $15.9 \cdot 10^{10}$ | $Nm^{-2}$ |
| $c_{13}$ | $7.43 \cdot 10^{10}$ | $5.43 \cdot 10^{10}$ | $0.63 \cdot 10^{10}$ | $11.1 \cdot 10^{10}$ | $Nm^{-2}$ |
| $c_{33}$ | $11.5 \cdot 10^{10}$ | $11.03 \cdot 10^{10}$ | $5.76 \cdot 10^{10}$ | $33.5 \cdot 10^{10}$ | $Nm^{-2}$ |
| $c_{44}$ | $2.56 \cdot 10^{10}$ | $2.8 \cdot 10^{10}$ | $0.89 \cdot 10^{10}$ | $7.1 \cdot 10^{10}$ | $Nm^{-2}$ |
| $e_{15}$ | 12.7 | n/a | n/a | n/a | $Cm^{-2}$ |
| $e_{31}$ | $-5.2$ | n/a | n/a | n/a | $Cm^{-2}$ |
| $e_{33}$ | 15.1 | n/a | n/a | n/a | $Cm^{-2}$ |
| $\epsilon_0$ | $8.85 \cdot 10^{-12}$ | n/a | n/a | n/a | $C^2m^{-2}N^{-1}$ |
| $\epsilon_{11}$ | $730 \cdot \epsilon_0$ | n/a | n/a | n/a | $C^2m^{-2}N^{-1}$ |
| $\epsilon_{33}$ | $635 \cdot \epsilon_0$ | n/a | n/a | n/a | $C^2m^{-2}N^{-1}$ |

Table 4.1: The material constants for a PZT-4 rod, aluminium, glass/epoxy and cobalt [4].

is similar to that of Honarvar el al [30], where we do not need to find the zeros of the characteristic equation. In this approach, the left hand sides of Eqns.(4.67) and (4.44) are calculated for a desired range of values of $\omega$ and $ka$; where $a$ is the radius of the cylinder. A three dimensional plot of the log of the modulus of the determinants $D_4$ and $D_3$ versus $\omega$ and $ka$ is then produced, which reveals the dispersion relation. Since the function whose

image is $\log(x)$ approaches $-\infty$ for $x$ approaching zero, the 3D surface plot described above gives rise to negative spikes at the zeros of the determinants $D_4$ and $D_3$ (i.e. Eqns.(4.68) and (4.45)) and positive spikes where the determinants diverge. A projection of the 3D surface plot unto the $ka$-$\omega$ plane gives rise to the desired dispersion curves. The above approach, though similar to that used by Honavar et al is different in two ways. Firstly, the authors in [30] made use of just the real part of the left hand side of the dispersion relation to generate the three dimensional surface plots. Secondly, the three dimensional plot of the dispersion curves were generated without making use of another function analogous to $\log(x)$ described above. Nevertheless, from the nature of the three dimensional plots of the curves in [30] (see appendix), it is evident that the sign function can be used in place of the log function in our model to generate these dispersion curves; so that the dispersion curves are actually boundaries where the left hand side of the dispersion relation changes sign from plus to minus in the neighborhood of a root. It is worth mentioning that this approach as discussed by Honavar et al is simple, more stable and very fast in comparison with the traditional root finding techniques, such as Newton-Raphson and bisection. This is because the one by one search of the individual roots of the dispersion relation is now avoided which is a characteristic of traditional root finding iteration techniques.

By making use of the above numerical technique, dispersion curves of the propagating modes of flexural waves with circumferential order m=1, for the non-piezoelectric model Eqn.(4.68) are displayed for the following solid cylinders: aluminium, cobalt, glass/epoxi fiber-reinforced composite and PZT-4 (with electromechanical coupling absent) in Figs.(4.1), (4.3), (4.5), (4.7), (4.8) and (4.9). The ranges of $ka$ and $w$ are 0 to 20 and 0 to $2\pi \cdot 9500$ respectively for Figs.(4.1), (4.3), (4.5), (4.7) and (4.8) and 0 to 5.7 and 0 to $2\pi \cdot 3000 s^{-1}$ respectively for Fig.(4.9).

We will now compare our results with those of Honarvar et al [4], who solved the same problem of non-axisymmetrical (flexural) waves in a non-piezoelectric solid cylinder of transversely isotropic symmetry. Honarvar et al made use of five displacement potentials as

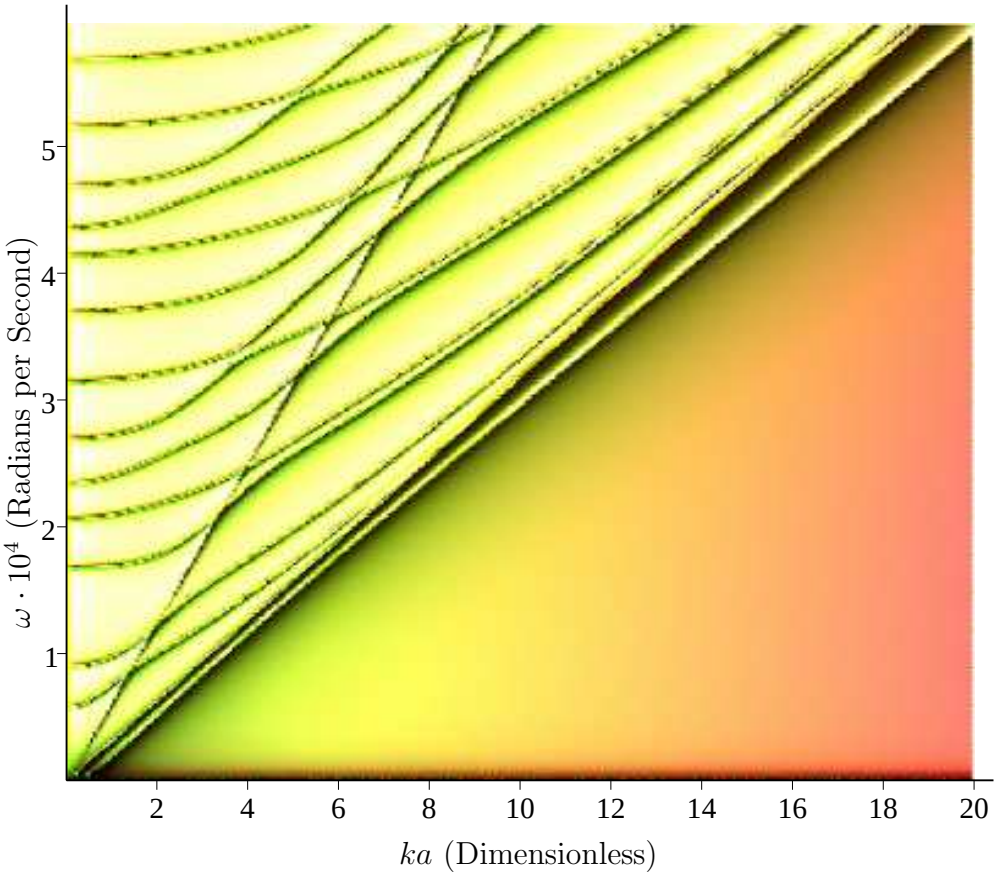


Figure 4.1: Dispersion curves for the flexural modes of a homogeneous isotropic aluminium solid cylinder by Mirsky's model ($m = 1$).

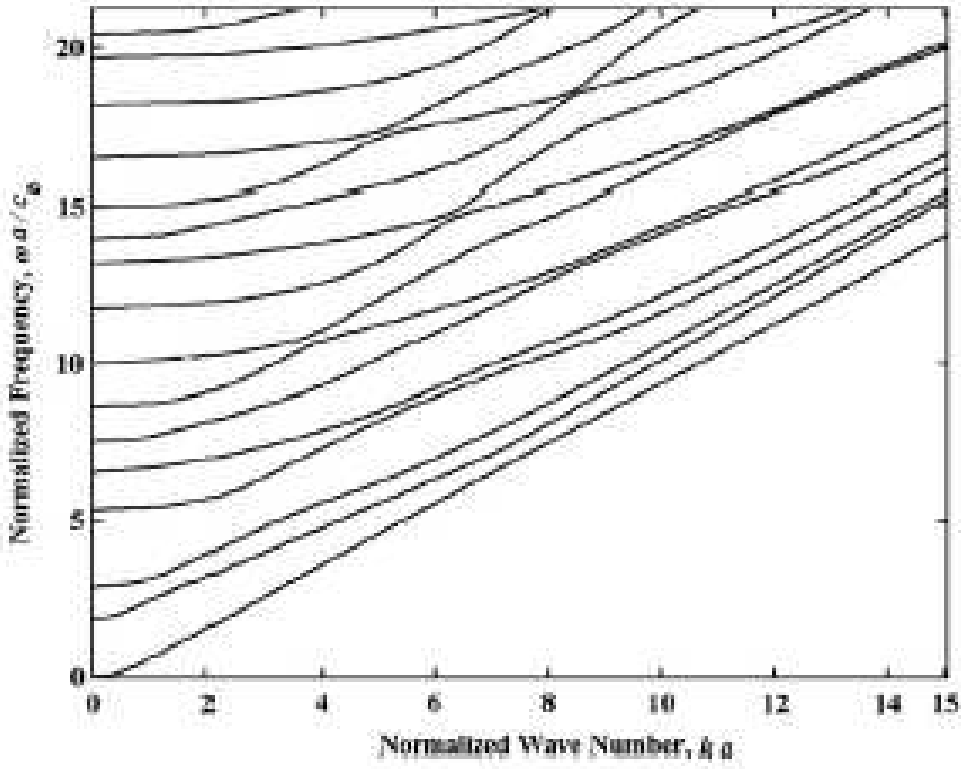


Figure 4.2: Dispersion curves for the flexural modes of a homogeneous isotropic aluminium solid cylinder by Honavar et al's model [4] ($m = 1$).

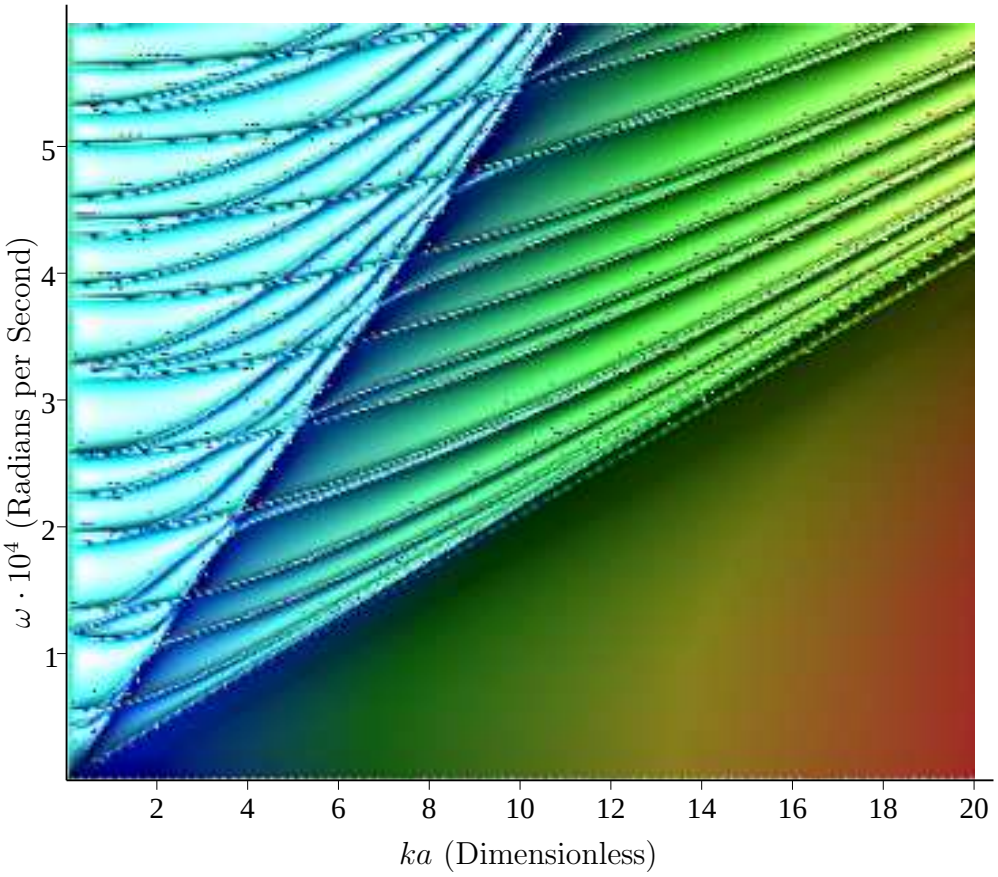


Figure 4.3: Dispersion curves for the flexural modes of a homogeneous transversely isotropic glass/epoxy fiber-reinforced composite solid cylinder by Mirsky's model ($m = 1$).

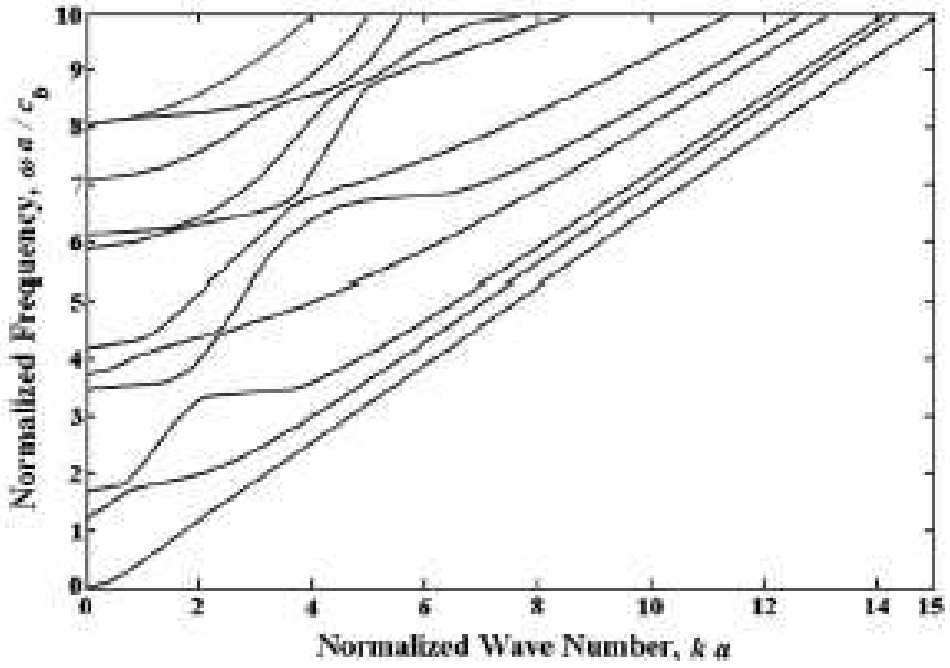


Figure 4.4: Dispersion curves for the flexural modes of a homogeneous transversely isotropic glass/epoxy fiber-reinforced composite solid cylinder by Honavar et al's model and produced from reference [4] ($m = 1$).

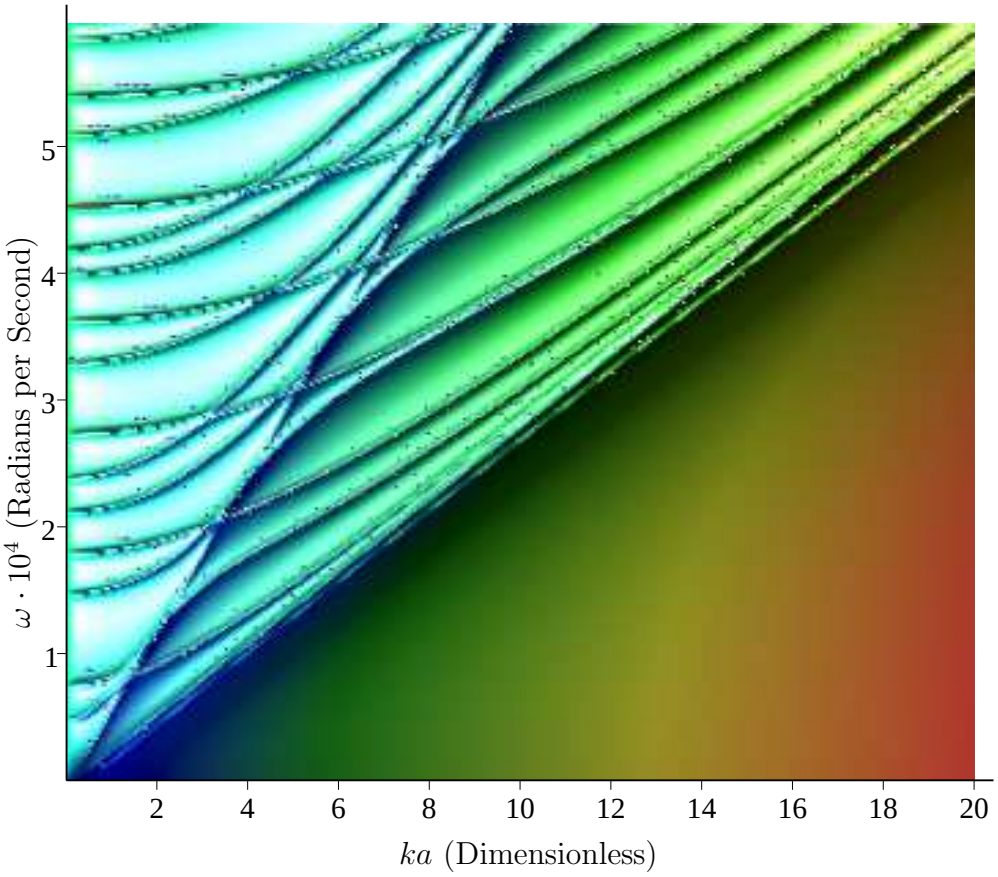


Figure 4.5: Dispersion curves for the flexural modes of a homogeneous transversely isotropic cobalt solid cylinder by Mirsky's model ($m = 1$).

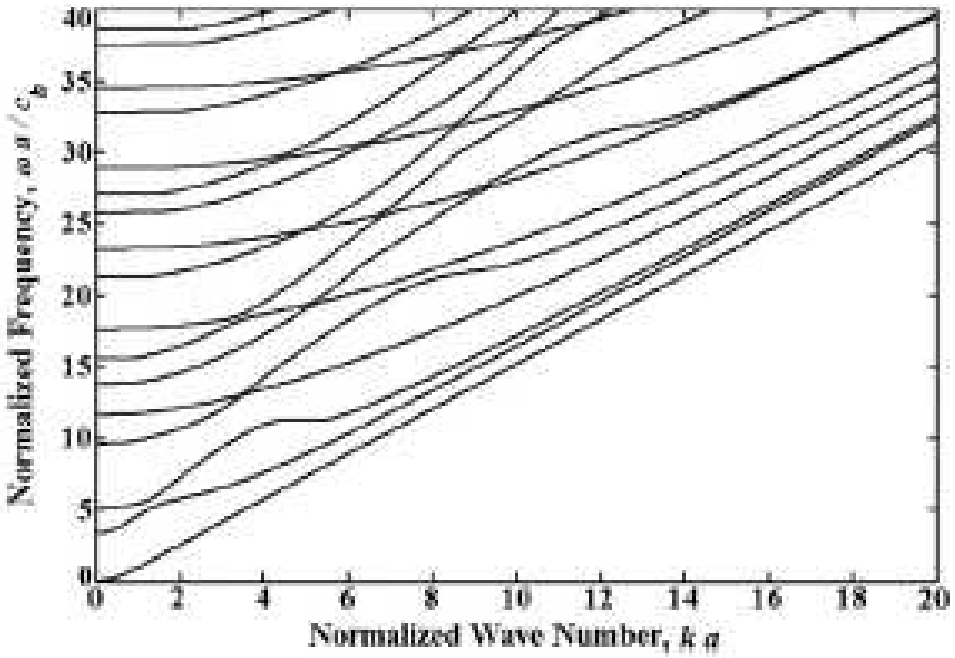


Figure 4.6: Dispersion curves for the flexural modes of a homogeneous transversely isotropic cobalt solid cylinder by Honarvar et al's model and produced from reference [4] ($m = 1$).

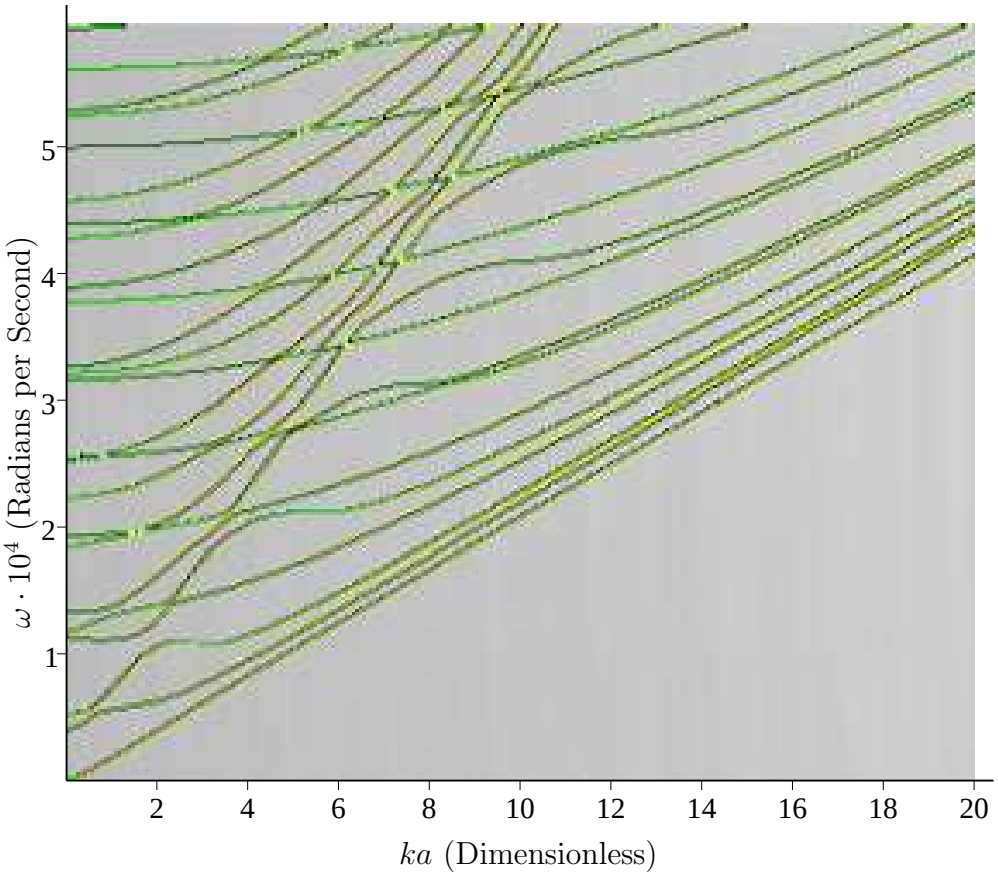


Figure 4.7: Dispersion curves for the flexural modes of a homogeneous transversely isotropic glass/epoxy fiber-reinforced composite solid cylinder by Mirsky's model ($m = 1$) and making use of the sign function.

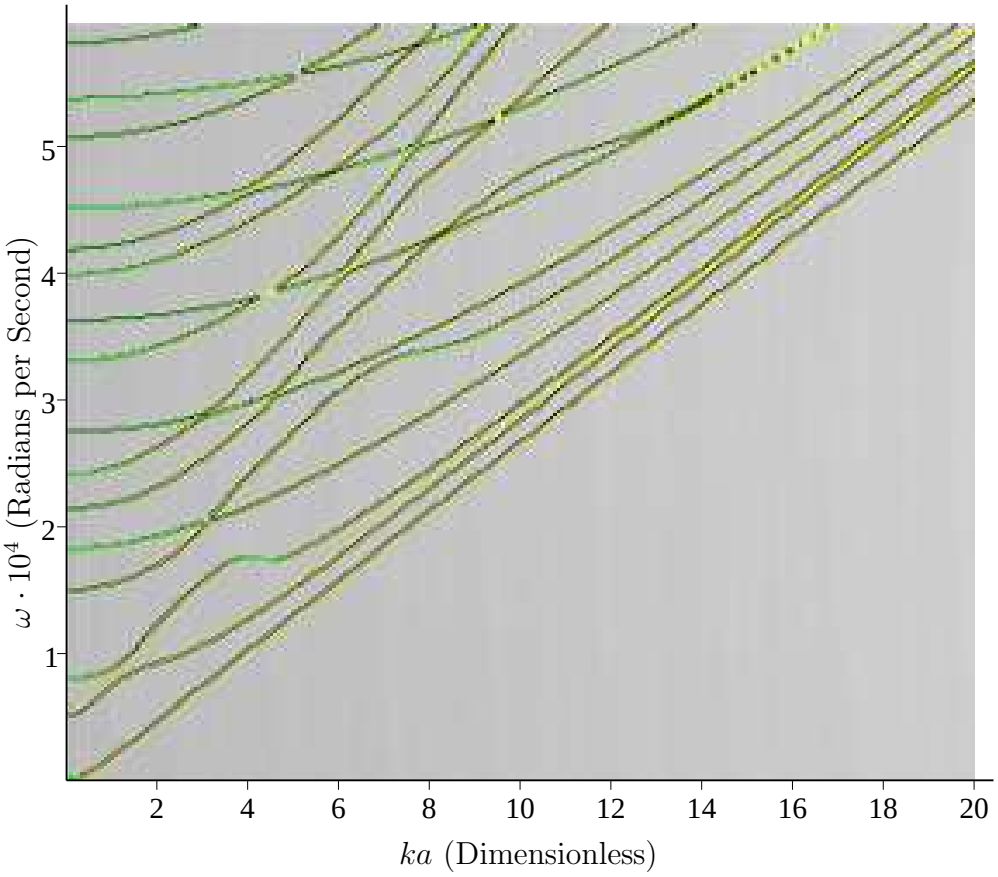


Figure 4.8: Dispersion curves for the flexural modes of a homogeneous transversely isotropic cobalt solid cylinder by Mirsky's model ($m = 1$) and making use of the sign function.

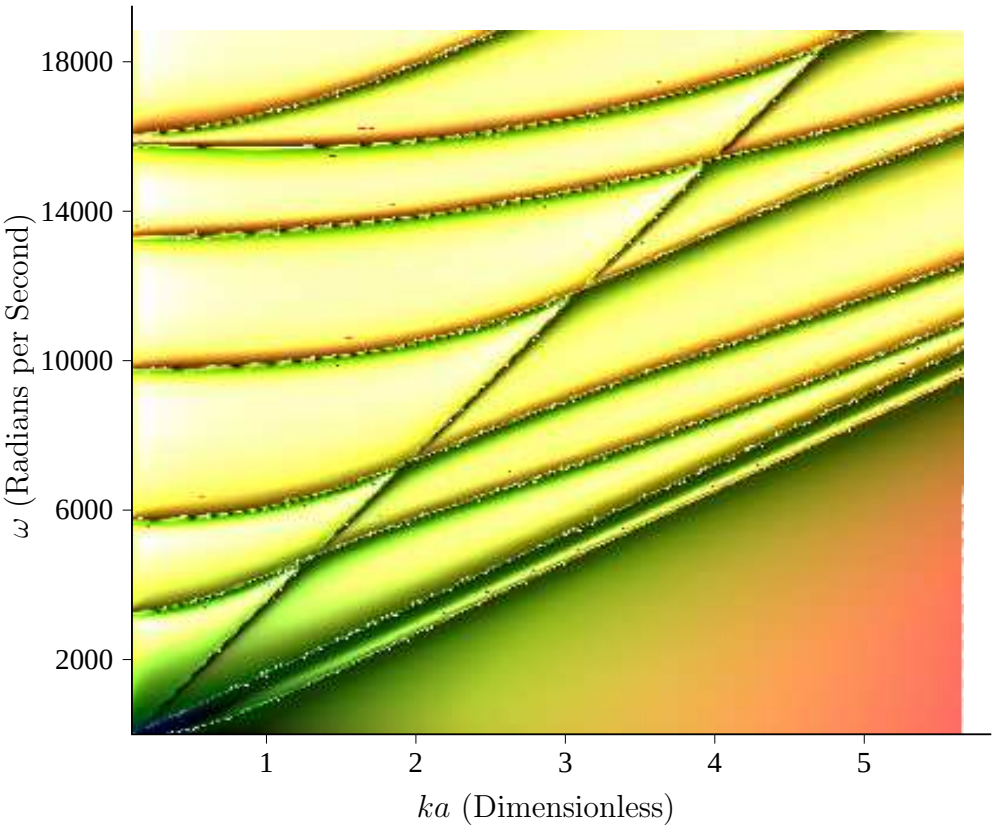


Figure 4.9: Dispersion curves for the flexural modes of a homogeneous transversely isotropic PZT-4 solid cylinder without electromecanical coupling by Mirsky's model ($m = 1$).

opposed to three used by Mirsky [15], Berliner et al [14] and in this dissertation. Also, to obtain dispersion curves, the authors in [4] plotted $\frac{\omega a}{c_b}$ (where $c_b = \sqrt{\frac{E_a}{\rho}}$ and $E_a$ the axial Young's modulus for a transversely isotropic rod) against $ka$, whereas we have plotted $\omega$ against $ka$ in this dissertation. However, both approaches are similar in that the characteristic arguments $\xi_1$, $\xi_2$ and $q$ obtained in this dissertation i.e. Eqns.(4.60) and (4.63) are the same with those obtained by Honarvar et al. It is also worth mentioning that in Honarvar et al's model, the expression for the displacement vector can be expressed via Helmholtz's decomposition into two parts; one with zero curl and the other with zero divergence. But the displacement vector field used in this dissertation i.e. Eqn.(4.2), doesn't satisfy this condition. The above remark is clearly a strong point in favour of Honarvar et al's model over ours.

The general form of the dispersion curves depicted in Figs.(4.1), (4.3) and (4.5) for aluminium, glass/epoxi fiber-reinforced composite and cobalt are very similar to those presented in [4] which are also shown in Figs.(4.2), (4.4) and (4.6). The straight lines in these figures, i.e. one very close to and above the fundamental mode (lowest order mode) and the other about 45-50 degrees from the horizontal axis, are artifacts and should be ignored as will be explained shortly. The general morphology of the curves for aluminium in Fig.(4.1) are exactly the same as that of Fig.(4.2) produced by Honarvar et al [4]. The only difference is that the curves in Fig.(4.1) are steeper than those in Fig.(4.2). This is because, the authors in [4] displayed the curves for $\frac{\omega a}{c_b}$ against $ka$, while we have plotted $\omega$ against $ka$; so that for a given point on a particular mode in Fig.(4.1) the phase velocity which is given by the tangent of the straight line from the origin to the point in question is $\frac{\omega}{ka}$, where $a = 1$. Whereas for the case in Fig.(4.2), the tangent of the straight line to the corresponding point is given by $\frac{\omega}{kc_b}$. This explains why the corresponding curves in Fig.(4.1) are steeper.

The dispersion curves for glass/epoxi and cobalt Figs.(4.3) and (4.5) are similar to those produced by Honarvar et al Figs.(4.4) and (4.6). The observed differences are: The curves in Figs.(4.3) and (4.5) are generally steeper than those in Figs.(4.4) and (4.6) for the same

reason as above. There are observed differences in the third and fifth modes for glass/epox in Fig.(4.3) and in the third, fifth and eighth modes for cobalt Fig.(4.5), which are less dispersive in nature for large $ka$ (i.e. less undulating in form) compared with those produced by Honavar et al i.e. Figs.(4.4) and (4.6); with the eighth mode not approaching the seventh mode very closely as it does in Fig.(4.6). However, by generating the 3D surface plot of the sign of the imaginary part of $D_3$, Eqn.(4.68) for glass/epoxi and cobalt and projecting it unto the $ka$-$\omega$ plane, we obtain the curves in Figs.(4.7) and (4.8) for glass/epoxi and cobalt respectively. These curves, are much more similar to those generated by Honaevar et al i.e. Figs.(4.4) and (4.6); and clearly are of very similar dispersive character. The small missing pieces of Figs.(4.7) and (4.8), is where two modes come very close to each other and then repel (e.g. the near meeting of the fourth and fifth modes in Fig.(4.8)). This effect is due to a shortcoming in the graphic resolution we are using in mathcad.

Finally, Fig.(4.9) represents the dispersion curves for a transversely isotropic rod without electromechanical coupling and having the same elastic stiffness constants as a PZT-4. The two straight lines in the figure are artifacts and should be ignored. The range of values of $ka$ and $w$ used for these curves are 0 to 5.7 and 0 to $2\pi \cdot 3000s^{-1}$ respectively. It is clear from Fig.(4.9) that the general form of these curves is similar to those of aluminium, cobalt and glass/epox, though less dispersive in nature.

Following from the above discussion, it is evident that the simpler model for non-axisymmetric (flexural) waves in a solid cylinder of transversely isotropic material presented in this dissertation is correct; since we have been able to reproduce very similar curves to those of Honavar et al who used a different mathematical model for the same problem.

Figs.(4.10) and (4.11) depicts results for a piezoelectric PZT-4 rod, but with the piezoelectric stress coefficients reduced by a factor of 1000; and with different electrical boundary conditions i.e. $[D_r]_{r=a} = 0$ and $[\phi]_{r=a} = 0$ respectively. The dispersion curves are observed to be very close to the non-piezoelectric results of Fig.(4.9); however, there are extra straight lines which are artifacts and as before should be ignored.

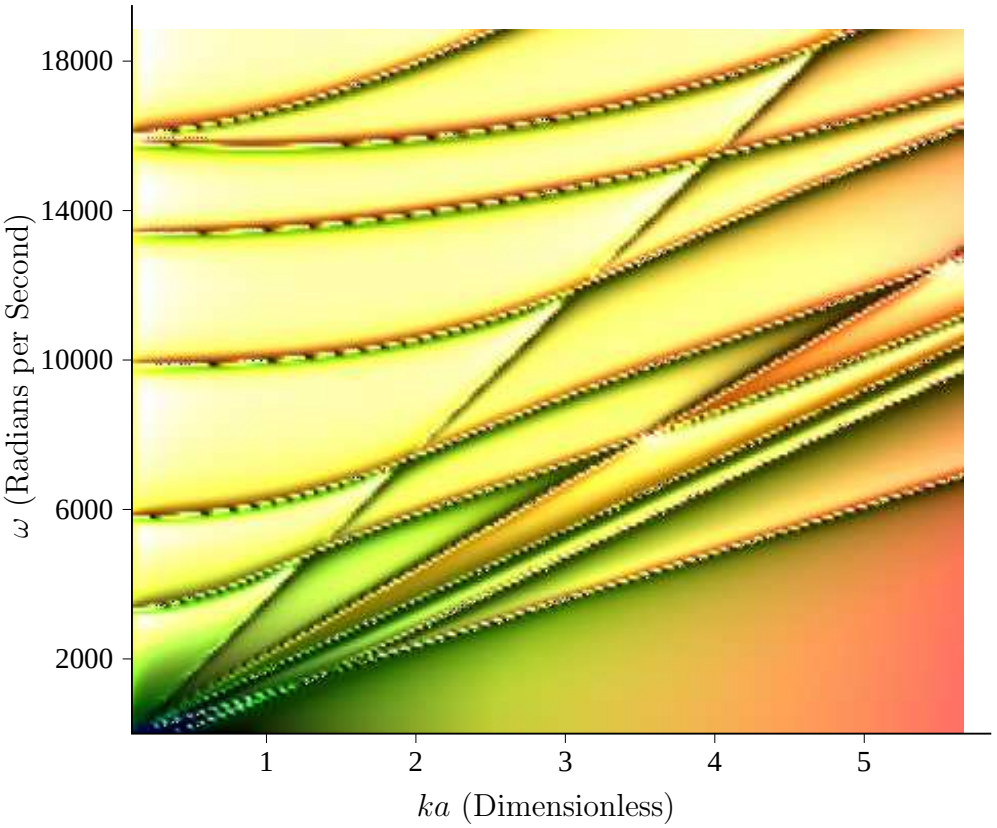


Figure 4.10: Dispersion curves for the flexural modes of a homogeneous transversely isotropic PZT-4 solid cylinder with $e_{ij} \cdot 0.001$ and $D_r|_a = 0$, $(m = 1)$.

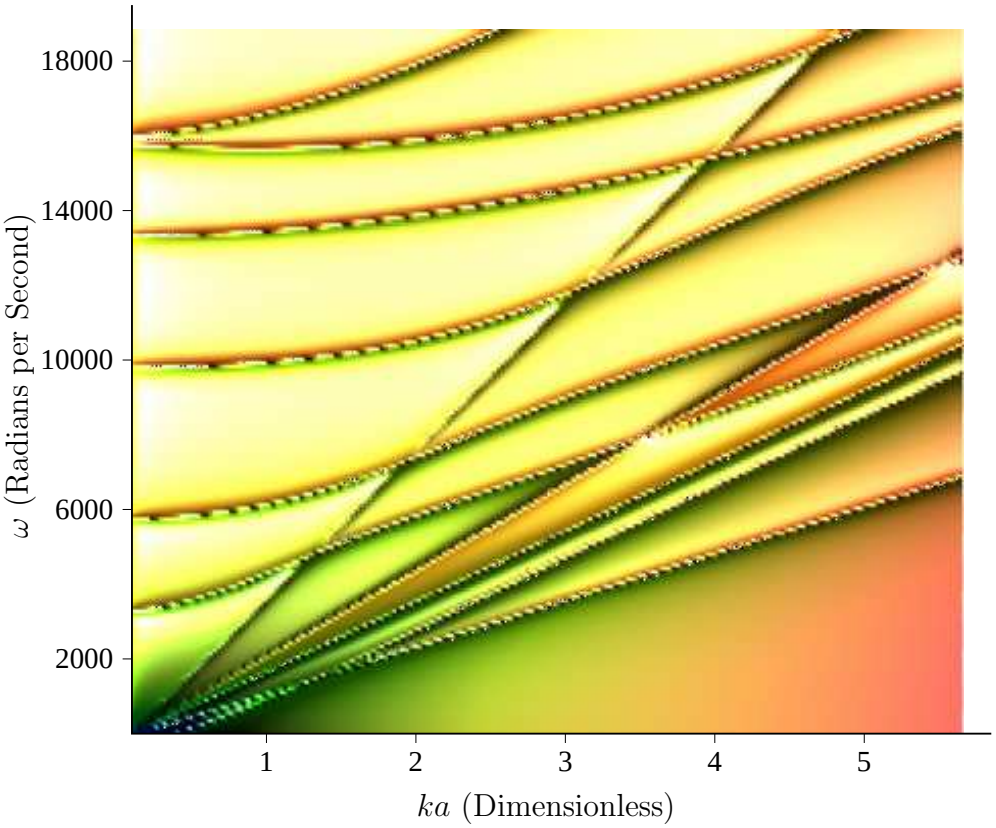


Figure 4.11: Dispersion curves for the flexural modes of a homogeneous transversely isotropic PZT-4 solid cylinder with $e_{ij} \cdot 0.001$ and $\phi|_a = 0$, $(m = 1)$

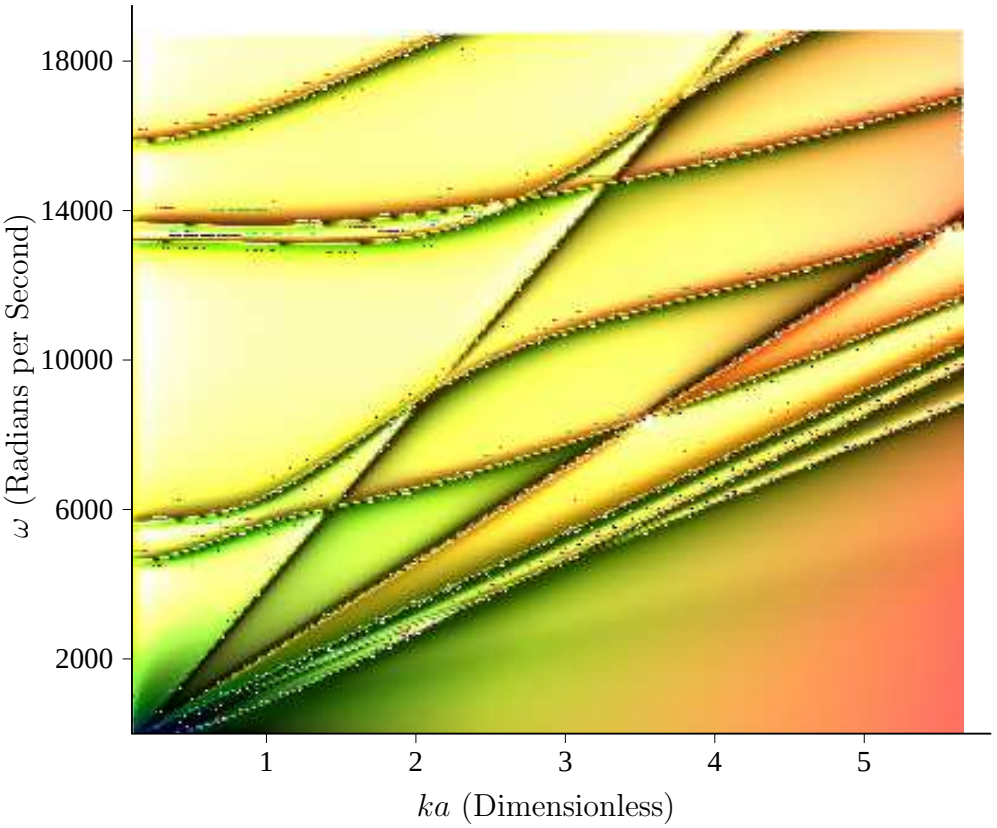


Figure 4.12: Dispersion curves for the flexural modes of a homogeneous transversely isotropic PZT-4 solid cylinder with $e_{ij} \cdot 1$ and $D_r|_a = 0$, $(m = 1)$.

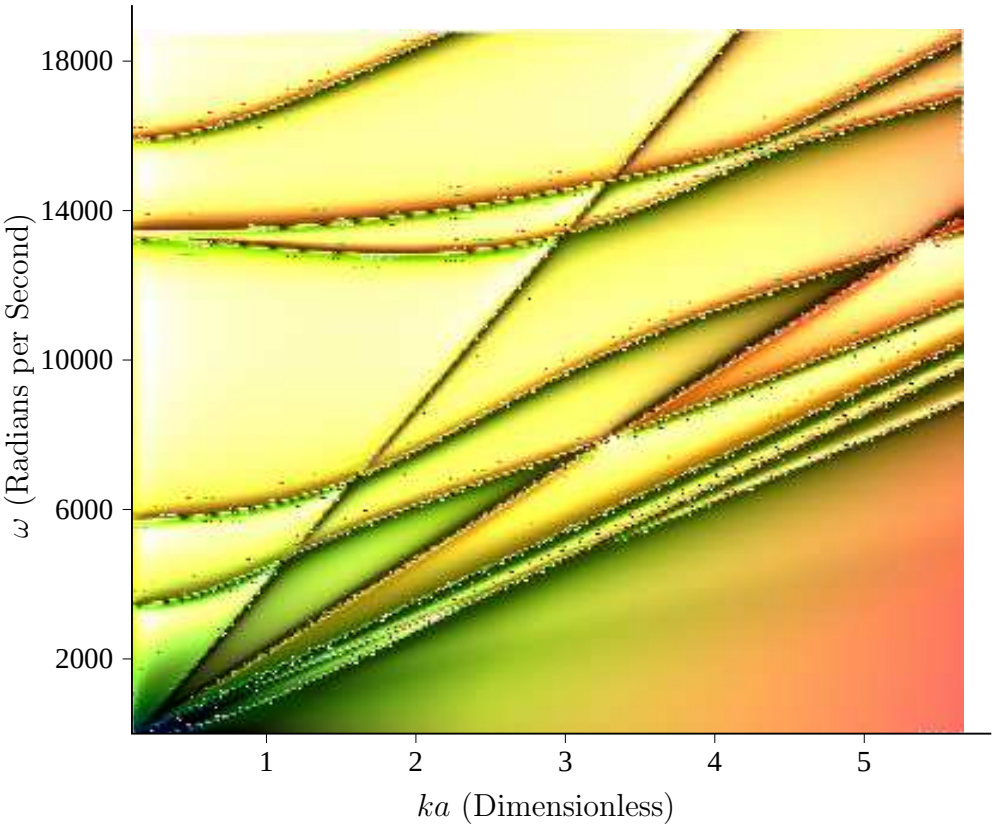


Figure 4.13: Dispersion curves for the flexural modes of a homogeneous transversely isotropic PZT-4 solid cylinder with $e_{ij} \cdot 1$ and $\phi|_a = 0$, $(m = 1)$

Finally, in Figs.(4.12) and (4.13), where the standard coupling coefficients of PZT-4 are used, the wave modes are seen to be sensitive to the electrical boundary conditions. The sensitivity is more pronounced for higher order modes. Comparing Fig.(4.9) with Figs.(4.12) and (4.13), we make the following observations with regard to the effect of piezoelectric coupling.

Firstly, we observe that the lowest order mode (the fundamental mode) is insensitive to the electro-mechanical coupling, since it does not change noticeably with the introduction of piezoelectric coupling in Figs.(4.12) and (4.13). Secondly, the higher order modes which are more sensitive to the piezoelectric coupling are more dispersive in character as indicated by the more undulating nature of the mode curves in Fig.(4.12) and (4.13). Thirdly, we notice that there is a significant shift in the cutoff frequencies (which occur in the limit as the phase velocity approaches infinity; the group velocity (by definition is the slope of the curves, Eqn.(1.4)) and the wave number approaching zero) of the second, fourth and seventh order modes to higher frequencies for the non-piezoelectric case Fig.(4.9) when piezoelectricity is introduced as seen in Figs.(4.12) and (4.13) (this effect is more pronounced for the case with $[D_r]_{r=a} = 0$). We also notice that, the number of modes observed for a given frequency range is smaller for Figs.(4.12) and (4.13). One could ascribe this to a form of piezoelectric stiffening which pushes velocities and frequencies to higher values. Finally, we observe that for the sixth mode in Fig.(4.9), and fourth and fifth modes in Figs.(4.12) and (4.13) there exist ranges of $ka$ and $\omega$ for which the group and phase velocity have opposite signs; implying that energy is being carried in one direction, while the wave (crest and troughs) appear to propagate in the opposite direction. These rages are $0.11 \leq ka \leq 0.97$ and $15660 \leq \omega \leq 15780$, $0.53 \leq ka \leq 1.16$ and $13240 \leq \omega \leq 13350$ and $0.05 \leq ka \leq 0.89$ and $13740 \leq \omega \leq 13860$ for the sixth mode in Fig.(4.9) and the fourth and fifth modes in Figs.(4.12) and (4.13) respectively.

Generally, each mode displayed in the above figures is a combination of coupled quasi-shear and quasi-longitudinal waves (these components of each mode are referred to as partial waves), as they interact at the boundary surface and after reflecting from the boundary

surface. However, at the cutoff frequencies, the phase velocities become infinite and the partial waves propagate strictly in the plane of isotropy (since the group velocity in the axial direction is zero); where they decouple into pure shear and longitudinal modes [10]; leading to standing wave modes in the radial direction of the cylinder after reflections from the boundary surface.

## 4.6 Discussion on the Artifacts

An artifact according to the American Heritage Dictionary [31], is an inaccurate observation, effect, or result, especially one resulting from the technology used in scientific investigation or from experimental error.

As stated previously the straight lines in Figs.(4.9) to (4.13) are artifacts. The following observations make us to conclude that these straight lines are artifacts:

These lines are non dispersive for all ranges of frequency and wave numbers and do not approach the fundamental mode in the limit of large wave number and angular frequency. This is contrary to characteristic dispersion curves of flexural waves for rods of both isotropic and transversely isotropic symmetry characteristics [13, 4]. Moreover, the result of introducing piezoelectricity and the quasistatic approximation into the model, is to make the material appear more stiffened and as such giving rise to stiffened propagating modes [6]. So, in principle the effect of piezoelectric coupling should only change the morphology of any existing modes in the non-piezoeletric model and not to introduce entirely new modes, such as the extra straight lines in Figs.(4.12) and (4.13). Also, we observe that these artifacts intersect with other modes, which is not a characteristic feature of guided wave modes in rods and plates [9, 4].

Naturally, we would like to know what are the sources of these artifacts in the given model. In order to accomplish this we carried out more investigations and made the following further observations about the artifacts:

- In Fig.(4.9) the slopes of the first and second artifacts from top are $\sqrt{\frac{c_{33}}{\rho}}$ and $\sqrt{\frac{c_{44}}{\rho}}$ respectively, which are equal to the speed of the shear and longitudinal wave modes in an infinite transversly isotropic media, propagating in the symmetry direction [10].

- The two artifacts in the non-piezoelectric case in Fig.(4.9) reappears in Figs.(4.10) to (4.13) where piezoelectricity is considered. However, the artifact with slope equal to $\sqrt{\frac{c_{33}}{\rho}}$ in Fig (4.9) (non-piezoelectric case) is changed to $\sqrt{\frac{c_{33}+\frac{e_{33}^2}{\epsilon_{33}}}{\rho}}$ in Figs.(4.12) and (4.13) (with piezoelectric effect included), while the artifact with slope in Fig.(4.9) equal to $\sqrt{\frac{c_{44}}{\rho}}$ is unaffected by the introduction of piezoelectric coupling. This is in perfect agreement with the observations made by Nayfeh et al [10]; a consequence of piezoelectric stiffening.

- The numerical values of the slopes of the second artifact from top and the fourth in Figs.(4.12) and (4.13) are respectively 2440 and 1573. These artifacts together with the first artifact from top are sensitive to the piezoelectric coupling, with their slopes changing as the piezoelectric stress constants are changed.

- By making use of mathcad's flexible 3D surface plot feature; where the surface plot can be rotated by any amount, we observed that the nature of the second artifact from the top in Figs.(4.12) and (4.13) is different from that of the other artifacts and the propagating modes. The difference is that, while the locus $(ka, \omega)$ generating the propagating modes and the other artifacts, causes the determinant, $D_4$, Eqn.(4.45) to approach zero, the set of $(ka, \omega)$ generating the second artifact from top causes $D_4$ to tend to infinity.

- Finally, we noticed that the artifacts are insensitive to the boundary conditions as depicted in Figs.(4.12) and (4.13). This implies that the source of these artifacts should exist before the boundary conditions of the model are imposed i.e. Eqn.(4.43).

Based on the last observation above, this important question arises; what will be our first guess for the source of the artifact amongst the numerous complicated equations in the

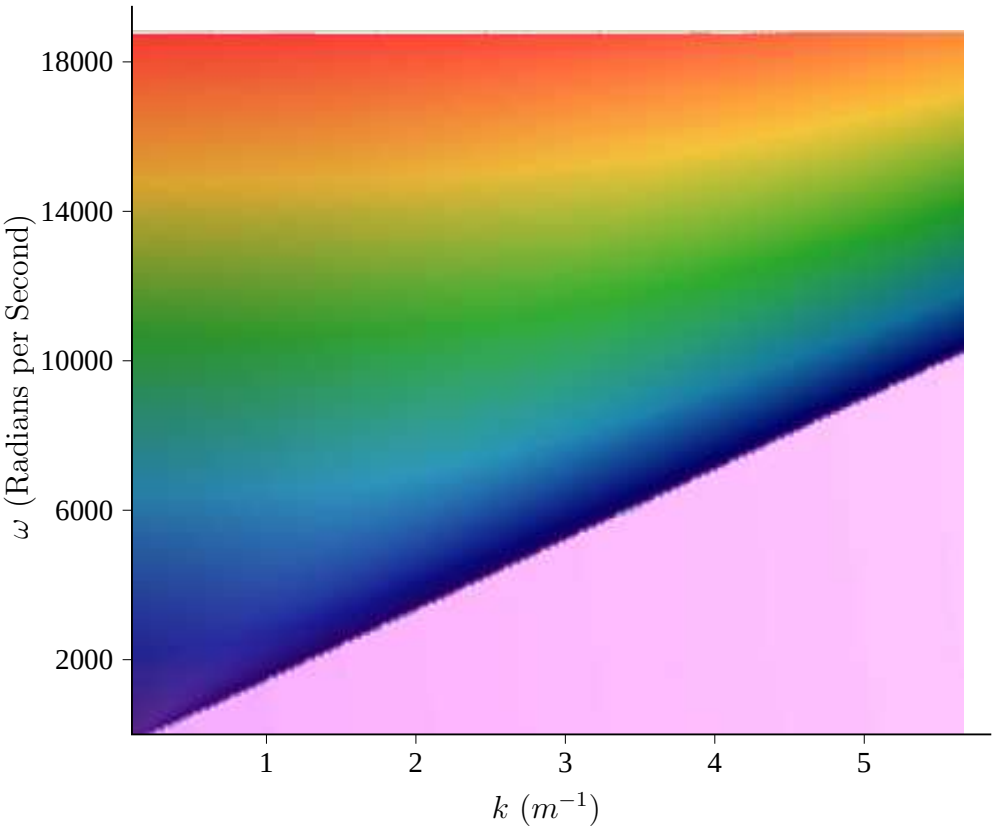


Figure 4.14: A 3D plot of $|\xi_1|$ projected unto the $k$-$\omega$ plane ($m = 1$).

model? Naturally, we should look for parameters that characterise and guarantee the existence of solutions. These parameters are the characteristic arguments $\xi_1$, $\xi_2$, $\xi_3$ and $\lambda$ and the characteristic factors $\eta_1$, $\eta_2$ and $\eta_3$.

We proceed by first investigating the nature of the characteristic arguments $\xi_1$, $\xi_2$, $\xi_3$ and $\lambda$. The projections of the three dimensional plots of $|\xi_1|$, $|\xi_2|$, $|\xi_3|$ and $|\lambda|$ which are all functions of $k$ and $\omega$ unto the $k$-$\omega$ plane, are shown in Figs.(4.14), (4.15), (4.16) and (4.17).

Clearly, the straight lines in the figures should suggest a relation to the artifacts. Doing further investigations on the nature of these straight lines, we observed the following:
The straight lines in Figs.(4.14) and (4.17) have exactly the same slope as the second artifact from bottom i.e $\sqrt{\frac{c_{44}}{\rho}}$ in Figs.(4.12) and (4.13). The two straight lines in Fig.(4.15)

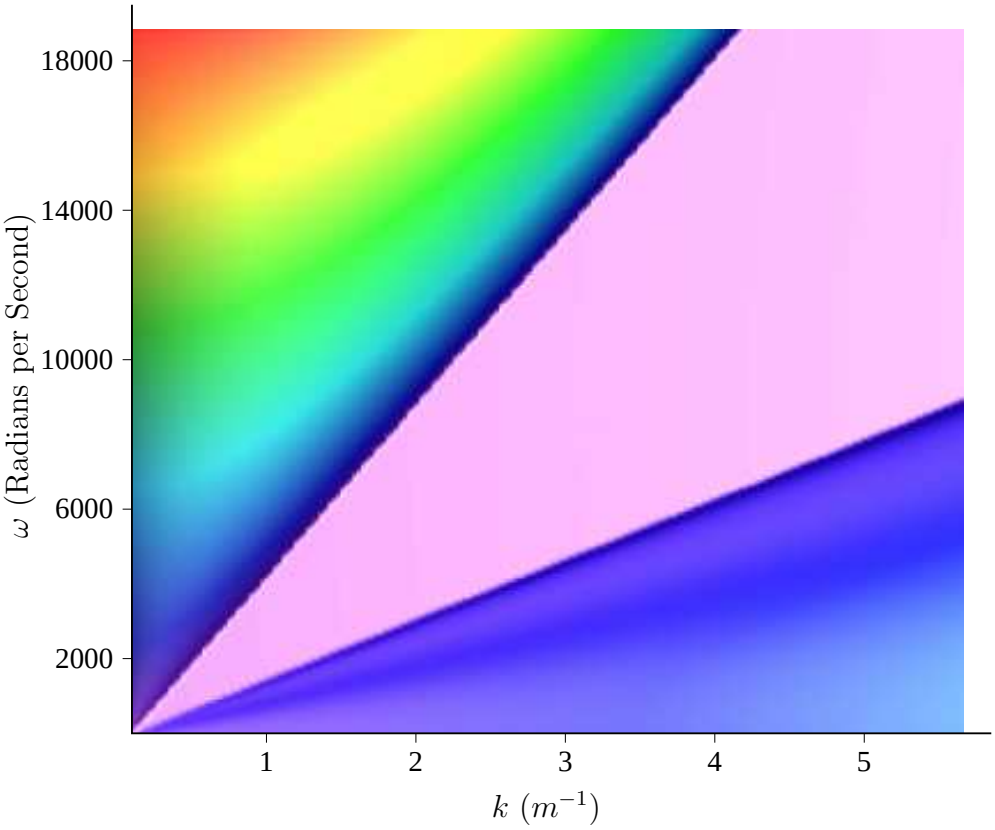


Figure 4.15: A 3D plot of $|\xi_2|$ projected unto the $k$-$\omega$ plane ($m = 1$).

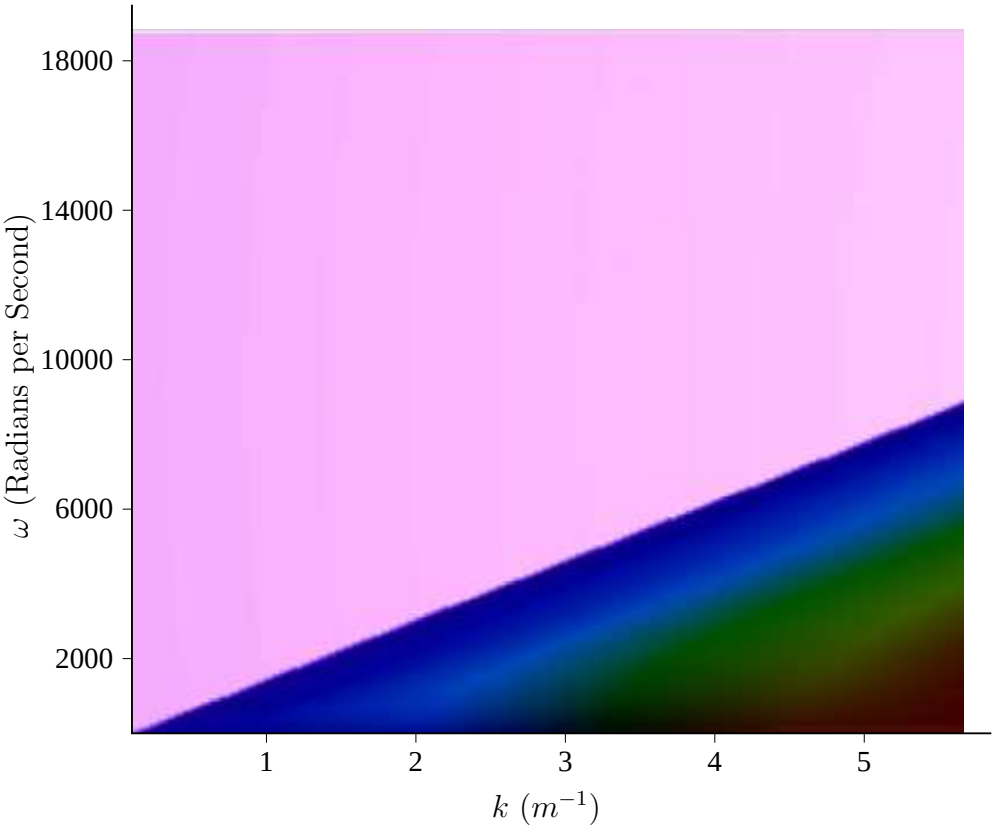


Figure 4.16: A 3D plot of $|\xi_3|$ projected unto the $k$-$\omega$ plane ($m = 1$).

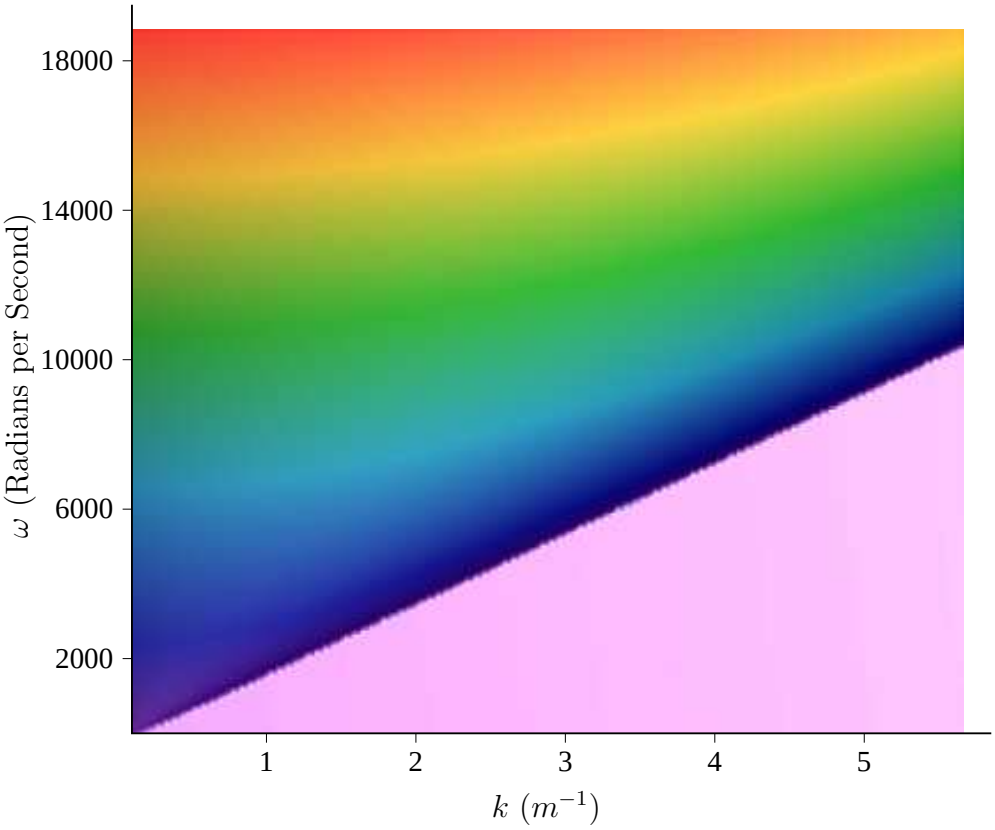


Figure 4.17: A 3D plot of $|\lambda|$ projected unto the $k$-$\omega$ plane ($m = 1$).

have slopes identical to $\sqrt{\frac{c_{33}+\frac{e_{33}^2}{\epsilon_{33}}}{\rho}}$ and 1573, which are the slopes of the first and fourth artifacts from top respectively in Figs.(4.12) and (4.13). Also, the slope of the straight line in Fig.(4.16) is same as that of the first artifact from bottom in Figs.(4.12) and (4.13) i.e 1573 as stated above.

Once more, making use of the ability to rotate mathcad's 3D surface plots we noticed that: The straight line in Figs.(4.14) and (4.17) is actually a boundary between two regions, where $\xi_1$ and $\lambda$ change character from being pure real in the upper region to being pure imaginary in the region below the line. Also, the two straight lines in Fig.(4.15) are also boundaries between regions in the nature of $\xi_2$; with $\xi_2$ changing from pure real in the upper region to pure imaginary in the middle region between the two straight lines and finally to complex in the region below the first line from bottom. Finally, the straight line in Fig.(4.16) also separates two regions in the character of $\xi_3$; with $\xi_3$ changing from pure imaginary in the upper region to complex in the lower region.

From the above observations about the artifact, we have noted that two of the artifacts, i.e. the first from top and the third from top occur where $\xi_1$ and $\xi_2$ changes from pure real to pure imaginary or equivalently, $\xi_1^2$ and $\xi_2^2$ changes sign on passing through zero. Setting $\xi$ equal to zero in the bi-cubic equation (i.e. Eqn.(4.17)) results in the following condition satisfied by the constant term (which is $c$ (i.e. Eqn.(4.19)) times $c_{11}\left(e_{15}^2+\epsilon_{11}c_{44}\right)$):

$$k^2\left[k^2c_{44}-\rho\omega^2\right]\left[k^2\left(c_{33}\epsilon_{33}+e_{33}^2\right)-\epsilon_{33}\rho\omega^2\right]=0. \tag{4.69}$$

Equation (4.69) is clearly satisfied if an only if

$$k=0 \quad \text{or} \quad \frac{\omega}{k}=\sqrt{\frac{c_{33}+\frac{e_{33}^2}{\epsilon_{33}}}{\rho}} \quad \text{or} \quad \frac{\omega}{k}=\sqrt{\frac{c_{44}}{\rho}}. \tag{4.70}$$

Clearly, the above observations leads to the slopes of the first and third artifacts from top as observed previously.

Also, as observed above, the fourth artifact from top occurs where $\xi_3$ changes from pure imaginary to complex. Looking at the expression for $\xi_3$ i.e. Eqn.(4.25), this will occur if

and only if $A - B = 0$; if and only if $A = B$ implying that $Q = 0$. Expressing $Q$ in terms of $a$, $b$ and $c$ (Eqn.(4.19)) (with help of mathcads symbolic package), we obtain the relation satisfied by the coefficients in the bi-cubic relation Eqn.(4.17) as follows:

$$-\frac{1}{108}a^2b^2 + \frac{1}{27}\left(b^3 + a^3c\right) - \frac{1}{6}abc + \frac{1}{4}c^2 = 0. \tag{4.71}$$

To show that Eqn.(4.71) has to be satisfied for this artifact to be generated, lets call the expression on the left of Eqn.(4.71) $V$; the 3D surface plot of $\log(|V|)$ projected unto the $k$-$w$ plane is depicted in Fig.(4.18).

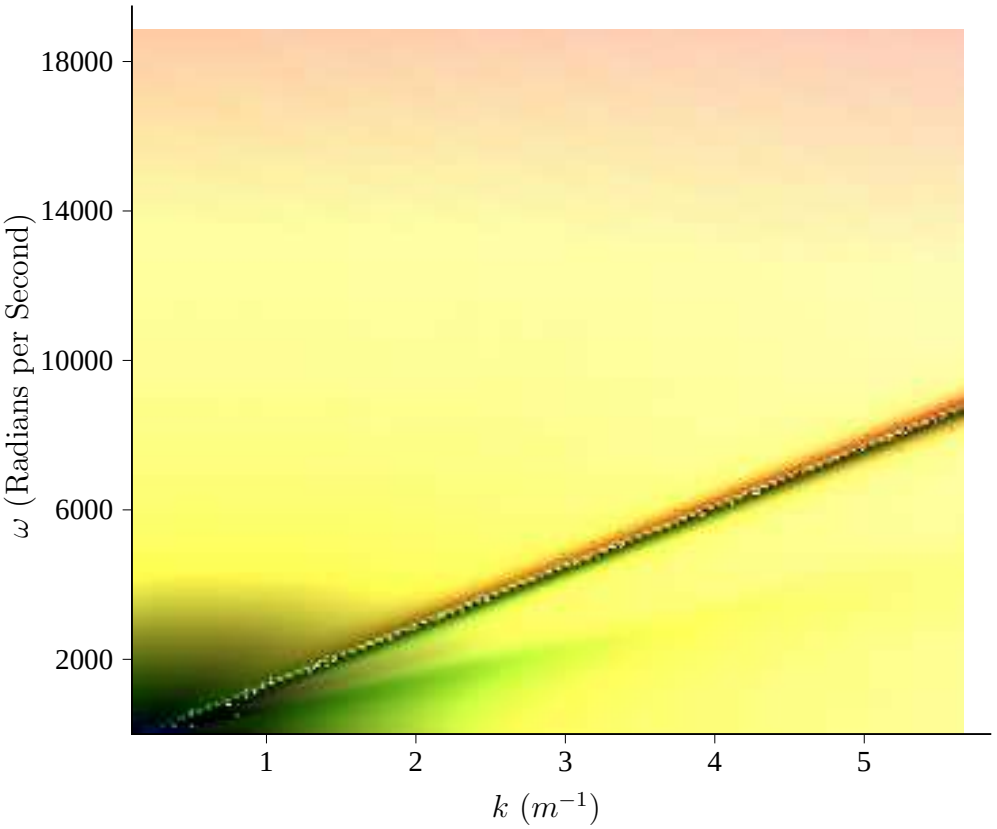


Figure 4.18: A surface plot of $\log(|V|)$ projected unto the $k$-$\omega$ plane ($m = 1$).

Clearly, the straight line in this figure is the fourth artifact from top and occurs for the set of values of $k$ and $\omega$ which lead to $|V| = 0$ as required by Eqn.(4.71).

Due to the above observations, it is evident that $\xi_1$, $\xi_2$, $\xi_3$ and $\lambda$ are the sources of the first, third and fourth artifact from top as they change their nature from one region to the other

separated by the artifacts.

So, we have successfully identified the sources of three artefacts. We are therefore now left to identify the source of the second artifact from top in Figs.(4.12) and (4.13). As mentioned before the source of this artifact is brought about by the set of points $(k, \omega)$ which cause $D_4$ to approach infinity. Hence, intuitively it's cause should be the result of some characteristic parameter or any other parameter dependent on the characteristic parameters approaching infinity, for the given set of $(k, \omega)$ values.

Taking a look at the expressions of the characteristic parameters $\xi_1$, $\xi_2$, $\xi_3$, $\lambda$, $\eta_1$, $\eta_2$ and $\eta_3$ in Eqns.(4.23), (4.24), (4.25), (4.28) and (4.16); it becomes obvious that only the $\eta$'s can tend to infinity (i.e. if their denominators tends to zero), because the denominators of the expressions for $\eta_1$, $\eta_2$ and $\eta_3$ are functions of $k$ and $\omega$, while the denominators of $\xi_1$, $\xi_2$, $\xi_3$ and $\lambda$ are independent of $k$ and $\omega$.

Further investigations of the denominators of $\eta_1$, $\eta_2$ and $\eta_3$ reveals the following for the denominator of $\eta_3$:

Let the denominator of $\eta_3$ be $B_3$; $B_3$ is expressed as follows from Eqn.(4.16):

$$B_3 = ik\Big(k^2\big[e_{33}(e_{15}+e_{31})+\epsilon_{33}(c_{13}+c_{44})\big]+\xi^2\big[e_{15}(e_{15}+e_{31})+\epsilon_{11}(c_{13}+c_{44})\big]\Big). \quad (4.72)$$

Figure (4.19) is a projection of the 3D surface plot of $\log(|B_3|)$ onto the $k$-$\omega$ plane. The three straight lines in the figure are actually values of $k$ and $\omega$ which cause the $\log(|B_3|)$ to approach $-\infty$ and hence cause $B_3$ to approach zero. Further determination of the slopes shows that the slope of the second straight line from the top and the third are 2440 and 1573; these values are exactly equal to the slopes of the second and fourth artifact from top in Figs.(4.12) and (4.13) respectively. Therefore, $\eta_3$ is responsible for the second artifact from top in Figs.(4.12) and (4.13) and the condition required for this artefact to occur is that $B_3 = 0$. One may ask, why is the effect of the first and third lines from top in Fig.(4.19) not displayed on the dispersion curves? We believe that their effect has been removed by some other multiplying factors in the numerical formulation of the problem.

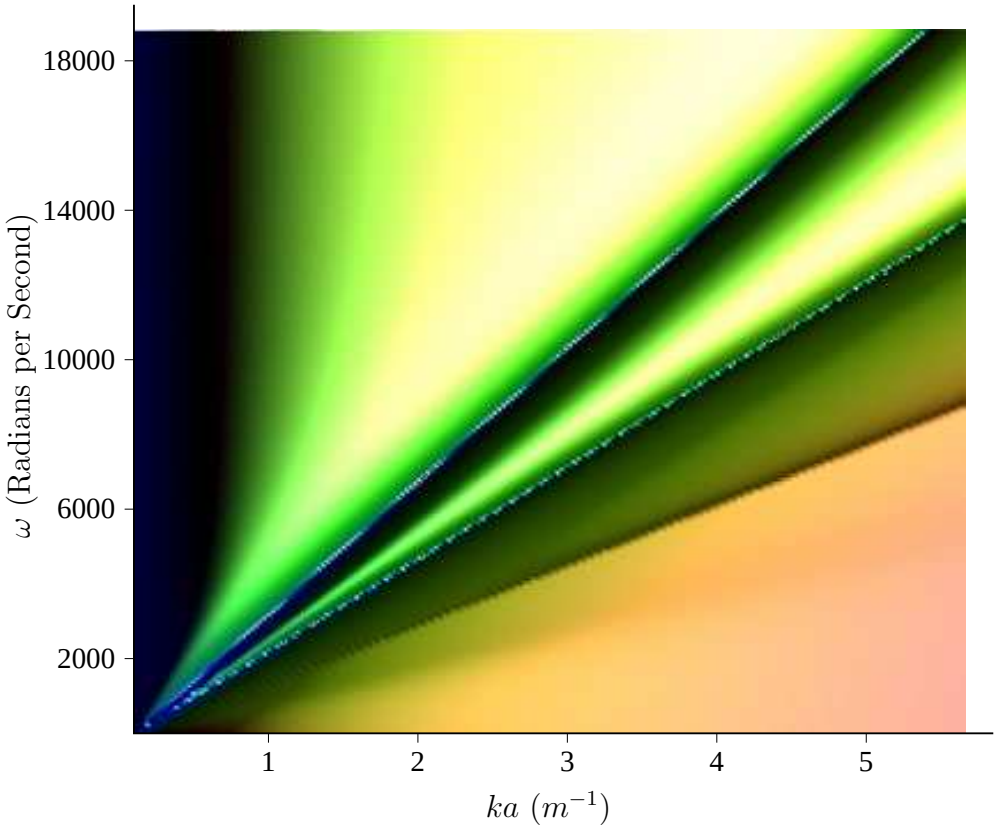


Figure 4.19: A 3D plot of $\log(|B_3)|$ projected unto the $k$-$\omega$ plane ($m = 1$).

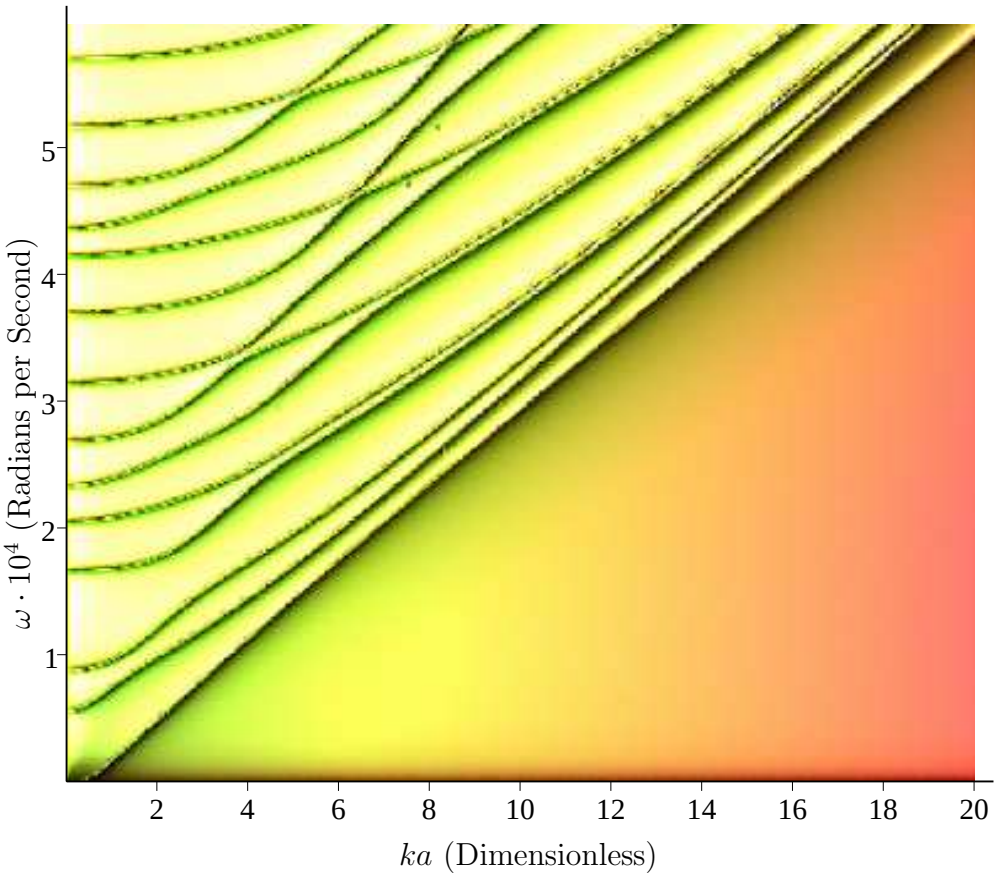


Figure 4.20: Dispersion curves for the flexural modes of a homogeneous isotropic aluminium solid cylinder by Mirsky's model ($m = 1$), with artifacts removed.

Now that we have identified the sources of the artifacts, ideally it will be good to display the dispersion curves with the artifacts absents. In order to accomplish this, we divided the characteristic equation by $(\omega - s_1 k)$, $(\omega - s_3 k)$, $(\omega - s_4 k)$ and multiplied it by $(\omega - s_2 k)$. Where $s_1$, $s_2$, $s_3$, $s_4$ are the slopes of the artifacts from top to bottom displayed in the dispersion curves respectively. The resulting dispersion curves without the artifacts are displayed in Figs.(4.20) to (4.27).

Clearly, from the above discussion we can say with certainty that the artifacts appearing in this model depend on the method of solution and do not reveal the nature of the dispersion curves for non-axisymmetric axial propagating modes in a transversely isotropic piezoelectric cylinder.

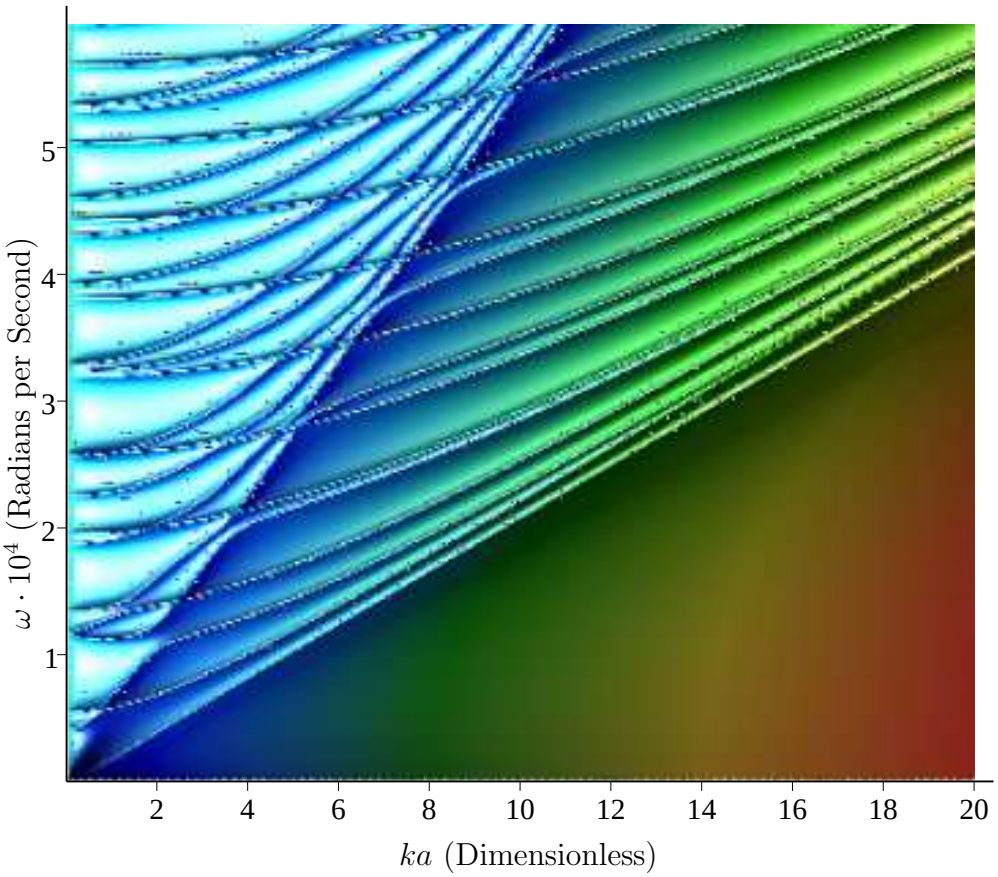


Figure 4.21: Dispersion curves for the flexural modes of a homogeneous transversely isotropic glass/epoxy fiber-reinforced composite solid cylinder by Mirsky's model ($m = 1$), with artifacts removed.

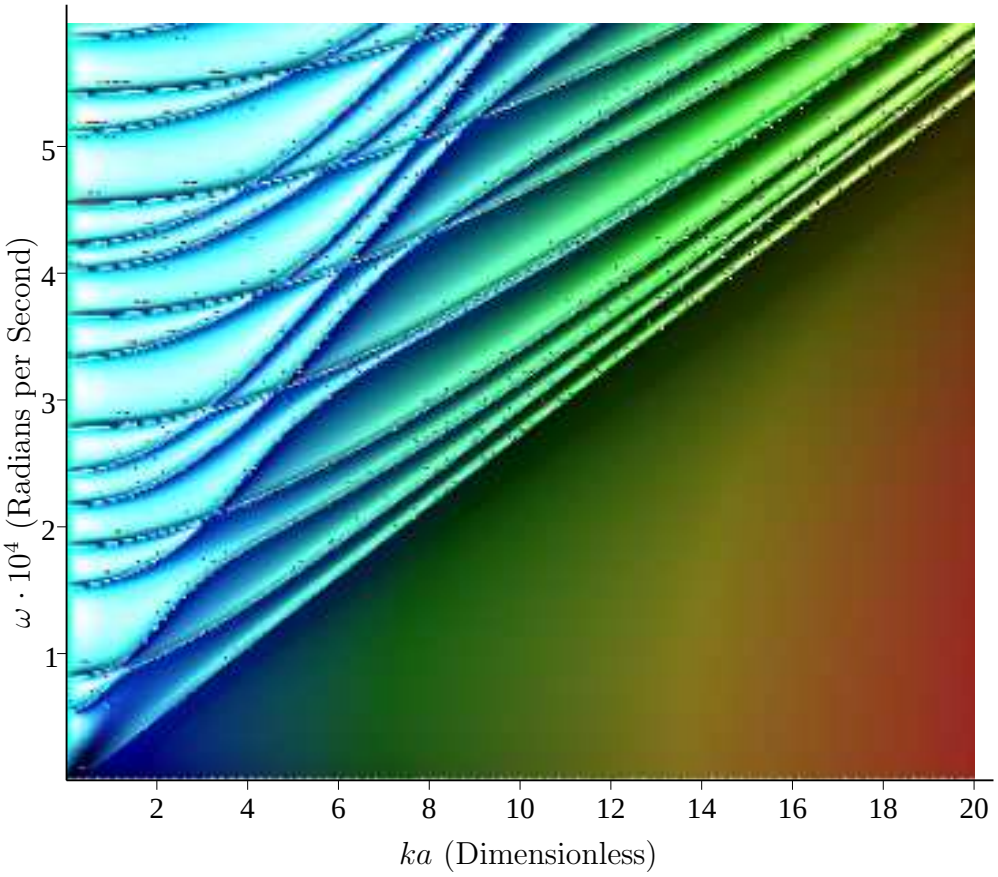


Figure 4.22: Dispersion curves for the flexural modes of a homogeneous transversely isotropic cobalt solid cylinder by Mirsky's model ($m = 1$), with artifacts removed.

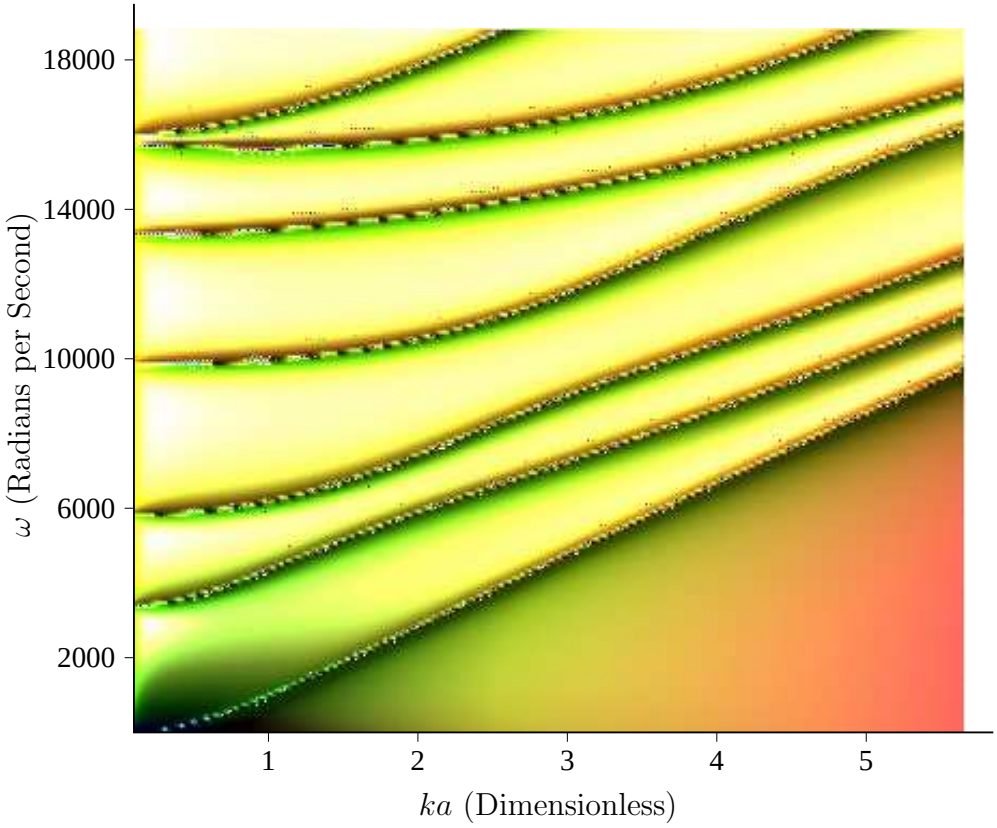


Figure 4.23: Dispersion curves for the flexural modes of a homogeneous transversely isotropic PZT-4 solid cylinder without electromecanical coupling by Mirsky's model ($m = 1$), with artifacts removed.

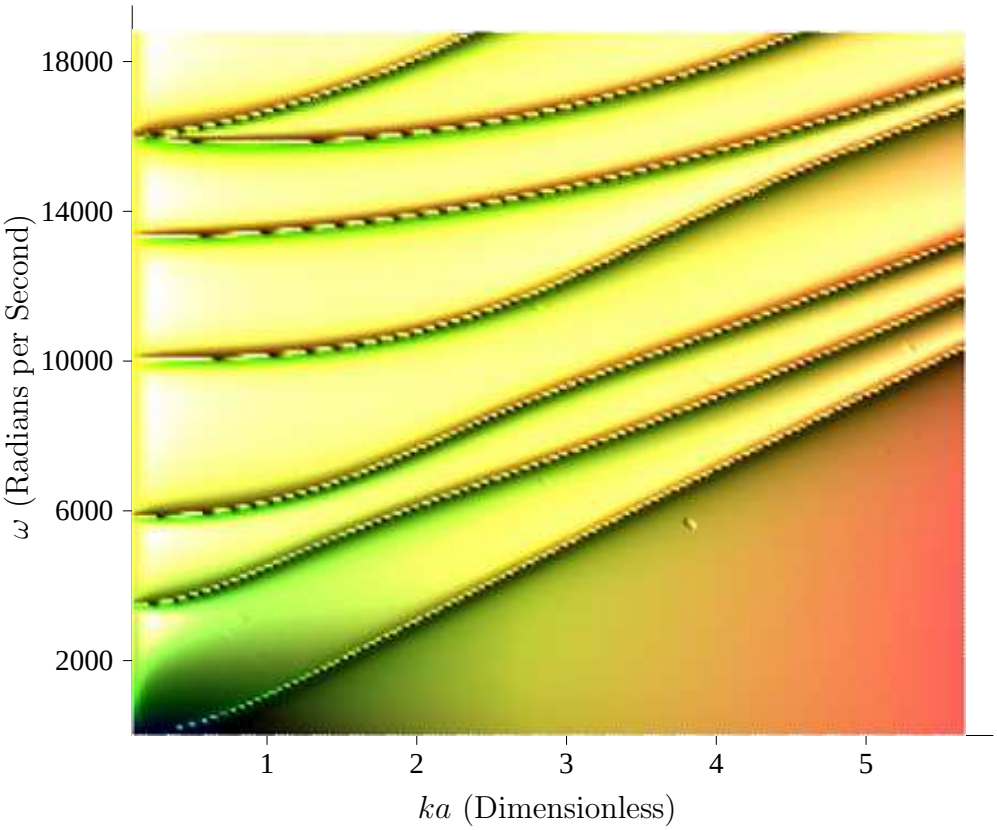


Figure 4.24: Dispersion curves for the flexural modes of a homogeneous transversely isotropic PZT-4 solid cylinder with $e_{ij} \cdot 0.001$ and $D_r|_a = 0$, $(m = 1)$, with artifacts removed.

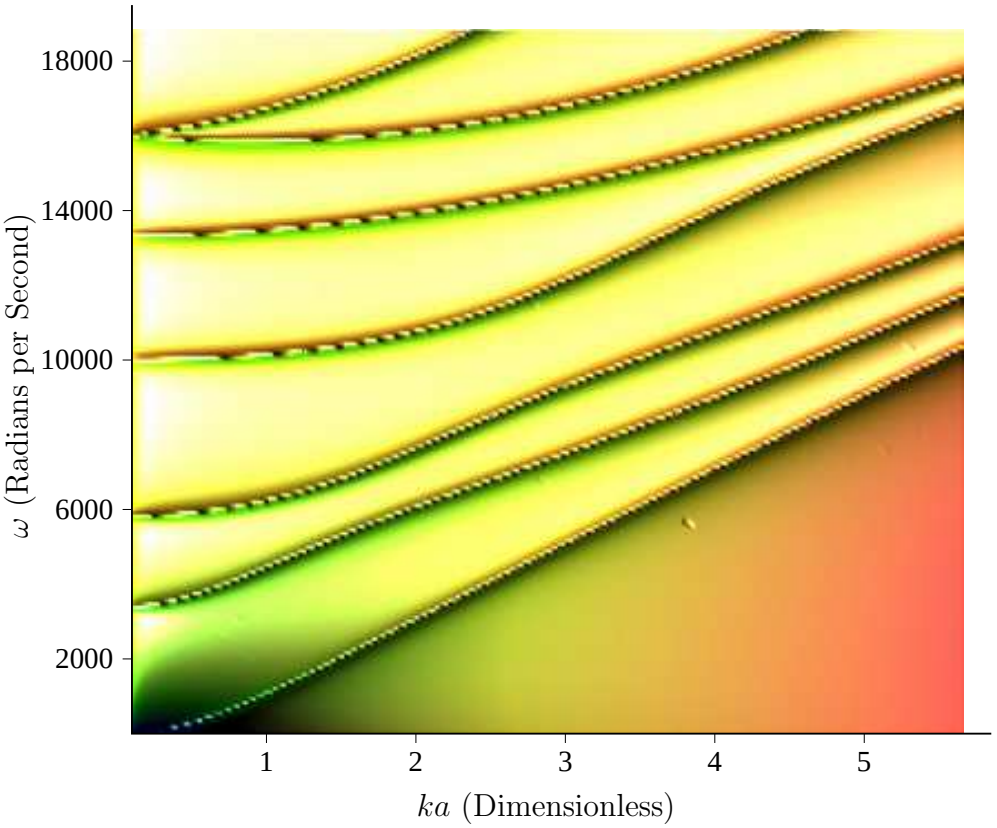


Figure 4.25: Dispersion curves for the flexural modes of a homogeneous transversely isotropic PZT-4 solid cylinder with $e_{ij} \cdot 0.001$ and $\phi|_a = 0$, $(m = 1)$, with artifacts removed.

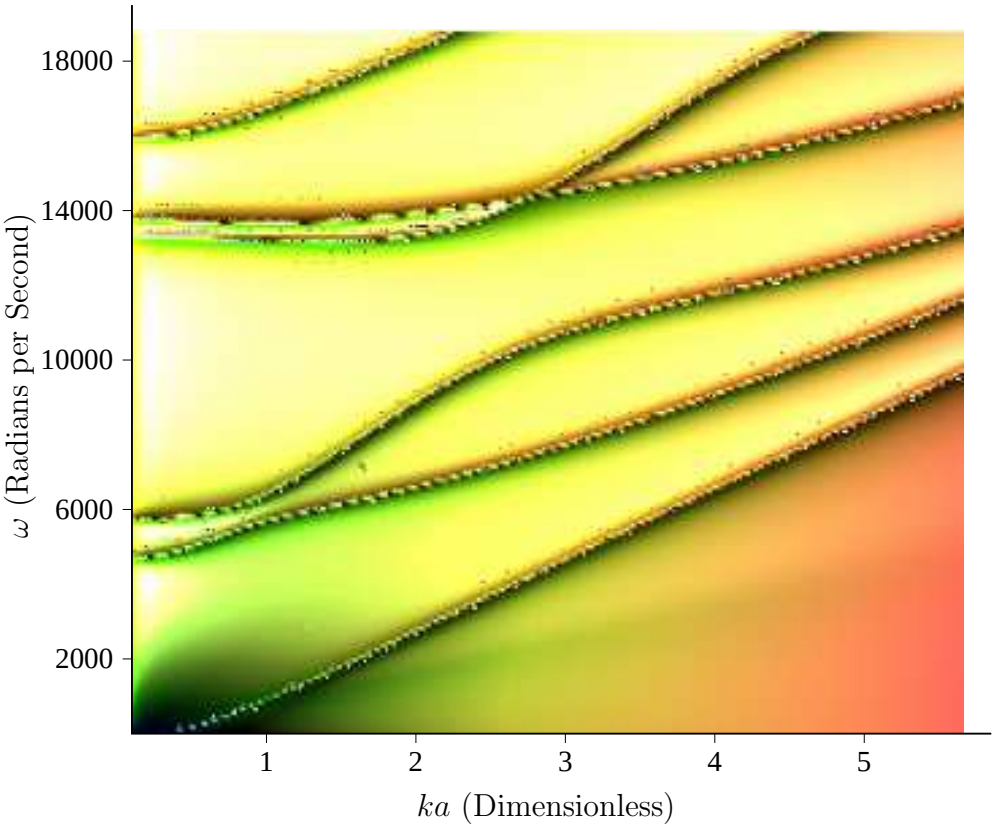


Figure 4.26: Dispersion curves for the flexural modes of a homogeneous transversely isotropic PZT-4 solid cylinder with $e_{ij} \cdot 1$ and $D_r|_a = 0$, $(m = 1)$, with artifacts removed.

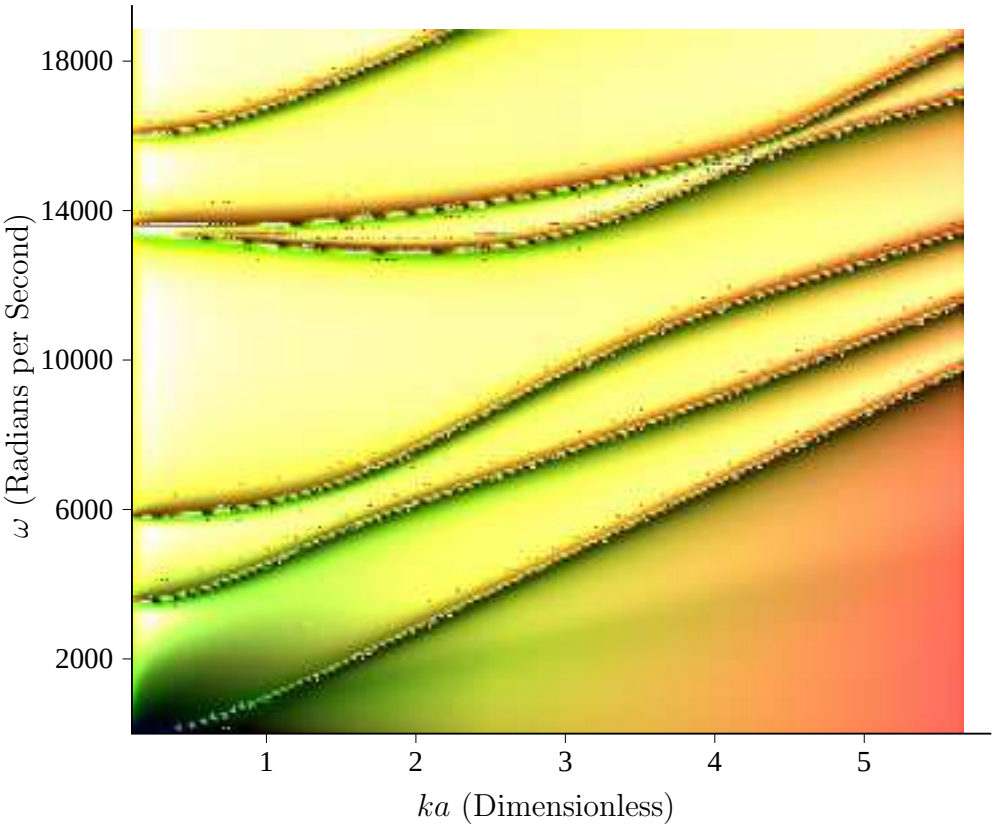


Figure 4.27: Dispersion curves for the flexural modes of a homogeneous transversely isotropic PZT-4 solid cylinder with $e_{ij} \cdot 1$ and $\phi|_a = 0$, $(m = 1)$, with artifacts removed.

# Chapter 5

# Conclusion

In summary, we have derived the governing equations of motion together with the allowed physical boundary conditions, for a homogeneous, piezoelectric rod, possessing transversely isotropic symmetry, and of class 6mm. The governing equations of motion have been solved analytically in terms of four displacement and three electric potentials each satisfying Helmholtz's equation. The characteristic equation for the system was then developed by application of the physical boundary conditions. We have also developed the characteristic equation (dispersion relation) for the simpler problem of non-axisymmetrical wave propagation in a non-piezoelectric solid cylinder possessing transversely isotropic symmetry; which has already been solved by Mirsky [15] and Berliner et al [14] via the same mathematical model; and Honarvar et al [4] through an entirely new and novel model. The characteristic equations for both the piezoelectric and the non-piezoelectric models have been solved numerically, for sample materials: PZT-4 rod, and aluminium, cobalt, glass/epoxi fiber-reinforced composite and PZT-4 (with electromechanical coupling absent) cylinders respectively. Dispersion curves for the allowed flexural propagating modes for both piezoelectric and non-piezoelectric models were presented. The dispersion curves presented had straight line artifacts intersecting the propagating modes which is due to our method of solution. We have shown that the dispersion curves produced using Mirsky [15] and Berliner

el al's [14] mathematical models are very similar to those produced by Honarvar et al [4]. We observed the following effects displayed by the propagating non-axisymmetric modes of a transversely isotropic rod when piezoelectric coupling was included:

- We observed that when the piezoelectric stress constants are reduced by a factor of 1000, the dispersion curves become very similar to those of the non-piezoelectric model.
- The lowest order mode (fundamental mode) is insensitive to piezoelectric coupling.
- The higher order modes become more dispersive in nature.
- The number of modes observed for a given frequency range is smaller for the piezoelectric rod, which can be interpreted as the effect of piezoelectric stiffening.
- Significant shifts in the cutoff frequencies in the non-piezoelectric cylinder for the second, fourth and seventh order modes to higher frequencies in the piezoelectric rod (especially for the case with $[D_r]_{r=a} = 0$).
- We observed that the group and phase velocities have opposite signs for some ranges of $ka$ and $\omega$ for the sixth order mode and for the fourth and fifth order modes for the non-pizoelectric and piezoelectric models respectively.
- Finally, we noticed that the mode characteristics were dependent on the nature of the electrical boundary condition; except for the lowest order mode.

Finally, we have shown that the sources of the artifacts are the characteristic arguments $\xi_1$, $\xi_2$, $\xi_3$, $\lambda$ and the characteristic factor $\eta_3$. We have also explained how the artifacts can be removed and presented the dispersion curves without the artifacts.

Therefore, from the above observations, we conclude that the introduction of piezoelectric coupling is crucial for the understanding of the elastodynamics of a PZT-4 rod; and the nature of the electrical boundary conditions play an important role in the study of propagating wave

modes in a piezoelectric rod. The effect of piezoelectric coupling are more pronounced for the higher order modes.

The results obtained in this dissertation, lay a good foundation for future investigations on modifications of the model system. For example, the model could be modified as follows: Flexural wave propagation could be studied in a hollow, transversely isotropic, piezoelectric cylinder, filled with and immersed in an iviscid fluid (i.e. fluid-loading). This is just the introduction of piezoelectric coupling to the problem solved by Berliner et al [14].

In this model, the equations of motion of the cylinder are developed and solved in exactly the same way as in this dissertation, except for the inclusion of the Bessel function of the second kind which was discarded in the model of the solid cylinder. The mechanical displacement equations of the internal and external fluids are developed using the constitutive relation of an irrotational inviscid fluid. Displacement potentials can be used to solve the equations of motion of the fluids; which are expressed in terms of Bessel functions of the first kind for the inner fluid and Hankel functions of the first kind for the outer fluid (so as to satisfy Sommerfeld radiation condition, for cylindrical waves propagating in infinite media [9]). However, due to the way in which we defined the phase dependence of the propagating modes in this dissertation, Hankel functions of the second will be the appropriate function for our purposes [9].

The frequency (characteristic) equation of the coupled cylinder and fluid system is obtained by assuming perfect-slip boundary conditions at the fluid-cylinder interfaces. With this assumption, only the surface stresses (i.e. $\sigma_{rr}$, $\sigma_{r\theta}$ and $\sigma_{rz}$), $u$, $D_r$ (due to absence of free charges at interface) and $\phi$ are continuous. The planar displacements $v$ and $w$ are discontinuous. It is worth noting that, wave number solutions to the propagating modes in the coupled fluid-cylinder system will be complex; this is to account for the attenuation due to fluid-loading of the hollow cylinder [9]. In this case, the imaginary part of the wave number is equivalent to the attenuation factor of the wave mode, while the ratio of the angular frequency to the real part of the wave number gives the phase velocity of the wave

mode in the cylinder.

We could also study the general problem of flexural wave propagation in a free multilayered fibre system (of arbitrary number of layers) and an embedded (immersed) multilayered fibre system in an infinite solid (liquid); with the constituent layers made of transversely isotropic piezoelectric materials. This problem is an extension of the problem solved by Nayfeh et al [10], who solved the corresponding problem for longitudinal waves using a different approach, i.e. without making use of displacement potentials as used in this dissertation.

The solution of the partial waves in each of the layers of the fibre system can be obtained in exactly the same way as done in this dissertation. The transfer matrix technique (which makes use of the continuity of $u$, $v$, $w$, $\sigma_{rr}$, $\sigma_{r\theta}$, $\sigma_{rz}$, $D_r$ and $\phi$ at the interfaces between layers of the fibre [10]) can then be implemented to relate the mechanical displacements, surface stresses, electric displacement and the electric potential at the outer surface of the outermost of the fibre layer to those of the outer surfaces of the inner layers including the core.

With the above result, the frequency (characteristic) equation for a free multilayered fibre can be obtained by applying boundary conditions of stress, electric displacement and electric potential as done in this dissertation.

To obtain the frequency equation of the fibre system embedded (immersed) in an infinitely extended solid (liquid) host, we first need to obtain solutions for waves propagating in the host. The displacement solutions for the solid host will be obtained in a manner similar to those of the fiber layers with the solid host made up of a transversely isotropic piezoelectric material. The only difference is that the Bessel's functions of the first and second kind are replaced by the Hankel function of the second kind in order to satisfy radiation conditions. The solutions for the case of an inviscid liquid host are obtained in a manner similar to that for the fluid-loaded hollow cylinder explained above. The frequency equation for the coupled fibre-host systems, is then obtained by applying the continuity and perfect-slip boundary condition of the field variables at the fibre-solid and liquid hosts interfaces respectively.

It is worth mentioning that inviscid fluids do not support shear stresses; so the shear stresses in the fluids of the above models are zero. Also, in the above model, the fibre layers are assumed to be perfectly bonded to each other at their interfaces. In the case of bonding imperfections as common in real life situations, the interfaces can be modelled as thin zones or layers, with a degenerate transfer matrix used to represent these layers as discussed by Nayfeh et al [10].

The above model as explained by Nayfeh et al, can be adjusted to solve the problem of a multilayered fibre systems uniformly distributed in a hexagonal fashion in a matrix, which models an infinite unidirectional fibre-reinforced composite as follows:
By taking advantage of the inherent periodicity and hexagonal symmetry of the unbounded composite system, the hexagonal repeating cells (composed of fiber and matrix) can be isolated and approximated by concentric cylindrical regions, with the fiber assembly as the core and surrounded by a matrix coaxial layer. As a result of the inherent periodicity and hexagonal symmetry of the system, the radial displacement($u$), the surface shear stresses ($\sigma_{r\theta}$ and $\sigma_{rz}$) and $D_r$ at the outer radius of the concentric fiber-matrix system vanishes. By applying this boundary condition for the radial displacement, the surface shear stresses and $D_r$, we obtain the frequency equation for a uniformly distributed fiber system in a matrix. Due to the hexagonal-cylindrical approximation to the geometry of this model, the results obtained will be approximate solutions and not exact solutions. But as described by Nayfeh et al [10], the result become more accurate at relatively low fibre volume fractions and at low frequencies.

Finally, flexural wave propagation in fibres of finite length together, with temperature effects taken into account could be considered. This will requre the machinery of finite element modelling and the theory of thermoelastic waves [9, 13]. All these further investigations are aimed at simulating real life situations found in industry.

# Appendix A

# Dispersion Curves Displayed by Honarvar et al via their Novel Method of Solving the Dispersion Relation

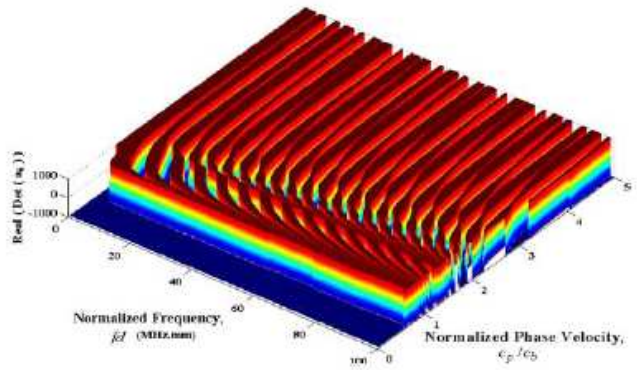


*Figure 1- Three-dimensional plot of the frequency equation for an isotropic aluminum cylinder,*

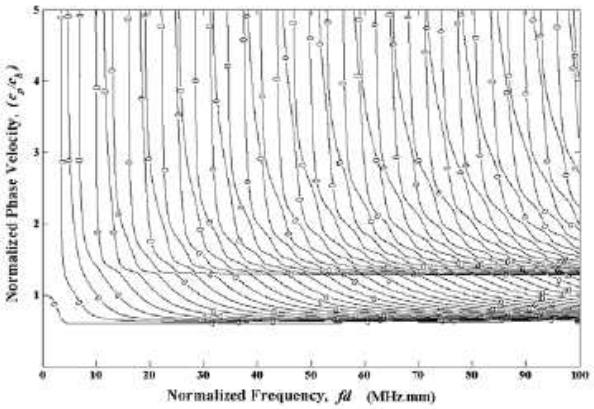


*Figure 2- Two-dimensional plot of the frequency equation for an isotropic aluminum cylinder,*

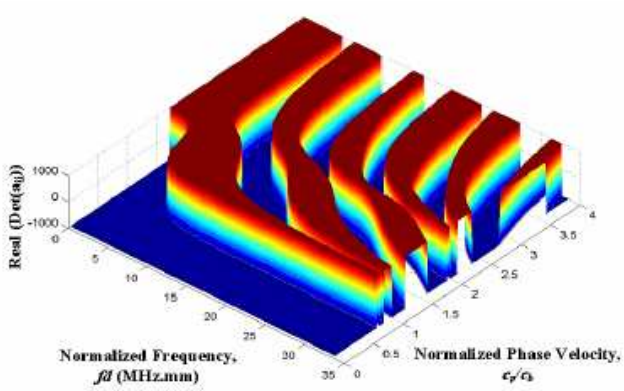


*Figure 3- Three-dimensional plot of the frequency equation for a transversely isotropic CFAMC cylinder,*

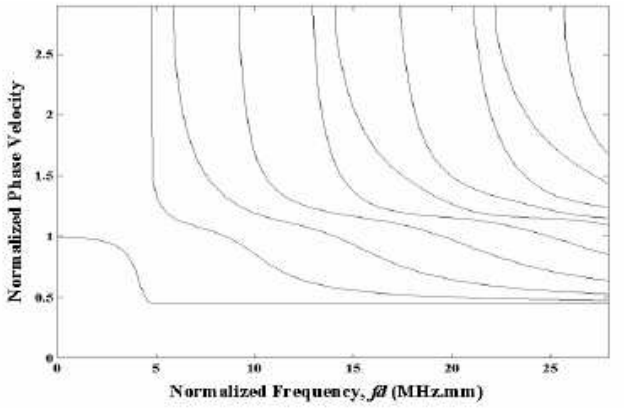


*Figure 4- Two-dimensional plot of the frequency equation for a transversely isotropic CFAMC cylinder,*

# Bibliography


[1] A. G. Every. *Handbook of Elastic Properties of Solids, Liquids and Gases*, volume 1. Academic Press, 2001.

[2] J. F. Nye. *Physical Properties of Crystals.* London: Oxford University Press, first edition, 1957.

[3] McGraw-Hill. *McGraw-Hill Concise Encyclopaedia of Science and Technology.* McGraw-Hill, fifth edition, 1989.

[4] F. Honarvar, E. Enjilela, A. N. Sinclair, and S.A. Mirnezami. Wave propagation in transversely isotropic cylinders. *International Journal of Solids and Structures*, (44):5236–5246, 2007.

[5] H. D. Young and R. Freedman. *University Physics.* Addison Wesley Longman, tenth edition, 2000.

[6] B. A. Auld. *Acoustic Fields and Waves in Solids.* Malabar: Krieger., 1990.

[7] C. Kittel. *Introduction to Solid State Physics.* John Wesley and Sons, Inc, fourth edition, 1979.

[8] H. J. Pain. *The Physics of Vibrations and Waves.* John Wiley and Sons Ltd, 1985.

[9] L. R. Joseph. *Ultrasonic waves in Solid Media.* Cambridge University Press, 1999.

[10] A. H. Nayfeh, W. G. Abdelrahman, and P. B. Nagy. Analyses of axisymmetric waves in layered piezoelectric rods and their composites. *Journal of Acoustical Society of America*, 108(4):1496–1504, 2000.

[11] A. G. Every and A. K. McCurdy. Phonon focusing in piezoelectric crystals. *Physical Review B*, 36(3):1432–1447, July 1987.

[12] J. D. Achenbach. *Wave Propagation in Elastic Solids*. New York: North-Holland, 1984.

[13] K. F. Graff. *Wave Motion in Elastic Solids*. New York: Dover, 1991.

[14] M. J. Berliner and R. Solecki. Wave propagation in fluid-loaded transversely isotropic cylinders. part 1. analytical formulation. *Journal of Acoustical Society of America.*, 99:1841–1847, 1996.

[15] I. Mirsky. Wave propagation in transversely isotropic circular cylinders part 1: Theory. *Journal of Acoustical Society of America*, 36:2106–2122, 1964.

[16] W. B. Frazer. Separable equations for a cylindrical anisotropic elastic waveguide. *Journal of Sound and Vibration*, 72:151–157, 1980.

[17] A. E. Armenakas and E. S. Reitz. Propagation of harmonic waves in orthotropic circular cylindrical shells. *Journal of Applied Mechanics*, 40:168–174, 1973.

[18] H. S. Paul. Vibrations of circular cylindrical shells of piezoelectric silver iodide crystals. *Journal of Acoustical Society of America*, 40:1077–1080, 1966.

[19] V. Winkel, J. E. B. Oliviera, J. D. Dai, and C. K. Jen. Acoustic wave propagation in piezoelectric fibers of hexagonal crystal symmetry. *IEEE Transactions on Ultrasonic, Ferroelectr and Frequency Control*, 42:949–955, 1995.

[20] J.P. Wei and X.Y. Su. Wave propagation in a piezoelectric rod of 6mm symmetry. *International Journal of Solids and Structures*, 42:3644–3654, January 2005.

[21] F. Honarvar, E. Enjilela, and A. N. Sinclair. Guided ultrasonic waves in composite cylinders. *Mechanics of Composite Materials*, 43(3):277–288, 2007.

[22] S. P. Timoshenko and J. N. Goodier. *Theory of Elasticity*. McGraw-Hill, third edition, 1970.

[23] B. L. Sidney, A. A. Marino, G. Berkovic, M. Fowler, and Abreo K. D. Piezoelectricity in the human pineal gland. *Bioelectrochemistry and Bioenergetics*, 41:191–195, 1996.

[24] A. G. Every and V. I. Neiman. Reflection of eletroacoustic waves in piezoelectric solids: Mode conversion into four bulk waves. *Journal of Applied Physics*, 71:6018–6024, 1992.

[25] L. Hassel. Sound velocities, elastic constants: Temperature dependence. *Material Science and Engineering A*, 442:31–34, April 2006.

[26] B. Kusse and E Westwig. *Mathematical Physics*. John Wiley and Sons, Inc, 1998.

[27] N. W. Hagood, W. H. Chung, and A. V. Flotow. Modelling of piezoelectric actuator dynamics for active structural control. *Journal of Intelligent Material Systems and Structures*, 1(3):327–354, 1990.

[28] S. H. Crandall, E. F. Karnopp, Jr. Kurtz, and D. C. Pridemore-Brown. *Dynamics of Mechanical and Electromechanical Systems*. Krieger Publishing Co, Malabar Florida, 1968.

[29] G. A. Korn and T. M. Korn. *Mathematical Handbook for Scientist and Engineers Definitions, Theorems and Formulas for Reference and Review*. Mc Graw-Hill, second, enlarged and revised edition, 1968.

[30] F. Honarvar, E. Enjilela, and A. N. Sinclair. Obtaining dispersion curves by a novel numerical method. *The Thirteenth International Congress on Sound and Vibration Vienna, Austria*, 2006.

[31] Houghton M. *The American Heritage Dictionary of the English Language*. Houghton Mifflin Company, fourth edition, 2000.